Doctoral Dissertation

博士論文

Searching for new physics with muon electric dipole moment

（ミューオン電気双極子能率による新物理探索）

A Dissertation Submitted for the Degree of Doctor of Philosophy

July 2022

令和４年7月　博士（理学）申請

Department of Physics, Graduate School of Science,
The University of Tokyo

東京大学 大学院 理学系研究科
物理学専攻

Shih-Yen Tseng

曾　師彦

THE UNIVERSITY OF TOKYO

Probing new physics by the muon electric dipole moment

by

Shih-Yen Tseng

in the

School of Science

Department of Physics

August 9, 2022

Abstract

In the thesis, we try to probe new physics by considering the muon electric dipole moment (EDM) induced from some new CP phases in the new physics model. More precisely, we study a Standard Model extension with two vector-like leptons, one $SU(2)_L$ singlet and one $SU(2)_L$ doublet. We consider a simple framework that only the muon couples to these new leptons. It leads to the mixing of muons with the extra heavy charged leptons and thus the muon mass receives contributions from these new particles. This contribution has a simple linear correlation with the muon $g-2$ at the leading order. Besides the muon dipole moments, an interesting feature is that the electron EDM is also induced in this framework, which is measured to very high precision and thus may give strong constraint on the parameters of the model if it predicts a too large electron EDM. With an appropriate choice of parameters, this model survives the experimental constraints on the Higgs-to-dimuon decay, heavy lepton masses, and electroweak precision measurements. We found parameter regions consistent with the observed deviation on muon $g-2$ between the experimental and theoretical results. Heavy lepton masses at the TeV scale are favored by the constraint on Higgs-to-dimuon decay, and typical values of the muon and electron EDMs are of order $\mathcal{O}(10^{-23} \sim 10^{-22})\ e \cdot \text{cm}$ and $\mathcal{O}(10^{-30})\ e \cdot \text{cm}$, respectively, which are just suitable for the proposed experiment on the measurement of these dipole moments.

Contents

List of Figures

List of Tables

Chapter 1

Introduction

Physicists have a dream, which is a theory of everything. In order to fulfill this quest, it is necessary to understand in detail what are the building blocks of our physical world, and what are the rules that lead to their specific properties and behaviors. This kind of study has currently been pushed to an extreme in the field of particle physics, considering the very sophisticated knowledge applied in experiments and theories of particle physics. Particle physics is a branch of physics studying the smallest constituents of the universe, which are called elementary particles. During the past seventy years or so, particle physicists had obtained fruitful results through the development of experimental techniques and the improvement of the theoretical framework. At the frontier of particle physics, researchers dive into a huge amount of experimental data and theoretical equations, search for the hint of the ultimate theory and try to figure out a single set of mathematical equations that well describes our physical world at the most fundamental level.

Today, to the best of our knowledge, most of the experimental results are consistent with the Standard Model (SM) of particle physics [1, 2, 3]. The SM of particle physics is the theory that describes the properties of elementary particles, the matter particles including leptons and quarks, and the fundamental forces, including electromagnetic, weak, and strong interactions, among the particles. Ten years ago, the last piece of the SM, the Higgs boson, was finally discovered at the Large Hadron Collider (LHC) by the effort of many experimental particle physicists at CERN [4, 5], which was a great achievement of particle physics and the triumph of the SM.

So far, the SM has been tested to work well through a wide range of energy scales up to $\mathcal{O}(1)$ TeV. However, we now certainly know that it is inherently an incomplete theory and therefore cannot be the ultimate theory that describes our physical world at the most fundamental level. There are several problems in both the theoretical and experimental aspects. First of all, it cannot explain gravity, since there is no description of gravity in the SM. Also, there are some ad hoc features in the SM. One is that the SM contains many free parameters which can only be determined by the experiments. These include 3 gauge couplings, 3 charged lepton masses, 6 quark masses, 3 quark mixing angles, 1 CP-violating phase, 1 Higgs mass, 1 Higgs vacuum expectation value, and 1 QCD vacuum angle, in total 19 parameters cannot be predicted from the theory (an extension with massive neutrinos need 7 more parameters [6]). Some physicists tried to find the relation among these free parameters, for example, the Koide formula proposed by Yoshio Koide [7, 8, 9, 10, 11] which shows an interesting relation among the masses of three charged leptons, although no one knows whether this kind of relation has any deeper implication or it is just a numerical coincidence. Another one is the well-known hierarchy problem which is related to the need for fine-tuning the Higgs mass to cancel out the large quantum corrections due to the virtual particles [12, 13].

Concerning the physical observations, the SM is not able to describe the phenomenon of neutrino oscillation [14, 15], because the neutrino mixings require neutrinos to have nonzero masses [16, 17], while in the SM, neutrinos are assumed to be massless particles. Another famous example is the mass-energy content of the universe. According to the standard Λ-CDM model of cosmology, the universe contains 5% of ordinary matter, 26% of dark matter, and 69% of dark energy [18]. Among them, only ordinary matter can be explained by the SM, and the remaining 95% of the universe is still a big puzzle in physics. There are no appropriate particle candidates for dark matter in the SM, and the SM prediction of the cosmological constant turns out to be 120 orders of magnitude too large compared to the observed dark energy [19, 20]. Recently, two new experimental results are claimed to be in disagreement with the predictions of the SM. One of them is the anomalous magnetic dipole moment of the muon or the so-called muon $g-2$. The discrepancy between the experimental result and the SM prediction has now increased from 3.7 to 4.2 standard deviations [21].

Inspired by this recently updated anomaly, especially the muon $g-2$, we investigate the physics beyond the SM related to the muon dipole moments, including both the magnetic

dipole moment (MDM) and electric dipole moment (EDM). The highly developed experimental techniques nowadays allow physicists to perform very precise measurements on the muon dipole moments, which can serve as the appropriate probes to the physics beyond the SM. One interesting feature is that a permanent EDM of an elementary particle is a direct observable which breaks the parity-inversion (P) and time-reversal (T) symmetries. Under the framework of quantum field theory, where CPT symmetry is respected (C is the charge conjugation symmetry), the existence of an EDM also implies the CP violation. There are several reasons why we should study the EDM of elementary particles. First of all, in the SM the only observed CP violation comes from the single complex phase in the Cabibbo-Kobayashi-Maskawa (CKM) quark mixing matrix [22], which explains the observed CP-breaking processes such as K-meson and B-meson decays. Such CP violation is in principle able to induce EDMs. However, due to the smallness and the symmetric property of the CP violation in the SM, the predicted values of the EDMs are highly suppressed and are beyond the scope of current and probably any foreseeable experiments in the future. For instance, the nonzero contribution to the lepton EDMs first appears at the 4-loop level in SM and is estimated to be around $10^{-38}\ e \cdot \mathrm{cm}$ [23].

Fortunately, physicists believe that there must be some new sources of CP violation. According to modern cosmology, the universe is initially in a symmetric state, with equal amounts of matter and antimatter. Under this condition, a CP violation is required to generate a finite amount of positive baryon numbers in the evolution of the universe, otherwise, baryons and antibaryons would proceed with pair annihilations and in the end, only radiations remain in the universe [24]. One problem of the SM is that the CP violation generated from the CKM matrix is too small and it cannot successfully reproduce the observed amount of the matter-antimatter asymmetry (baryogenesis) in the universe. Therefore, any discovery of new sources of CP violation is possibly an important key to solving this mystery. Of course, there is no guarantee that the source of CP violation in the particle EDM is identical or correlated to the one needed for the baryogenesis. Nevertheless, it would doubtlessly be a new milestone in particle physics and would definitely be a breakthrough in the history of physics. Furthermore, many new physics models predict relatively large EDMs. For example, to explain the deviation of muon $g-2$, a large class of supersymmetric models is proposed. These models contain many hypothetical new particles and couplings, whose corresponding parameters can be complex in general, and thus render new sources of CP violation. This leads to several

loop contributions to the muon EDM whose magnitudes may be large enough to be probed in the future experiments with the required precision [25, 26, 27, 28, 29, 30, 31, 32, 33, 34]. Other new physics models which also predict sizable particle EDMs include leptoquarks [35, 36, 37], two Higgs doublet models [38, 39, 40], vector-like leptons [41], etc. Once a particle EDM is detected in the experiment, it would certainly be an unambiguous sign of the physics beyond the SM and is therefore quite motivated in this sense.

In this thesis, we consider the possibility of probing the physics beyond the SM with a specific extension in the lepton sector by vector-like leptons. These hypothesized leptons are different from their partner in the SM, in the sense that the leptons in the SM are chiral, i.e. left-handed leptons and right-handed leptons act differently under the $SU(2)_L \times U(1)_Y$ transformations. Through the mixing among the muon and the vector-like leptons, the deviation of the measured value of the anomalous magnetic dipole moment of the muon from its SM prediction can be explained successfully. Besides the muon $g-2$, this lepton mixing has several interesting features. In this framework, the muon Yukawa coupling in the SM is combined with new parameters, including the Yukawa couplings and masses of the vector-like leptons, after the mass diagonalization. This means that the vector-like leptons also contribute to the muon mass at the same time and it is possible to find a correlation between the muon $g-2$ and the muon mass. The Higgs couplings are also affected by the lepton mixing in general. To be specific, the Higgs decay rates such as $\Gamma(h \to \mu^+\mu^-)$ are modified with respect to their SM prediction, and these effects from the vector-like leptons can be examined by the experiment like LHC.

Our goal in this study is to examine whether the considered vector-like lepton model has any parameter region that is consistent with the deviation of the muon $g-2$ between the experimental result and the theoretical prediction, and to scrutinize how large the muon EDM can be generated, taking into account the experimental constraints on the model.

The organization of the thesis is as follows. In chapter 2, we briefly describe the Standard Model of particle physics and the CP violation generated in the CKM matrix. In chapter 3, general properties of the electromagnetic dipole moments of the charged lepton are introduced. The anomalous magnetic dipole moment and electric dipole moment generated in the framework of SM is also discussed, with a brief mention of the experimental aspect and prospect of future experiments of EDM measurement. In chapter 4, we describe the general structure of the new physics contributions to the dipole moments through the

quantum corrections in the loops of the Feynman diagrams. In chapter 5, the analysis of the vector-like lepton model is performed. The results are shown to be consistent with the favored region of the muon $g-2$ anomaly and the constraints from the experiments on the Higgs decay $h \to \mu^+\mu^-$ [42] and the electron EDM [43], etc. Finally, in chapter 6, we summarize the content of this thesis.

Chapter 2

Standard model of particle physics

In this chapter, we briefly describe the content of the standard model (SM) of particle physics. Since the electric dipole moment is a physical quantity that breaks the CP symmetry, we also discuss the structure of the CP violation in the standard model.

2.1 Theoretical framework

As already mentioned in the introduction, the SM [1, 2, 3] is a theory that describes the strong, weak, and electromagnetic interactions. In the SM, the electromagnetic and weak interactions are unified into an electroweak interaction which is associated with the gauge symmetry of $SU(2)_L \times U(1)_Y$. Combining with the strong interaction associated with the $SU(3)_C$ symmetry, it forms the gauge group $SU(3)_C \times SU(2)_L \times U(1)_Y$ as the foundation of the SM. In the sector of matter particles, there are three sets of generation and each of them consists of one electrically charged lepton, one neutral lepton (neutrino), and two charged quarks. All particles in the SM are summarized in table 2.1, with their spins, representations of the gauge groups, electric charges, baryon numbers, and lepton numbers shown. The electric charge Q of a particle is defined by its weak isospin T_3 and hypercharge Y through the relation $Q = T_3 + Y$. The Lagrangian of the SM is

$$\mathcal{L}_{\text{SM}} = \mathcal{L}_{\text{gauge}} + \mathcal{L}_{\text{fermion}} + \mathcal{L}_{\text{Yukawa}} + \mathcal{L}_{\text{Higgs}}, \tag{2.1}$$

	spin	$SU(3)_C$	$SU(2)_L$	$U(1)_Y$	$Q = T^3 + Y$	B	L
$Q_L = \begin{pmatrix} u_L \\ d_L \end{pmatrix}$	$\frac{1}{2}$	**3**	**2**	$\frac{1}{6}$	$\begin{pmatrix} \frac{2}{3} \\ -\frac{1}{3} \end{pmatrix}$	$\frac{1}{3}$	0
u_R	$\frac{1}{2}$	**3**	**1**	$\frac{2}{3}$	$\frac{2}{3}$	$\frac{1}{3}$	0
d_R	$\frac{1}{2}$	**3**	**1**	$-\frac{1}{3}$	$-\frac{1}{3}$	$\frac{1}{3}$	0
$L_L = \begin{pmatrix} \nu_L \\ e_L \end{pmatrix}$	$\frac{1}{2}$	**1**	**2**	$-\frac{1}{2}$	$\begin{pmatrix} 0 \\ -1 \end{pmatrix}$	0	1
e_R	$\frac{1}{2}$	**1**	**1**	-1	-1	0	1
G^a_μ	1	**8**	**1**	0	0	0	0
$\begin{pmatrix} W^+_\mu \\ W^0_\mu \\ W^-_\mu \end{pmatrix}$	1	**1**	**3**	0	$\begin{pmatrix} +1 \\ 0 \\ -1 \end{pmatrix}$	0	0
B	1	**1**	**1**	0	0	0	0
$\Phi = \begin{pmatrix} \phi^+ \\ \phi^0 \end{pmatrix}$	0	**1**	**2**	$\frac{1}{2}$	$\begin{pmatrix} +1 \\ 0 \end{pmatrix}$	0	0

TABLE 2.1: The quantum numbers of the particles in the SM. For quarks and leptons, only one generation is shown for simplicity.

where

$$\mathcal{L}_{\text{gague}} = -\frac{1}{4}G^a_{\mu\nu}G^{a\mu\nu} - \frac{1}{4}W^a_{\mu\nu}W^{a\mu\nu} - \frac{1}{4}B_{\mu\nu}B^{\mu\nu}, \tag{2.2}$$

$$\mathcal{L}_{\text{fermion}} = \overline{q'}_L i\not{D} q'_L + \overline{u'}_R i\not{D} u'_R + \overline{d'}_R i\not{D} d'_R + \overline{\ell'}_L i\not{D} \ell'_L + \overline{e'}_R i\not{D} e'_R, \tag{2.3}$$

$$\mathcal{L}_{\text{Yukawa}} = -(y_u)_{ij}\overline{q'}_{Li}\widetilde{\Phi}u'_{Rj} - (y_d)_{ij}\overline{q'}_{Li}\Phi d'_{Rj} - (y_e)_{ij}\overline{\ell'}_{Li}\widetilde{\Phi}e'_{Rj} + \text{h.c.},\ \widetilde{\Phi} = i\sigma_2\Phi*, \tag{2.4}$$

$$\mathcal{L}_{\text{Higgs}} = (D_\mu\Phi)^\dagger(D^\mu\Phi) - V(\Phi^\dagger,\Phi),\ V(\Phi^\dagger,\Phi) = -\mu^2(\Phi^\dagger\Phi) + \lambda(\Phi^\dagger\Phi)^2. \tag{2.5}$$

In the above expression, the spinor with a prime means that it is in the flavor eigenbasis and the indices i, j indicate the generation of the particle. The covariant derivative is given by

$$D_\mu = \partial_\mu + ig_s t^a G^a_\mu + igT^a W^a_\mu + ig'Y B_\mu. \tag{2.6}$$

The strength tensors of the gauge fields are

$$G^a_{\mu\nu} = \partial_\mu G^a_\nu - \partial_\nu G^a_\mu + g_s f^{abc} G^b_\mu G^c_\nu, \tag{2.7}$$

$$W^a_{\mu\nu} = \partial_\mu W^a_\nu - \partial_\nu W^a_\mu + g\epsilon^{abc} W^b_\mu W^c_\nu, \tag{2.8}$$

$$B_{\mu\nu} = \partial_\mu B_\nu - \partial_\nu B_\mu, \tag{2.9}$$

where the generator of G^a_μ is $t^a = \lambda^a/2$ with λ^a the Gell-Mann matrices, and the generator of W^a_μ is $T^a = \sigma^a/2$ with σ^a the Pauli matrices. f^{abc} and ϵ^{abc} are the structure constants of the $SU(3)$ and $SU(2)$ groups.

In order to generate the masses of leptons and gauge bosons, the Higgs mechanism is introduced into the SM. An $SU(2)$ scalar doublet field is added with a non-zero vacuum expectation value and this breaks the original $SU(2)_L \times U(1)_Y$ symmetry spontaneously into $U(1)_{\mathrm{EM}}$. First of all, we can rewrite the Higgs potential as

$$V(\Phi^\dagger, \Phi) = \lambda \left(\Phi^\dagger \Phi - \frac{\mu^2}{2\lambda} \right)^2 - \frac{\mu^4}{4\lambda}. \tag{2.10}$$

Based on this, the vacuum expectation value of the Higgs field is

$$\langle \Phi \rangle = \begin{pmatrix} 0 \\ \frac{v}{\sqrt{2}} \end{pmatrix} = \begin{pmatrix} 0 \\ \sqrt{\frac{\mu^2}{2\lambda}} \end{pmatrix}, \ \lambda v^2 = \mu^2. \tag{2.11}$$

We can expand the Higgs field around the vacuum as

$$\Phi = \frac{1}{\sqrt{2}} \begin{pmatrix} \sqrt{2}\phi^+_W \\ v + h + i\phi_Z \end{pmatrix}. \tag{2.12}$$

Here the scalar fields $\phi^\pm_W$ and ϕ_Z are eaten by the $W^\pm$ and Z bosons in the process of spontaneous symmetry breaking, and h corresponds to the physical Higgs particle. Substituting this expansion into the Higgs potential, we obtain a Higgs mass term

$$\mathcal{L}_{m_h} = -\frac{1}{2}(2\mu^2)h^2. \tag{2.13}$$

This means that the Higgs mass is

$$m_h = \sqrt{2\mu^2} = \sqrt{2\lambda v^2}. \tag{2.14}$$

The masses of the gauge field can be obtained from the kinetic term of the Higgs field by setting the Higgs field at its vacuum expectation value. We then obtain the mass terms of the gauge bosons

$$\mathcal{L}_{m_V} = \frac{g^2 v^2}{4} W_\mu^+ W^{-\mu} + \frac{g^2 v^2}{8\cos\theta_W} Z_\mu Z^\mu. \tag{2.15}$$

In order to write the above result, we have applied the linear combination of W_μ^1 and W_μ^2

$$W_\mu^\pm = \frac{1}{2}(W_\mu^1 \pm W_\mu^2), \tag{2.16}$$

and the linear combination of W_μ^3 and B_μ

$$Z_\mu = \cos\theta_W W_\mu^3 - \sin\theta_W B_\mu, \tag{2.17}$$

$$A_\mu = \sin\theta_W W_\mu^3 + \cos\theta_W B_\mu, \tag{2.18}$$

with the weak mixing angle defined by

$$\cos\theta_W = \frac{g}{\sqrt{g^2 + g'^2}},\ \sin\theta_W = \frac{g'}{\sqrt{g^2 + g'^2}}. \tag{2.19}$$

Now, as we can see, after the spontaneous symmetry breaking, it correctly gives three massive gauge bosons with masses

$$m_W = \frac{1}{2} g v,\ m_Z = \frac{g v}{2\cos\theta_W} = \frac{m_W}{\cos\theta_W}, \tag{2.20}$$

and a massless photon

$$m_A = 0, \tag{2.21}$$

corresponds to the remaining $U(1)_{EM}$ symmetry.

Similarly, we can obtain the mass of the fermions by setting the Higgs field to its vacuum expectation value in the Yukawa interactions

$$\mathcal{L}_{m_f} = -\frac{(y_u)_{ij} v}{\sqrt{2}} \overline{u'_{Li}} u'_{Rj} - \frac{(y_d)_{ij} v}{\sqrt{2}} \overline{d'_{Li}} d'_{Rj} - \frac{(y_e)_{ij} v}{\sqrt{2}} \overline{e'_{Li}} e'_{Rj} + \text{h.c.}. \tag{2.22}$$

The matrix of Yukawa couplings are in general complex, and can be diagonalized by bi-unitary transformations with two unitary matrices U and W. The unitary matrices are

defined by

$$yy^\dagger = U(y^d)^2U^\dagger,\ y^\dagger y = W(y^d)^2W^\dagger\ \rightarrow\ y = Uy^dW^\dagger, \tag{2.23}$$

where y^ds are the diagonal matrices whose diagonal elements are the positive square roots of the eigenvalues of the combinations $yy^\dagger$ and $y^\dagger y$.

Correspondingly, we have the following relations between the fermion flavor and mass eigenbases after the diagonalization of the Yukawa matrices in eq. (2.22),

$$u'_L = U_u u_L,\ u'_R = W_u u_R, \tag{2.24}$$

$$d'_L = U_d d_L,\ d'_R = W_d d_R, \tag{2.25}$$

$$e'_L = U_e d_L,\ e'_R = W_e e_R, \tag{2.26}$$

$$\nu'_L = U_e \nu L. \tag{2.27}$$

The mass matrices of the fermions are then defined as the product of the diagonalized Yukawa matrices and the vacuum expectation value of the Higgs field

$$m_i = \frac{y_i^d v}{\sqrt{2}},\ i = u, d, e. \tag{2.28}$$

Most of the terms in the Lagrangian are not affected by the unitary transformation of the fermion fields, except the interaction that couples the quarks to the W bosons (the charged current)

$$\mathcal{L}_{CC} = -\frac{g}{\sqrt{2}}\overline{u'_{Li}}\gamma^\mu d'_{Li}W^+_\mu + \text{h.c.} = -\frac{g}{\sqrt{2}}\overline{u_{Li}}\gamma^\mu (U_u^\dagger U_d)_{ij} d_{Lj}W^+_\mu + \text{h.c.}. \tag{2.29}$$

Therefore, we see that the charged current connects the up-type quarks with a unitary rotation of the three down-type quarks, with the rotation given by the unitary matrix

$$V = U_u^\dagger U_d = \begin{pmatrix} V_{ud} & V_{us} & V_{ub} \\ V_{cd} & V_{cs} & V_{cb} \\ V_{td} & V_{ts} & V_{tb} \end{pmatrix}. \tag{2.30}$$

This unitary matrix is the well-known Cabibbo-Kobayashi-Maskawa (CKM) mixing matrix [22, 44].

Under the CP transformation the interaction with the W bosons changes in the following way

$$-\frac{g}{\sqrt{2}}\overline{u_L}\gamma^\mu V d_L W_\mu^+ - \frac{g}{\sqrt{2}}\overline{d_L}\gamma^\mu V^\dagger u_L W_\mu^- \tag{2.31}$$

$$\xrightarrow{CP} -\frac{g}{\sqrt{2}}\overline{d_L}\gamma^\mu V^T u_L W_\mu^- - \frac{g}{\sqrt{2}}\overline{u_L}\gamma^\mu V^* d_L W_\mu^+. \tag{2.32}$$

According to the result of the transformation, the interaction with the W boson does not respect the CP symmetry when we have the following condition

$$V \neq V^*, \tag{2.33}$$

which means V must be complex to establish the CP violation. Let us now turn to consider the number of parameters in V, assuming N generations of quarks. In general, an $N \times N$ unitary matrix contains N^2 parameters. Among these parameters, $N(N-1)/2$ are related to the rotation or mixing of the generations, and the remaining ones are related to the phases. Since we have in total $2N$ up-type and down-type quarks, it is possible to absorb $2N-1$ phases by the field redefinition of the quark fields. In the end, the number of physical phases of V is

$$N^2 - \frac{N(N-1)}{2} - (2N-1) = \frac{(N-1)(N-2)}{2}. \tag{2.34}$$

From this result, we understand that only when the number of generations is no smaller than 3 do we have a complex phase in V for the CP violation.

2.2 CP violation in the SM

The CP symmetry is a combination of the charge conjugation and parity transformations. In the theoretical framework of the SM, there are two sources of the CP violation. One is the complex phase in the CKM matrix, the other one is called the QCD θ term which can contribute to the electric dipole moment of the neutron. Basically, the θ parameter is a free parameter in the range of 0 to 2π. According to the experimental result on the neutron EDM, the θ parameter is strongly constrained to a very tiny number and is consistent with zero. Why its value is so small is a puzzle called the strong CP problem, which we will not discuss in this thesis and assume that it is solved by some physics

mechanism beyond the SM, such as the Peccei-Quinn mechnism [45, 46]. In the following discussion, we will focus on the CP violation in the CKM matrix.

As we have already seen in the previous section, the CKM matrix must be complex in order to violate the CP symmetry. Let us first see why the existence of complex numbers implies CP violation by considering the CPT invariance in the quantum field theory. Any terms we write down in the Lagrangian must preserve the CPT symmetry, regardless of whether they are real or complex. We also know that the property of the time-reversal transformation T is to send the imaginary number i to $-i$. Therefore, if the real part of a term is invariant under the time reversal, then its imaginary part must break the time-reversal symmetry. Then, by the CPT invariance, we can conclude that the imaginary part of that term must also violate the CP symmetry.

Following the discussion made in the previous section, and taking into account the fact that we have three generations of quarks, the CKM matrix thus has four degrees of freedom, containing three rotation angles and one complex phase. We can denote the rotation angle by θ_{ij} for the rotation between the i and j quark flavors, and the complex phase by δ. Then, the most general CKM matrix is given by

$$V = \begin{pmatrix} c_{12}c_{13} & s_{12}c_{13} & s_{13}e^{-i\delta} \\ -s_{12}c_{23} - c_{12}s_{23}s_{13}e^{i\delta} & c_{12}c_{23} - s_{12}s_{23}s_{13}e^{i\delta} & s_{23}c_{13} \\ s_{12}s_{23} - c_{12}c_{23}s_{13}e^{i\delta} & -c_{12}s_{23} - s_{12}c_{23}s_{13}e^{i\delta} & c_{23}c_{13} \end{pmatrix}, \tag{2.35}$$

where $c_{ij} = \cos\theta_{ij}$ and $s_{ij} = \sin\theta_{ij}$, respectively. The numerical values for these parameters are [47]

$$\begin{aligned} \sin\theta_{12} &= 0.22500 \pm 0.00067, \\ \sin\theta_{13} &= 0.00369 \pm 0.00011, \\ \sin\theta_{23} &= 0.04182^{+0.00085}_{-0.00074}, \\ \delta &= 1.144 \pm 0.027. \end{aligned} \tag{2.36}$$

We know that the CKM matrix is unitary by construction. Therefore, the precise measurement of the parameters of the CKM matrix also serves as a test for the assumption of three-generation in the SM, because if there were a fourth generation, the three-generation subsector in the CKM matrix cannot be unitary. If we substitute the values listed above

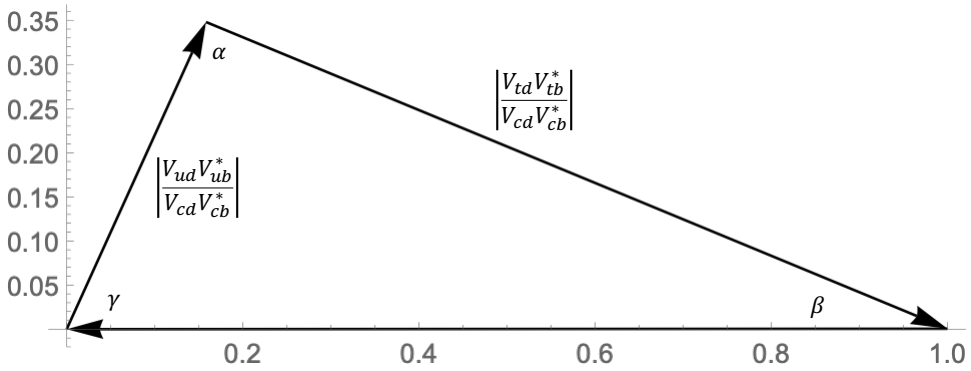

FIGURE 2.1: The unitarity triangle corresponding to eq. (2.38).

for the mixing angles and the phase in the CKM matrix, we can see that the CKM matrix is in good agreement with being a unitary matrix. Physicists had come up with a clever way to visualize the unitarity of the CKM matrix by means of a unitarity triangle. The unitarity of a matrix means that its rows are orthonormal to each other and so are its columns, which indicates that we have

$$\sum_{i=u,c,t} V_{ij}V_{ik}^* = \delta_{jk}. \tag{2.37}$$

From this we have, for example, $V_{ud}V_{ub}^* + V_{cd}V_{cb}^* + V_{td}V_{tb}^* = 0$. We can interpret this equation geometrically as a triangle formed by three complex vectors . According to this equation, we can further divide by by $V_{cd}V_{cb}^*$ and normalize its length to 1

$$\frac{V_{ud}V_{ub}^*}{V_{cd}V_{cb}^*} + \frac{V_{td}V_{tb}^*}{V_{cd}V_{cb}^*} + 1 = 0. \tag{2.38}$$

In figure 2.1, we plot the vector sum on the complex plane directly by using the matrix elements obtained in eq. (2.35) with the parameter values listed in eq. (2.36). It is clear from the figure that the three vectors indeed form a perfect triangle. Therefore, the three-generation quark mixing is correctly described by the CKM matrix. Since it is in principle possible to parameterize the CKM matrix in several different ways, it would be convenient if we can measure the CP violation that is independent of the parametrization we use. It turns out such an invariant quantity exists, which is called the Jarlskog invariant J.

Let us recall the diagonalization of the Yukawa coupling in eq. (2.23), we have

$$y_{u,d} = U_{u,d}y_{u,d}^d W_{u,d}^\dagger. \tag{2.39}$$

Without loss of generality, we can perform a rotation to the right-handed field by $u'_R = W_u U_u^\dagger u_R$ and $d'_R = W_d U_d^\dagger d_R$. This makes the Yukawa matrices become hermitian

$$y_{u,d} = U_{u,d} y^d_{u,d} U^\dagger_{u,d}. \tag{2.40}$$

If they can be diagonalized simultaneously, then $U_u = U_d$. In this case, V is a unit matrix and no CP violation at all. What this tells us is that CP violation is encoded in the commutator of the two Yukawa matrices

$$-iC \equiv [y_u, y_d] = \left[U_u y^d_u U^\dagger_u, U_d y^d_d U^\dagger_d\right] = U_u \left[y^d_u, V_d y^d_d V^\dagger_d\right] U^\dagger_u. \tag{2.41}$$

From the last expression, we know that the matrix C is Hermitian and traceless. We can compute its determinant as an invariant quantity, which is given by

$$\det C = -\frac{16}{v^6}(m_t - m_c)(m_t - m_u)(m_c - m_u)(m_b - m_s)(m_b - m_d)(m_s - m_d)J, \tag{2.42}$$

where the Jarlskog invariant shows up and is given by the following different combinations

$$\begin{aligned} J &= \mathrm{Im}(V_{ud}V_{cs}V^*_{us}V^*_{cd}) = \mathrm{Im}(V_{cd}V_{ts}V^*_{cs}V^*_{td}) = \mathrm{Im}(V_{td}V_{us}V^*_{ts}V^*_{ud}) \\ &= -\mathrm{Im}(V_{ud}V_{cb}V^*_{ub}V^*_{cd}) = -\mathrm{Im}(V_{cd}V_{tb}V^*_{cb}V^*_{td}) = \mathrm{Im}(V_{td}V_{ub}V^*_{tb}V^*_{ud}), \end{aligned} \tag{2.43}$$

which can be written in a more compact form

$$J\sum_{m,n}\epsilon_{ikm}\epsilon_{j\ell n} = \mathrm{Im}(V_{ij}V_{k\ell}V^*_{i\ell}V^*_{jk}), \tag{2.44}$$

where $i,k,m = u,c,t$ and $j,l,n = d,s,b$, respectively. One interesting feature of the Jarlskog invariant is that its value is twice the area of the unitary triangle in figure 2.1. In terms of the standard parametrization eq. (2.35), we have [47]

$$J = s_{12}s_{13}s_{23}c_{12}c^2_{13}c_{23}\sin\delta = (3.08^{+0.15}_{-0.13}) \times 10^{-5}. \tag{2.45}$$

From this expression, we see that if V is real, then J vanishes and so does the determinant of the Yukawa commutator C. To preserve the CP violation, two degenerate up-type or down-type quarks are not allowed, too, as implied by eq. (2.42).

Chapter 3

Lepton dipole moments

In this chapter, we discuss the general properties of the magnetic dipole moment (MDM) and electric dipole moment (EDM) of leptons. First, we look at the behavior of these dipole moments under discrete symmetry transformations such as parity inversion and time reversal. Then, we describe the general structure of the dipole moments in the framework of quantum field theory.

3.1 General properties

In nonrelativistic electrodynamics, the interaction between an electromagnetic field and a particle with a spin $\vec{S}$ is described by the Hamiltonian

$$H = -\mu \frac{\vec{S}}{|\vec{S}|} \cdot \vec{B} - d \frac{\vec{S}}{|\vec{S}|} \cdot \vec{E}, \tag{3.1}$$

where μ is the magnetic dipole moment (MDM) and d is the electric dipole moment (EDM). From table 3.1, we found that the interaction between the MDM and the magnetic field conserves the parity P and time-reversal T transformations, while the interaction

	$\vec{B}$	$\vec{E}$	$\vec{S}$
P	$+$	$-$	$+$
T	$-$	$+$	$-$

TABLE 3.1: Properties of the electromagnetic field and the spin under the parity P and time reversal T transformations.

between the EDM and the electric field violates both symmetries. Assuming the CPT invariance of the quantum field theory, we conclude that the EDM interaction also violates the CP symmetry. The interaction in eq. (3.1) are induced by the following relativistic effective operators

$$-\mu\frac{\vec{S}}{|\vec{S}|}\cdot\vec{B} \;\leftrightarrow\; -eQ_\ell\overline{\psi}\gamma^\mu\psi A_\mu - \frac{eQ_\ell a_\ell}{4m_\ell}\overline{\psi}\sigma^{\mu\nu}\psi F_{\mu\nu}, \tag{3.2}$$

$$-d\frac{\vec{S}}{|\vec{S}|}\cdot\vec{E} \;\leftrightarrow\; -i\frac{d_\ell}{2}\overline{\psi}\sigma^{\mu\nu}\gamma_5\psi F_{\mu\nu}. \tag{3.3}$$

We note that the magnetic dipole moment consists of two operators, where the first one corresponds to the part with $g = 2$ predicted by the Dirac equation, and the second one corresponds to the part of the so-called anomalous magnetic dipole moment with $g - 2$.

In the language of quantum field theory, the anomalous magnetic moment and electric dipole moment of a lepton are defined through the vertex function. The dipole moments are induced by quantum corrections to the interaction of the leptons with a static electromagnetic background field. These corrections are represented by the Feynman diagrams with loops. Their structure and calculation are the topics of the next chapter and more details can be found in appendix A. The electromagnetic vertex function is given by

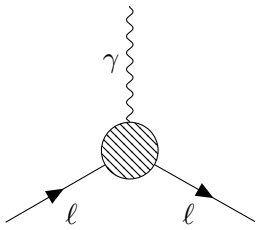

$$= -ieQ_\ell\overline{u}(p')\Gamma^\mu(p',p)u(p), \tag{3.4}$$

where the blob in the diagram represents the quantum corrections to the interaction between the charged lepton ℓ and the photon. The vertex function can be decomposed into several Lorentz-invariant form factors as

$$\Gamma^\mu = F_1(q^2)\gamma^\mu + F_2(q^2)\frac{i\sigma^{\mu\nu}}{2m_\ell}q_\nu - F_3(q^2)\sigma^{\mu\nu}q_\nu\gamma_5 + F_4(q^2)\frac{q^2\gamma^\mu - q^\mu\not{q}}{m_\ell^2}\gamma_5, \tag{3.5}$$

where $q^\mu = p'^\mu - p^\mu$ is the incoming photon four-momentum. The mass m_ℓ is the physical mass of the charged lepton ℓ. The charged leptons in the external legs are on shell, $p'^2 = p^2 = m_\ell^2$. The factor e in eq. (3.4) is determined by the renormalization condition

$$F_1(0) = 1, \tag{3.6}$$

and represents the traditional definition of the charge of electron. Q_ℓ is the value of electric charge in the unit of e and for charged leptons it is simply $Q_\ell = -1$.

The anomalous magnetic dipole moment is defined by the form factor F_2 at the limit of zero momentum transfer

$$a_\ell = F_2(0) = \frac{g_\ell - 2}{2}, \tag{3.7}$$

and the electric dipole moment corresponds to the form factor F_3 at the limit of zero momentum transfer

$$d_\ell = eQ_\ell F_3(0). \tag{3.8}$$

The form factor F_4 at the limit of zero momentum transfer is called the anapole moment. In the vertex function considered here, its contribution is zero since the photon is on-shell, which means $q^2 = 0$, and also q^μ is contracted with a photon polarization vector ϵ_μ such that $\epsilon_\mu q^\mu = 0$.

3.2 Electromagnetic dipole moments in the SM

3.2.1 Magnetic dipole moment

Last year, the Muon $g-2$ collaboration at the Fermilab published their latest precise measurement on the muon $g-2$ [21]. The new result shows a 4.2σ deviation from the theoretical prediction of the SM, which has stimulated many theoretical works related to physics beyond the SM. In this section, we review the current state-of-the-art predictions and briefly summarize the characteristics of each process from the theoretical point of view. We will also discuss the contribution of hadron vacuum polarization (HVP) from the Standard Model predictions, which is an issue from the viewpoint of theoretical refinement.

According to the White Paper of muon $g-2$ [48], the theoretical prediction currently has a value of

$$a_\mu^{\mathrm{SM}} = 116591810(43) \times 10^{-11}. \tag{3.9}$$

The value of muon $g-2$ calculated in the framework of SM can be separated into several dominated parts

$$a_\mu^{\mathrm{SM}} = a_\mu^{\mathrm{QED}} + a_\mu^{\mathrm{EW}} + a_\mu^{\mathrm{HVP}} + a_\mu^{\mathrm{HLbL}}, \tag{3.10}$$

including the contributions from QED, electroweak, and hadronic processes. Their values are also given in the White Paper [48],

$$a_\mu^{\mathrm{QED}} = 116584718.931(104) \times 10^{-11}, \tag{3.11}$$

$$a_\mu^{\mathrm{EW}} = 153.6(1.0) \times 10^{-11}, \tag{3.12}$$

$$a_\mu^{\mathrm{HVP}} = 6845(40) \times 10^{-11}, \tag{3.13}$$

$$a_\mu^{\mathrm{HLbL}} = 92(18) \times 10^{-11}. \tag{3.14}$$

The QED contribution can be divided into components with different dependence on the lepton mass, which appears as ratios since $g-2$ is a dimensionless quantity,

$$a_\mu^{\mathrm{QED}} = A_1 + A_2\left(\frac{m_\mu}{m_e}\right) + A_2\left(\frac{m_\mu}{m_\tau}\right) + A_3\left(\frac{m_\mu}{m_e}, \frac{m_\mu}{m_\tau}\right), \tag{3.15}$$

where A_1 is the term independent of the mass ratios and therefore universal for all leptons. Thanks to the small QED coupling constant, which is the fine structure $\alpha \simeq 1/137$, we are able to compute the terms in eq. (3.15) by perturbative expansions

$$A_i = \left(\frac{\alpha}{2\pi}\right) A_i^{(2)} + \left(\frac{\alpha}{2\pi}\right)^2 A_i^{(4)} + \left(\frac{\alpha}{2\pi}\right)^3 A_i^{(6)} + \cdots, \ i = 1, 2, 3. \tag{3.16}$$

The current theoretical prediction of the QED contribution to the muon $g-2$ is shown in eq. (3.11). By comparing the value with the total theoretical prediction in eq. (3.9), we can see that the QED contribution is the largest one, as it accounts for around 99.994% of the total prediction after summing all different contributions. Yet it has the smallest uncertainty among different components. This is because physicists put a lot of effort into the loop calculations of the QED contribution, some of them are shown in figure 3.1, and it has now been pushed to the amazing five-loop level [49].

The hadronic contribution includes the diagrams of hadronic vacuum polarization (HVP) and the hadronic light-by-light scattering (HLbL). The HVP contribution originates from the quantum corrections in the photon propagator, and the lowest-order HVP diagram

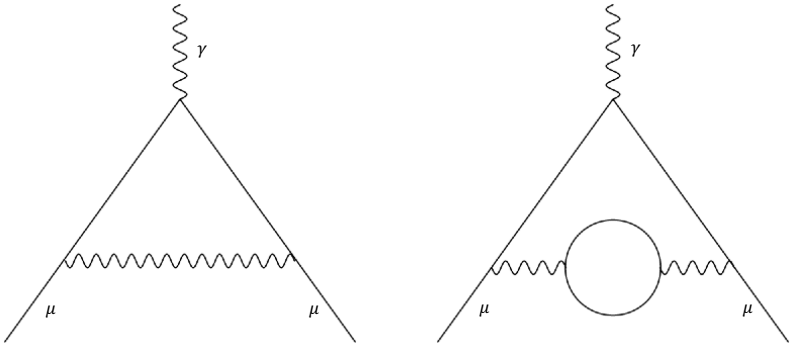

FIGURE 3.1: Examples of QED loop diagrams at one-loop and two-loop levels.

is shown in figure 3.2. In contrast to the QED contributions, the HVP ones cannot be computed solely from the theory because most of the hadronic contributions come from the nonperturbative QCD regime at low energy. Nevertheless, it is still possible to calculate the diagrams by applying the analyticity and unitarity in the HVP correlator.

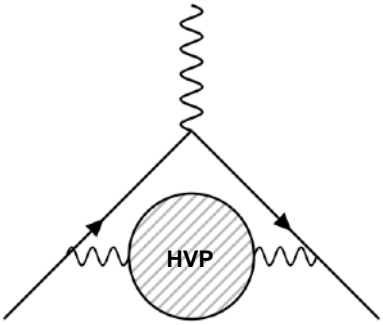

FIGURE 3.2: The lowest-order contribution from HVP. The blob inside the photon propagator represents the hadronic quantum fluctuations.

The leading-order contribution from HVP is computed via the dispersion integral [50, 51]

$$a_\mu^{\mathrm{HVP,LO}} = \frac{\alpha^2}{3\pi^2}\int_{m_\pi^2}^{\infty}\frac{K(s)}{s}R(s)ds, \tag{3.17}$$

where $K(s)$ is called the kernel function

$$K(s) = \int_0^1 dx \frac{x^2(1-x)}{x^2+(1-x)s/m^2}, \tag{3.18}$$

and R(s) is called the R-ratio

$$R(s) = \frac{\sigma^0(e^+e^- \to \text{hadrons})}{4\pi\alpha^2/3s}, \tag{3.19}$$

$\sqrt{s}$ is the center-of-mass energy of e^+e^-. The R-ratio is a physical observable and is measured in the experiment. On the other hand, from the expression of the kernel function, eq. (3.18), we can see that the contributions from higher energy are suppressed due to the factor s/m^2 in the denominator, and therefore most of the contributions come from the low-energy regime. One disadvantage of the data-driven method is that we need to take into account the experimental uncertainties for the theoretical predictions. The actual value of the leading-order HVP contribution given in the White Paper is [48]

$$a_\mu^{\mathrm{HVP,LO}} = 6931(28)_{\mathrm{stat}}(28)_{\mathrm{sys}}(7)_{\mathrm{others}} \times 10^{-11}, \tag{3.20}$$

where the subscripts stat and sys correspond to the statistical and systematic uncertainties from the experiments, respectively. After summing up contributions to the next-to-next-to-leading order (NNLO), the final prediction is shown in eq. (3.13). As you can see, the HVP uncertainty is the largest among all contributions due to the large uncertainties in the experimental data. The HVP contribution has been a challenge in terms of refining theoretical calculations due to its large errors, and there is one more issue that should be mentioned. Currently, a discrepancy exists between the results in the White Paper and the lattice QCD calculations performed by the Budapest-Marseille-Wuppertal (BMW) group [52]. Lattice QCD, first formulated by Ken Wilson [53], is a first-principle approach for tackling the nonperturbative strong interactions, unlike the data-driven method which relies on the data inputs such as the R-ratio. According to the lattice QCD simulation, the leading-order HVP contribution is

$$a_{\mu,\mathrm{BMW}}^{\mathrm{HVP,LO}} = 7075(55) \times 10^{-11}. \tag{3.21}$$

This is 2.1σ larger than the recommended data-driven result eq. (3.13). Naturally, the two values should be compatible with each other because they correspond to the same physical processes in the SM, even though the calculation methods are different. However, the current situation is that there is a significant difference even between the different theoretical approaches, and the cause of this difference is not yet clear. More intriguingly, recently other lattice QCD groups published their result on the HVP calculation [54, 55] and it seems to agree with the result obtained by the BMW group. If the result is further confirmed, it is then necessary to first investigate what is the main reason that causes the discrepancy between the data-driven method and the lattice QCD simulation.

Let us also mention that in the meantime, the experimental side also proposed a new approach, the MUonE experiment [56, 57], as a crosscheck of the leading HVP contribution to the muon $g-2$ obtained from the R-ratio method, by measuring the hadronic contribution to the effective electromagnetic coupling α in the muon-electron scattering[1].

The hadronic light-by-light contributions (HLbL, figure 3.3), by the same argument, can be obtained by applying the data-driven dispersive approach or doing a first-principle lattice QCD simulation. The difference from the HVP contributions is that the data-driven and lattice QCD predictions are in good agreement in the case of HLbL, and the results are combined to give the value listed in eq. (3.14).

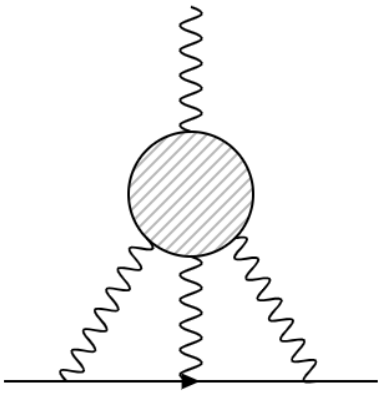

FIGURE 3.3: The Feynman diagram representing the hadronic light-by-light contributions. The blob in the plot corresponds to the interaction of photons with hadrons.

The electroweak contributions consist of those diagrams containing the electroweak bosons, the Z, W, and Higgs bosons. Because of the heavy masses of these gauge bosons, the electroweak contributions are highly suppressed compared to the QED contributions. The typical one-loop diagrams of the electroweak contribution are shown in figure 3.4, which we will calculate in the next chapter after discussing the general structure of one-loop contributions of the dipole moments. Depending on the choice of gauge fixing, for example, the Feynman gauge, diagrams with unphysical Goldstone bosons may also need to be taken into account. The value listed in eq. (3.12) is obtained by combining the one-loop and two-loop calculations, with an estimation on the three-loop leading contributions [63, 64].

[1] As a brief digression, we also note that the MUonE experiment has the capability for probing the $U(1)_{L_\mu - L_\tau}$ boson [58], which is one hypothetical particle proposed for solving the muon $g-2$ deviation between the experimental result and the theoretical prediction [59, 60, 61, 62].

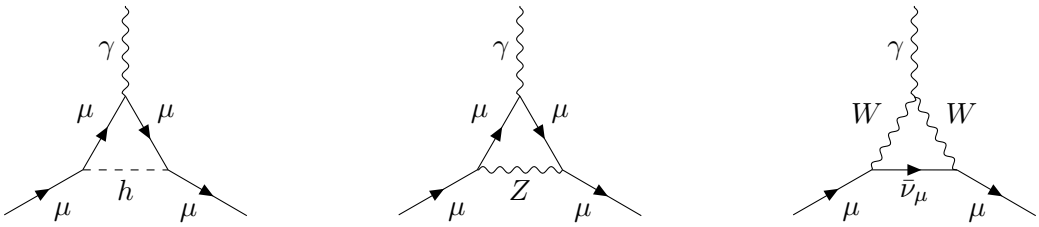

(a) Higgs boson (b) Z boson (c) W boson

FIGURE 3.4: One-loop diagrams of the electroweak contribution to muon $g-2$.

3.2.2 Electric dipole moment

In this section, we review the EDM of charged leptons in the SM. In the SM, the CP violation originates from the physical complex phase of the CKM matrix, so the contributions to the charged lepton EDM necessarily contain quark loops, and the flavor mixings must be sufficient to satisfy the Jarlskog invariant [65], which is given by the product of four CKM matrix elements [47]

$$J = \mathrm{Im}[V_{td}V_{us}V_{ts}^{*}V_{ud}^{*}] = (3.08^{+0.15}_{-0.13}) \times 10^{-5}. \tag{3.22}$$

From the expression of the Jarlskog invariant, we see that the quark loops must include four W boson-quark vertices. Considering the requirement of quark loops, the simplest diagrams are the two-loop contributions with a quark loop connected to a charged lepton by the W boson propagators. In such diagrams, since the W bosons are attached to the line of a charged lepton, there are only two flavor-changing vertices containing the complex phases in the quark loop. As a consequence, the Jarlskog invariant is not fulfilled at the two-loop level, and it does not contribute to the EDM because the signs of two complex phases are always opposite and cancel out each other, that is, one vertex with V_{ij} and the other with V_{ij}^{*}.

Taking into account the requirement of the Jarlskog invariant, the first reasonable contribution appears at the three-loop level [66]. However, after some detailed analyses of the three-loop diagrams, physicists found that the contributions from the three-loop level also vanish due to the antisymmetric characteristic of the Jarlskog invariant under the flavor exchange [67, 68, 69]. Therefore, we anticipate that the first nonvanishing contribution keeping away from the cancellation of the CP phase appears at the four-loop level, an

example of such a diagram is shown in figure 3.5. It seems that there is yet no complete analysis of the four-loop calculation. Nevertheless, it is possible to make a rough estimation. For example, in [23] the electron EDM is claimed to be

$$d_e^{\mathrm{SM}} \leq 10^{-38}\ e \cdot \mathrm{cm}. \tag{3.23}$$

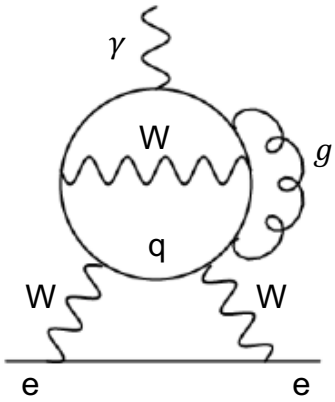

FIGURE 3.5: An example of the four-loop contribution to the electron EDM. A gluon is attached to the internal quark propagators to prevent the cancellation due to the antisymmetric character of the Jarlskog invariant.

From the above discussion, it can be seen that the lepton EDMs in the framework of SM induced by the CP-violating phase in the CKM matrix are vanishing small and are out of the capability of current experimental techniques. The measurement with the best sensitivity was performed by the ACME collaboration, which set an upper bound on the electron EDM as $< 1.1 \times 10^{-29}\ e \cdot \mathrm{cm}$ [43], about 10 orders of magnitude larger than the prediction of electron EDM in the SM. This fact indicates that when we consider physics beyond the SM, the lepton EDMs are highly sensitive to the new CP-violating sources because the background events of the SM are very small. This is one of the main motivations that physicists should pursue the experimental searches for the lepton EDMs because there is a huge space for the discovery of new physics before the experiments become sensitive to the SM EDMs in the far future.

As a brief digress, if we take the possible strong CP angle θ into account, it is pointed out in [70] that the contribution from θ to the electron EDM can be in a similar order to those from the CKM phase, considering the latest constraint on the neutron EDM set by the experiment at Paul Scherrer Institute [71] giving $|\theta| < \mathcal{O}(10^{-10})$.

3.3 Magnetic and electric dipole moments in new physics

New physics effects on the lepton dipole moments can be described by the following effective operators

$$\mathcal{L}_{\text{eff}} = -\frac{1}{2}\frac{m_\ell\, c_{M,\ell}}{\Lambda^2}\,\bar{\ell}\sigma^{\mu\nu}\ell F_{\mu\nu} - \frac{i}{2}\frac{m_\ell\, c_{E,\ell}}{\Lambda^2}\,\bar{\ell}\sigma^{\mu\nu}\gamma_5\ell F_{\mu\nu}, \tag{3.24}$$

where m_ℓ is the mass of the charged lepton ℓ, Λ is a mass scale at which these operators are generated, $F_{\mu\nu}$ is the electromagnetic field strength tensor, and $c_{M,\ell}$ and $c_{E,\ell}$ are model-dependent coefficients. We put the lepton mass in the coefficients of these operators explicitly as these interactions flip chirality. However, we note that there are many models (including the one discussed in this thesis) where the chirality flip is not associated with the lepton mass term but with other, more sizable terms (denoted collectively by M). In such cases, the resultant contributions to the dipole moments are enhanced by a factor of $\sim M/m_\ell$.

The first and second terms in eq. (3.24) for $\ell = \mu$ correspond to muon $g-2$ and EDM, respectively. Comparing with the expression in eq. (3.2), we see that the muon anomalous magnetic dipole moment is given by

$$\Delta a_\mu = -\frac{2m_\mu^2}{e\Lambda^2}c_{M,\mu}, \tag{3.25}$$

while the muon EDM is expressed as

$$d_\mu = \frac{m_\mu}{\Lambda^2}c_{E,\mu}. \tag{3.26}$$

From these equations, we find a relation between these two quantities:

$$d_\mu = -\frac{e}{2m_\mu} \times \frac{c_{E,\mu}}{c_{M,\mu}} \times \Delta a_\mu \tag{3.27}$$

$$\simeq -2.3 \times 10^{-22}\ e\cdot\text{cm} \times \left(\frac{c_{E,\mu}}{c_{M,\mu}}\right) \times \left(\frac{\Delta a_\mu}{2.51\times 10^{-9}}\right). \tag{3.28}$$

This relation indicates that a new-physics effect that explains the observed muon $g-2$ discrepancy can induce a value of the muon EDM within the reach of future muon EDM experiments, e.g. $|d_\mu| \lesssim 6\times 10^{-23}\ e\cdot\text{cm}$ [72].

On the other hand, the electron $g-2$ and EDM can be expressed in a similar manner as in eq. (3.25) and eq. (3.26), respectively. We can thus relate the anomalous magnetic dipole moments of electron and muon as

$$\Delta a_e = \frac{m_e^2}{m_\mu^2} \times \frac{c_{M,e}}{c_{M,\mu}} \times \Delta a_\mu \tag{3.29}$$

$$\simeq 6 \times 10^{-14} \times \left(\frac{c_{M,e}}{c_{M,\mu}}\right) \times \left(\frac{\Delta a_\mu}{2.51 \times 10^{-9}}\right). \tag{3.30}$$

The size of the prefactor is smaller than the uncertainty in the measured value of the electron $g-2$, $a_e = 115965218073(28) \times 10^{-14}$ [73], by a factor of around 5. This explains why many models for the muon $g-2$ discrepancy can evade the constraint from the electron $g-2$ measurement.

Similarly, the EDMs of electron and muon are related to each other as

$$d_\mu = \frac{m_\mu}{m_e} \times \frac{c_{E,\mu}}{c_{E,e}} \times d_e \tag{3.31}$$

$$\simeq 2.3 \times 10^{-27}\ e \cdot \mathrm{cm} \times \left(\frac{c_{E,\mu}}{c_{E,e}}\right) \times \left(\frac{d_e}{1.1 \times 10^{-29}\ e \cdot \mathrm{cm}}\right). \tag{3.32}$$

The current limit on the electron EDM is $|d_e| < 1.1 \times 10^{-29}\ e \cdot \mathrm{cm}$ [43]. By using this limit and the relation eq. (3.32), we can obtain an upper limit on the muon EDM $|d_\mu|$, which is smaller than the sensitivities of the future muon EDM experiments by orders of magnitude if $c_{E,\mu} \simeq c_{E,e}$.

The implications of the eq. (3.27) and eq. (3.31) for the expected value of muon EDM, which apparently contradict with each other, are based on the assumption that the ratio of the relevant coefficients, $c_{M,\ell}$ and $c_{E,\ell}$, is $\mathcal{O}(1)$. This corresponds to the following assumptions on the underlying physics:

(i) Sizable CP violation: if CP phases in the new-physics sector are highly suppressed, then we have $c_{E,\ell} \ll c_{M,\ell}$.

(ii) Lepton-flavor universality: if the BSM particles interact with electron and muon differently, we do not expect $c_{M/E,e} \simeq c_{M/E,\mu}$.

(iii) Chirality flip by the lepton mass: if the dipole moments in eq. (3.24) are generated in processes where the chirality flip is caused by other sources than the corresponding lepton mass terms, we do not have the lepton-mass factors in eq. (3.29) and eq. (3.31).

As it turns out, these assumptions do not necessarily hold in the models that can explain the muon $g-2$ discrepancy. To see the deviation from (or consistency with) the above arguments, we consider a concrete example of the vector-like lepton model as an extension to the SM in the following chapters and discuss the implications for the muon EDM.

3.4 Muon EDM measurement in a storage ring

3.4.1 Basic concept

In order to detect an EDM in the experiment, it is necessary to measure the interaction of the EDM with an electric field in an environment as clean as possible, since its signal is expected to be very small due to the smallness of particle EDM. Also, there is a technical challenge to handle charged particles in an electric field for a sufficient period, because they will be accelerated by the electric field, becoming faster and faster and hard to control. This is the reason why the muon EDM measurements are performed by means of the storage-ring experiment, which can avoid difficulty. With an external magnetic field applied to the muons, they move circularly in the storage. In the rest frame of the particle, it feels a motional electric field transformed from the magnetic field relativistically, which can be of the same order or much greater than the external electric field applied in the laboratory.

To understand how an EDM is measured in a storage ring, we have to first learn how the muon $g-2$ experiment works. In such kind of experiment, the spin-polarized beam of muons are generated from the charged pion decay

$$\pi^+ \to \mu^+ + \nu_\mu, \tag{3.33}$$

$$\pi^- \to \mu^- + \overline{\nu}_\mu. \tag{3.34}$$

A schematic plot of the positively charged pion decay is shown in figure 3.6. In the following discussion, we fix the positive charge and simply call μ^+ a muon, since this case is the one used in the real muon $g-2$ experiment [21]. Because pion is a spin-0 particle, muons are emitted isotropically in the rest frame of the pion. Also, the helicity of the decay particles is fixed by the property of weak interaction, that is, neutrinos must be left-handed. By the conservation of angular momentum, we know that the muon must also be left-handed. When boosted to the laboratory frame, the highest-energy and lowest-energy muon are produced from pion decays in the forward and backward directions, which are highly polarized. We can obtain the spin-polarized muon beams by selecting the energy of muons appropriately.

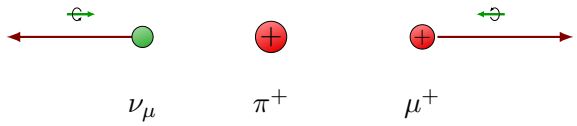

FIGURE 3.6: A schematic plot showing the charged pion decay in the rest frame.

For a muon moving in a magnetic field, the spin precession is induced by the interaction between the magnetic dipole moment of muon and the magnetic field, which is given by [74]

$$\vec{\omega}_s = -g\frac{e\vec{B}}{2m} - \frac{e\vec{B}}{\gamma m}(1-\gamma), \tag{3.35}$$

where $\gamma = (1-\beta^2)^{-1/2}$, $\beta = v/c$.

The cyclotron angular frequency of a muon in a storage ring is [74]

$$\vec{\omega}_c = -\frac{e\vec{B}}{\gamma m}, \tag{3.36}$$

which indicates the frequency that the muon goes around in a circle.

Since both $\vec{\omega}_s$ and $\vec{\omega}_c$ pointing in the same direction, the difference between the frequency of the spin precession and the cyclotron precession is then

$$\vec{\omega}_a = \vec{\omega}_s - \vec{\omega}_c = -\frac{g-2}{2}\frac{e\vec{B}}{m} = -a\frac{e\vec{B}}{m}, \tag{3.37}$$

where a is the anomalous magnetic dipole moment of the particle. This represents the angular frequency which the spin of a particle rotates relative to its momentum vector. Since we know that g is greater than 2, the spin precession is faster than the cyclotron motion of the momentum vector of the particle. Note that in eq. (3.37), the angular frequency only depends on the size of the magnetic field and there is no dependence on the momentum of the particle. This behavior will change once we apply an external electric field to the particle since in such a case the spin motion does strongly depend on its momentum.

The muon has a lifetime of 2.2 μs in its rest frame and decays via the parity-violating weak interaction to one electron and two neutrinos.

$$\mu^+ \rightarrow \overline{\nu}_\mu + \nu_e + e^+. \tag{3.38}$$

In the rest frame of the muon, the maximum energy of the positron appears when it is emitted in the opposite to the pair of neutrinos which goes in the same direction, see figure 3.7. Since the two neutrinos in the pair have opposite spin directions, the positron must have the same spin direction as the muon by the conservation of angular momentum. For a light particle like a positron, the right-handed production is more favorable than the left-handed production in the weak decays. We can conclude that for the case when the positron obtains maximum energy in the muon decay, it has a higher probability to move parallel to the muon spin direction. The conclusion is the opposite for the case with negatively charged particles.

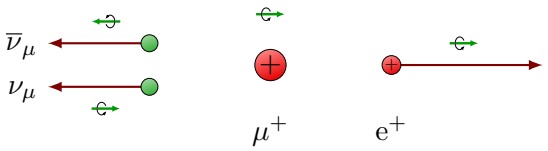

FIGURE 3.7: A schematic plot showing the muon decay in the rest frame with a maximum energy of the decay electron.

The positron energy is maximum when its direction of motion is parallel to the muon momentum in the laboratory frame, and when its center-of-mass energy is maximum too. With the conclusion that we reached for the muon decay in the last paragraph, it is now clear that such kind of high-energy positron appears more frequently when the spin

direction is parallel to the muon momentum. Because the muon spin rotates relative to the muon momentum with an angular frequency ω_a, it means that the number of positrons with maximum energy in the laboratory frame also oscillates at this frequency, that is, the number of decay positrons reaches a maximum when the spin and the momentum of muon are parallel, and a minimum when they are antiparallel. We can set an energy threshold E_{th} to select the high-energy positrons from the muon decay in the experiment, the variation of the positron number is given by [74]

$$N(t, E_{\text{th}}) = N_0(E_{\text{th}})e^{-\lambda t}[1 + A(E_{\text{th}})\cos(\omega_a t + \phi(E_{\text{th}}))], \tag{3.39}$$

where $\lambda^{-1} = \gamma\tau$ is the dilated muon lifetime. The normalization N_0, the weak asymmetry of the muon decay A and the initial phase ϕ depend on the threshold energy. By monitoring the number of the decay positrons, we can know the spin direction at a certain time.

If there is no any field gradient applied for confining muons in the storage ring, then the capture efficiency of muons would be low such that muons cannot move in a static trajectory. In the actual experiment at Fermilab, the focusing of the muon beam is achieved by using an electric quadrupole field [21]. When an electric field is applied, eq. (3.37) is modified to [74]

$$\vec{\omega}_a = -\frac{e}{m}\left[a\vec{B} - \left(a - \frac{1}{\gamma^2 - 1}\right)\frac{\vec{\beta} \times \vec{E}}{c}\right], \tag{3.40}$$

with the assumption $\vec{\beta} \cdot \vec{B} = 0$. In order to eliminate the effect from the electric field on the muon spin, it is necessary to tune the muon momentum to the so-called "magic" momentum

$$p_{\text{magic}} = \frac{mc}{\sqrt{a}} \simeq 3.094 \text{ GeV/c}, \tag{3.41}$$

which corresponds to $\gamma = \sqrt{1 + a^{-1}} \simeq 29.3$. With this magic momentum, the effect of the electric field on the muon momentum and spin are equal and the second term in eq. (3.40) vanishes and it brings us back to the simple eq. (3.37). This method led to the 0.46 ppm measurement of the muon $g - 2$ at Fermilab [21].

As we learnt from the course of special relativity, the electric field and magnetic field

transform into each other. We have already seen that in eq. (3.40) the muon spin does receive a contribution from the motion magnetic field $\propto \vec{\beta} \times \vec{E}$ that is transformed from the applied electric field. Similarly, if the muon EDM exists, then the motional electric field $\propto \vec{\beta} \times \vec{B}$ would create a torque to the EDM and induce a spin precession around the motional electric field. With this consideration in mind, eq. (3.40) becomes [74]

$$\vec{\omega} = -\frac{e}{m}\left[a\vec{B} - \left(a - \frac{1}{\gamma^2 - 1}\right)\frac{\vec{\beta} \times \vec{E}}{c} + \frac{\eta}{2}\left(\vec{\beta} \times \vec{B} + \frac{\vec{E}}{c}\right)\right], \tag{3.42}$$

where η is an analog of the g-factor in the magnetic dipole moment and is related to the muon EDM d by

$$d = \eta\frac{e\hbar}{4mc}. \tag{3.43}$$

Tuning the muon momentum to be p_{magic}, the frequency reduces to

$$\vec{\omega} = -\frac{e}{m}\left[a\vec{B} + \frac{\eta}{2}\left(\vec{\beta} \times \vec{B} + \frac{\vec{E}}{c}\right)\right]. \tag{3.44}$$

In the actual experiment, the static electric quadrupole field is much smaller than the motional electric field, $|\vec{E}| \ll c|\vec{\beta} \times \vec{B}|$, and the expression can be further approximated by

$$\vec{\omega} \simeq -\frac{e}{m}\left[a\vec{B} + \frac{\eta}{2}\left(\vec{\beta} \times \vec{B}\right)\right]. \tag{3.45}$$

If the muon does have an EDM, the observed angular frequency in the experiment becomes the sum of two components, $\vec{\omega} = \vec{\omega}_a + \vec{\omega}_\eta$, where the first one comes from muon $g-2$ and the second one comes from muon EDM. A schematic plot is shown in figure 3.8 for the two components of the spin precession frequency. The x-direction is the direction of muon momentum, the y-direction points radially inward to the center of the circular ring, and the z-direction points upward. The magnetic field is applied in the negative z direction.

The existence of muon EDM would change our interpretation of the $\vec{\omega}_a$ measured in the experiment, since it becomes a combination of the contributions from muon $g-2$ and muon EDM. From figure 3.8, we know that one effect of the muon EDM is that the spin

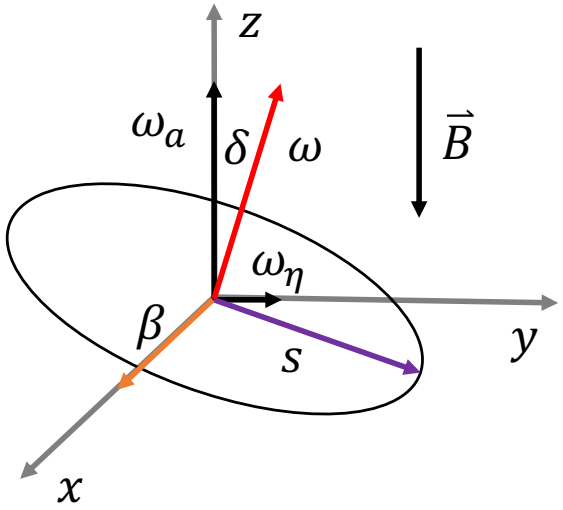

FIGURE 3.8: This schematic plot shows the spin precession frequency $\vec{\omega}_a$ and $\vec{\omega}_\eta$ induced by the muon $g-2$ and muon EDM, respectively. The sum of the two vectors makes the spin precess out of the horizontal plane of the storage ring.

precession plane is tilted by an angle δ

$$\delta = \tan^{-1}\left(\frac{\omega_\eta}{\omega_a}\right) = \tan^{-1}\left(\frac{\eta\beta}{2a}\right), \tag{3.46}$$

The tilt of the precession plane leads to an up-down oscillation of the muon spin, and a phase shift of $\pi/2$ relative to the precession caused by the muon $g-2$. These characteristics were the main objectives of the muon EDM search performed by the E821 experiment at Brookhaven National Laboratory (BNL) [75]. It turned out that the experiment obtained a null result and set an upper limit on the muon EDM,

$$|d_\mu| < 1.8 \times 10^{-19}\ e \cdot \text{cm}\ \ (95\%\ \text{C.L.})\,. \tag{3.47}$$

The overall magnitude of the precession frequency also changes and given by

$$|\vec{\omega}| = \frac{e|\vec{B}|}{m}\sqrt{a^2 + \left(\frac{\eta\beta}{2}\right)^2}. \tag{3.48}$$

If we consider new physics as an explanation of the 4.2σ deviation between the experimental result and the theoretical prediction of muon $g-2$, assuming that $\beta \simeq 1$, it can be rewritten as

$$|\vec{\omega}| = |\vec{B}|\sqrt{\left(\frac{e}{m}\right)^2 (a^{\text{SM}} + a^{\text{NP}})^2 + \left(\frac{2c}{\hbar}\right)^2 d^2}, \tag{3.49}$$

Figure 3.9 shows the possible combinations of ω_a and ω_η in terms of the new physics

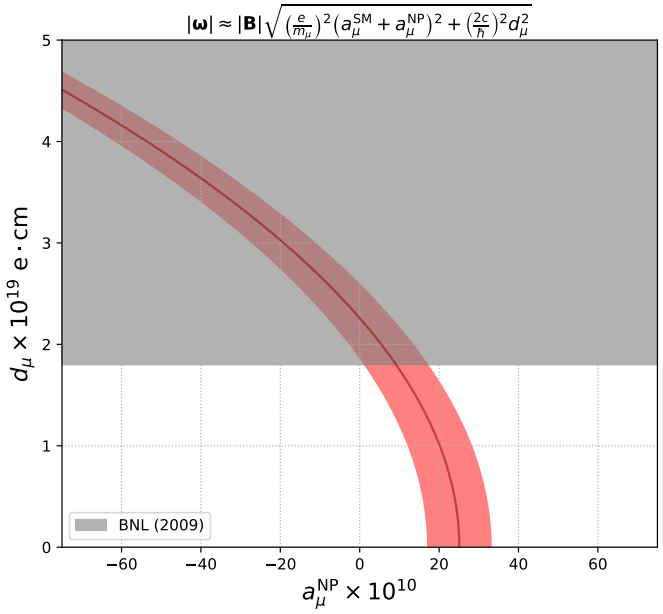

FIGURE 3.9: Regions on the $(a_\mu^{\mathrm{NP}}, d_\mu)$ plane which are consistent with the measured value of precession frequency at its central value and 1σ level. The gray area is already excluded by the E821 experiment at BNL.

contributions to the muon $g-2$ and the muon EDM that give the correct value of the spin precession frequency measured by the E989 experiment at Fermilab [21], with the region excluded by the latest constraint on the muon EDM obtained from the E821 experiment at BNL [75].

3.4.2 Prospects of future experiments

Here we would like to briefly mention without technical details the three proposed experiments related to the muon EDM measurement. One is the E989 experiment at Fermilab, another one is at Japan Proton Accelerator Research Complex (J-PARC), and the last one is at Paul Scherrer Institute (PSI).

3.4.2.1 Fermilab [76]

After many upgrades for the muon $g-2$ experiment at Fermilab, the E989 experimental setup can probe the muon EDM with higher sensitivity. The segmentation of the calorimeters is adapted in the experiment, which can make physicists better control the

pileup, and also the systematic uncertainty from the position and tilt angle of the detectors which were the large ones in the E821 EDM measurement. The energy acceptance of the calorimeters is also improved to cover a broader range of energy. The voltage of the electrostatic quadrupole applied in the E989 experiment is also chosen appropriately to reduce a significant systematic uncertainty from the coherent betatron oscillation. Other improvements include the increasing amount of experimental data, the number of trackers, and better tracker acceptance. They give an order of 1000 times more statistics compared to the E821 EDM experiment. Considering all these effects, the collaboration claims a preliminary estimation of the EDM sensitivity to be at the level of 10^{-21} e·cm.

3.4.2.2 J-PARC [77]

The idea of the experiment at Fermilab basically follows the discussion in section 3.4.1, where the momentum of the muon is tuned to the magic momentum in order to cancel the effect from the motional magnetic field generated by the electrostatic focusing. In the proposed experiment E34 at J-PARC, a different approach is adapted to measure the muon dipole moments. The experimentalists try to reduce the requirement of muon focusing by applying a technique called reaccelerated thermal muon beam. This leads to a significant improvement in the emittance of the muon beam, which is smaller by a factor of 1000. Such kind of small emittance makes the very weak magnetic focusing and the low-energy muons (around 300 MeV/c) in a compact storage ring become possible, without using an external electric field for the muon focusing. This means in the J-PARC scenario, eq. (3.45) becomes exact

$$\vec{\omega} = -\frac{e}{m}\left[a\vec{B} + \frac{\eta}{2}\left(\vec{\beta}\times\vec{B}\right)\right], \tag{3.50}$$

with no effect coming from the electric field and thus it reduces some possible sources of systematic uncertainty. Also, instead of the horizontal injection of muon beams into the storage ring, the J-PARC group proposed a novel vertical helix injection that can store the muon beams in the storage ring more efficiently. With this whole new approach different from the one at Fermilab, the collaboration estimated the muon EDM sensitivity to be of 1.5×10^{-21} e·cm, which is 60 times better than the muon EDM measurement performed by E821 experiment previously.

3.4.2.3 PSI [72]

The experimental group at PSI plan to use another novel approach for measuring the muon EDM. This method is called the frozen-spin technique [78, 79]. The idea is to totally cancel the contribution from the anomalous magnetic dipole moment in eq. (3.42). This can be achieved by carefully choosing the electric field applied in the experiment. We can solve for the required electric field by imposing the following requirement,

$$a\vec{B} - \left(a - \frac{1}{\gamma^2 - 1}\frac{\vec{\beta} \times \vec{E}}{c}\right) = 0. \tag{3.51}$$

From this equation, we obtain the desired size of the electric field as

$$E = \frac{aBc\beta}{1 - (1 + a)\beta^2} \simeq aBc\beta\gamma^2. \tag{3.52}$$

Under this condition, there is no time-dependent relative precession between the muon momentum vector and spin vector if the muon EDM is absent, that is, the spin is "frozen" without an EDM. It is clear that with the frozen-spin technique, we are able to suppress the contamination from the precession of the frequency induced by the anomalous magnetic dipole moment in the measurement and maximize the signal of muon EDM. The experimental group estimates the sensitivity to be of order around 6×10^{-23} e·cm.

As a recap of this section, we summarize the prospects of the three different proposals for muon EDM measurement.

$\lvert\vec{p}\rvert$ (GeV/c)	γ	$\lvert\vec{B}\rvert$(T)	$\lvert\vec{E}\rvert$(kV/cm)	$\lvert\vec{E}'\rvert/\gamma$(kV/cm)	R(m)	$\sigma_d^{\text{goal}}(e\cdot\text{cm})$	Ref.
3.094	29.3	1.45	$\mathcal{O}(10)$	4300	7.11	$\mathcal{O}(10^{-21})$	E989 [76]
0.3	3.0	3.0	0.0	8500	0.333	1.5×10^{-21}	E34 [77]
0.125	1.55	3.0	20	7000	0.28	6×10^{-23}	PSI [72]

TABLE 3.2: Comparison among different proposals of the muon EDM measurement. $\vec{p}$ is the momentum of muon. γ is the boost factor. $\vec{B}$ is the applied magnetic field. $\vec{E}$ is the applied electric field. $\vec{E}'$ is the electric field that muon feels in its rest frame. R is the radius of the storage ring. σ_d^{goal} is the goal of the sensitivity of muon EDM.

Chapter 4

General structure of new physics contributions to dipole moments

In this chapter, we discuss the general structure of the new physics contributions to dipole moments. To be specific, we explain the procedure of deriving the general formulas for all possible one-loop contributions to the vertex function, and also the two-loop ones which are necessary for the model we consider in the next chapter.

4.1 One-loop contributions

One-loop contributions to the electromagnetic vertex function can be divided into four categories generically, which are shown in figure 4.1 and figure 4.2. We note that in the left diagrams of figure 4.1 and 4.2, both neutral and charged bosons are possible depending on the model considered, while in the right diagrams, only charged bosons are available because they need to carry electric charges to interact with the photon electromagnetically. Now we explain the general steps for obtaining the electromagnetic dipole moments of the charged leptons.

Our goal is to extract the form factors corresponding to the magnetic and electric dipole

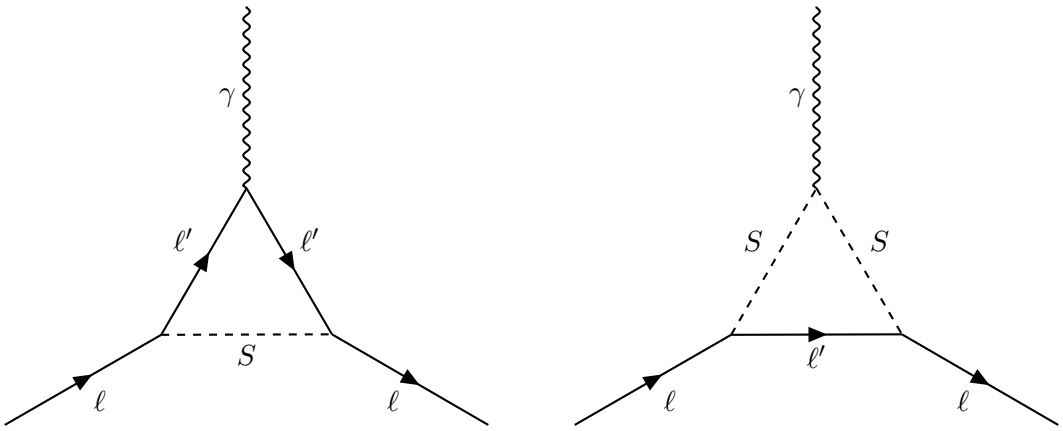

(a) Neutral/Charged scalar (b) Charged scalar

FIGURE 4.1: One-loop contributions to dipole moments with scalar bosons. The left diagram is for the neutral scalar boson and the right one is for the charged scalar boson.

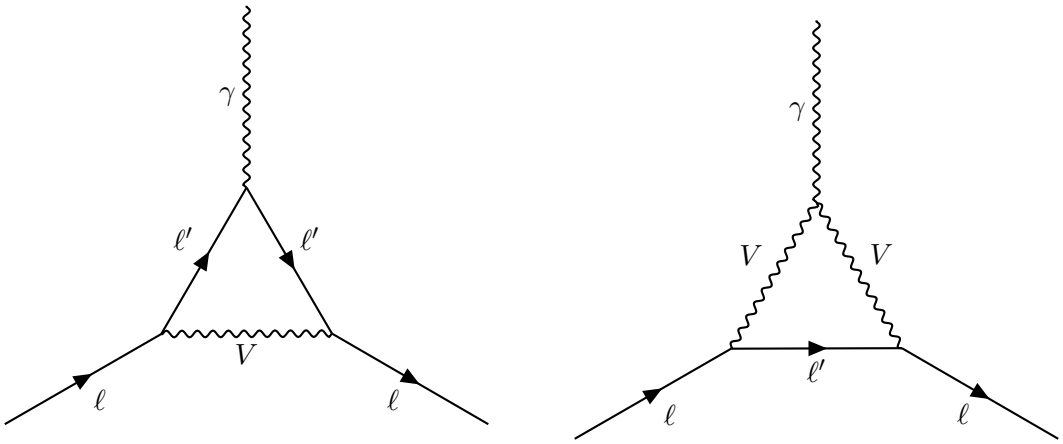

(a) Neutral/Charged vector (b) Charged vector

FIGURE 4.2: One-loop contributions to dipole moments with vector bosons. The left diagram is for the neutral vector boson and the right one is for the charged vector boson.

moments in the vertex function, eq. (3.4), that is, F_2 and F_3. For convenience, the necessary parts of the vertex function are reproduced here

$$\Gamma^\mu \supset F_2(q^2)\frac{i\sigma^{\mu\nu}}{2m_\ell}q_\nu - F_3(q^2)\sigma^{\mu\nu}q_\nu\gamma_5. \tag{4.1}$$

Let us first define the momentum flow in the diagram. This is given in figure 4.3.

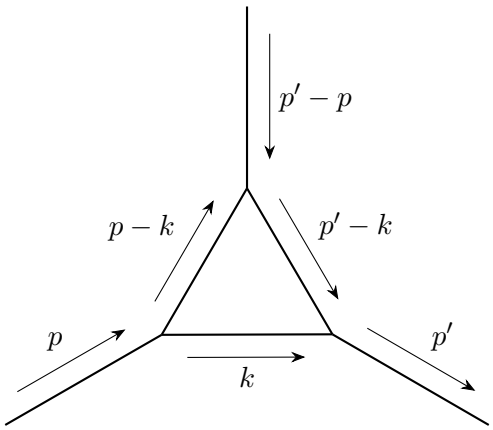

FIGURE 4.3: The convention of the momentum flow in the one-loop diagram.

We then write down the expression for each one-loop diagram according to the Feynman rules. The general form looks like

$$-ieQ_\ell \Gamma^\mu = \int \frac{d^4k}{(2\pi)^4} \text{ (a product of couplings and propagators).} \tag{4.2}$$

As an example, let us explicitly show the expression in the case of a neutral scalar boson

$$\begin{aligned} -ieQ_\ell \Gamma^\mu = -i^6 eQ_{\ell'} \int \frac{d^4k}{(2\pi)^4} \\ \left(g_s^* - g_p^* \gamma_5\right) \frac{\not{p}' - \not{k} + m_{\ell'}}{(p'-k)^2 - m_{\ell'}^2} \gamma^\mu \frac{\not{p} - \not{k} + m_{\ell'}}{(p-k)^2 - m_{\ell'}^2} \left(g_s + g_p \gamma_5\right) \frac{1}{k^2 - m_S^2}. \end{aligned} \tag{4.3}$$

where we move the electric charge factor in the coupling with the external photon outside the integration of the loop momentum k. The factors like $(g_s + g_p\gamma_5)$ are the couplings of the scalar boson with charge leptons, where g_s and g_p are the scalar and pseudoscalar couplings, respectively. We will summarize the general Feynman rules used in each category of the diagram in the following section.

The next step is to simplify the numerator and the denominator in the product of couplings and propagators. The denominator can be simplified by taking advantage of Feynman's formula

$$\frac{1}{A_1 \cdots A_n} = \int dF_n \frac{1}{(x_1 A_1 + \cdots + x_n A_n)^n}, \tag{4.4}$$

where the integration measure over the Feynman parameters x_i is

$$\int dF_n = (n-1)! \int_0^1 dx_1 \cdots dx_n \delta\left(x_1 + \cdots + x_n - 1\right). \tag{4.5}$$

For instance, in the case of neutral scalar boson, we have

$$x_1\left[\left(p'-k\right)^2 - m_{\ell'}^2\right] + x_2\left[\left(p-k\right)^2 - m_{\ell'}^2\right] + x_3\left(k^2 - m_S^2\right) \equiv \ell^2 - D, \tag{4.6}$$

where

$$\ell = k - \left(x_1 p' + x_2 p\right), \tag{4.7}$$

$$D = -x_1 x_2 q^2 + \left(x_1 + x_2\right)\left(x_1 + x_2 - 1\right) m_\ell^2 + \left(x_1 + x_2\right) m_{\ell'}^2 + x_3 m_S^2. \tag{4.8}$$

Now we use the fact that the dipole moments correspond to the dimensional-five operators in the Lagrangian eq. (3.24), which are nonrenormalizable. This means that there are no counterterms for absorbing the infinities, and therefore the contributions to the dipole moments must come from the finite part in the vertex function. After shifting the momentum from k to ℓ, we get terms up to quadratic order in ℓ. The terms with ℓ^2 contain divergences, but since these terms only contribute to the form factor F_1 in eq. (3.5), we can ignore the ℓ^2 terms in the numerator. Next, by using the fact that terms linear in ℓ are odd functions, these terms integrate to zero in the end. It turns out that we only need to focus on terms independent of ℓ in the integration for the extraction of the dipole moments. In the case with a neutral scalar boson, it is given by

$$\left(g_s^* - g_p^* \gamma_5\right)\left[\left(1-x_1\right)\not{p}' - x_2 \not{p} + m_{\ell'}\right]\gamma^\mu\left[-x_1\not{p}' + \left(1-x_2\right)\not{p} + m_{\ell'}\right]\left(g_s + g_p\gamma_5\right). \tag{4.9}$$

Recalling that the vertex function is actually sandwiched between a pair of lepton spinor like $\overline{u}(p')\Gamma^\mu u(p)$. We can use the fact that the external leptons are on-shell to further simplify the numerator by applying the Dirac equation. This replaces factors $\not{p}$ and $\not{p}'$ to the mass of external lepton, m_ℓ.

In order to extract the form factor, we rearrange the simplified numerator and extract the term proportional to $(p'+p)^\mu$. Then, applying the Gordon identity

$$\overline{u}\left(p'\right)\gamma^\mu u\left(p\right) = \frac{1}{2m_\ell}\overline{u}\left(p'\right)\left[\left(p'+p\right)^\mu + i\sigma^{\mu\nu}q_\nu\right]u\left(p\right) \tag{4.10}$$

to obtain the desired term proportional to $\sigma^{\mu\nu}q_\nu$ and $\sigma^{\mu\nu}q_\nu\gamma_5$, where $q = p' - p$. The coefficients of these terms give us the form factors, $F_2(q^2)$ and $F_3(q^2)$, of the electromagnetic dipole moments. Finally, we can translate the form factors into the dipole moment in the limit of zero momentum transfer, $q^2 = 0$,

$$a_\ell = F_2(0), \tag{4.11}$$

$$d_\ell = eQ_\ell F_3(0). \tag{4.12}$$

4.2 Feynman rules

Here we list down the general Feynman rules used in the calculation of the contributions.

4.2.1 Lepton propagator

The lepton propagator is given by

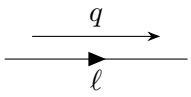

$$= i\frac{\not{q} + m_\ell}{q^2 - m_\ell^2}. \tag{4.13}$$

4.2.2 Photon couplings

The couplings of a photon with leptons or charged scalar bosons are

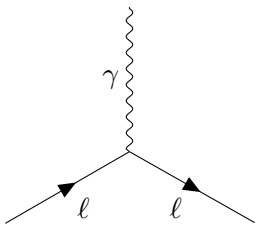

$$= -ieQ_\ell\gamma^\mu\ ,$$

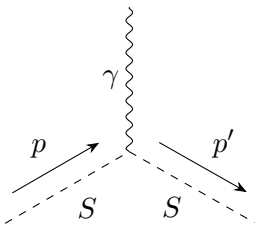

$$= -ieQ_S\left(p + p'\right)^\mu . \tag{4.14}$$

The couplings of a photon with charged vector bosons are

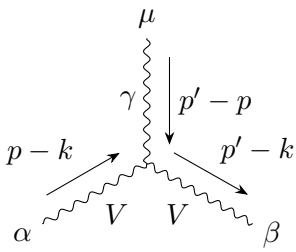

$$= iG[g^{\alpha\beta}(p+p'-2k)^{\mu} + g^{\beta\mu}(p-2p'+k)^{\alpha} + g^{\mu\alpha}(-2p+p'+k)^{\beta}], \tag{4.15}$$

where G denotes the coupling constant.

4.2.3 Scalar boson sector

The following Feynman rules are derived from the Lagrangian with both the scalar and pseudoscalar couplings,

$$\mathcal{L} = \overline{\ell}'(g_s + g_p\gamma_5)\ell S^*. \tag{4.16}$$

The general couplings of a scalar boson with leptons are written as

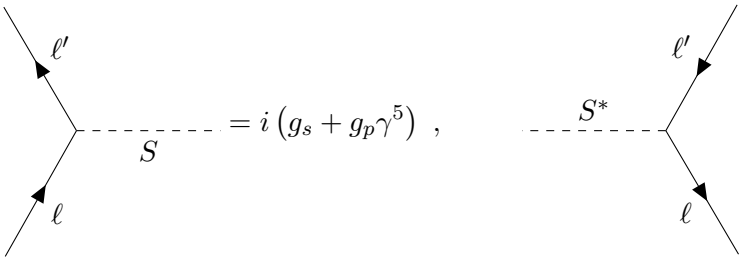

(4.17)

The propagator of a scalar boson is given by

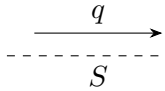

$$= \frac{i}{q^2 - m_S^2}. \tag{4.18}$$

4.2.4 Vector boson sector

The following Feynman rules are derived from the Lagrangian with both the vector and axial-vector couplings,

$$\mathcal{L} = \overline{\ell}'\gamma^{\mu}(g_v + g_a\gamma_5)\ell V_{\mu}^*. \tag{4.19}$$

The general couplings of a vector boson with leptons are written as

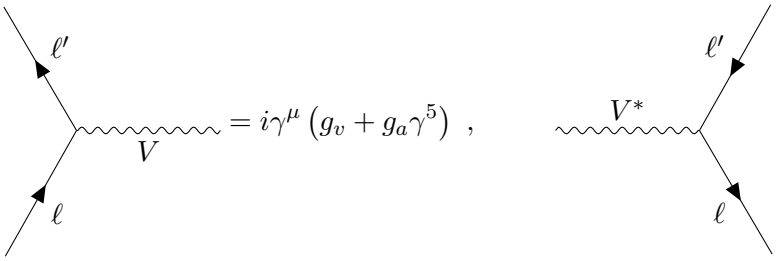

The propagator of a vector boson in the Feynman gauge is

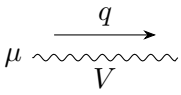

4.2.5 Unphysical scalar boson

Since we choose to work in the Feynman gauge, we need to take into account the contribution from the unphysical Goldstone bosons. Their Yukawa couplings can be obtained by matching the amplitude with the unphysical scalar boson replaced by the vector one and requiring that the gauge dependent part must vanish. The resulting Yukawa couplings is given by

$$g_s^{\text{unphy}} = \frac{g_v}{m_V}(m_\ell - m_{\ell'}) \ , \ g_p^{\text{unphy}} = -\frac{g_a}{m_V}(m_\ell + m_{\ell'}). \tag{4.22}$$

A photon-vector-scalar coupling is given by

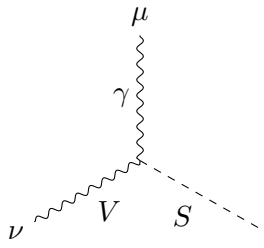

where $\widetilde{G}$ denotes the coupling constant.

4.3 Summary of the one-loop general structure

In this section, we write down the exact form of all contributions from the four categories of diagrams to the muon anomalous magnetic dipole moment and the electric dipole moment, after the tedious calculations. More details of the calculation can be found in appendix A.

4.3.1 Neutral/charged scalar boson

The general structure of the magnetic dipole moment and electric dipole moment in figure 4.1a are

$$a_\ell = \frac{Q_{\ell'}}{Q_\ell}\frac{m_\ell}{8\pi^2}\int_0^1 dx\,(1-x)^2\,\frac{m_{\ell'}\left(g_s^* g_s - g_p^* g_p\right) + x m_\ell\left(g_s^* g_s + g_p^* g_p\right)}{x m_S^2 + (1-x)\,m_{\ell'}^2 - x\,(1-x)\,m_\ell^2}, \tag{4.24}$$

$$d_\ell = -i\frac{eQ_{\ell'}}{16\pi^2}\int_0^1 dx\,(1-x)^2\,\frac{m_{\ell'}\left(g_s^* g_p - g_s g_p^*\right)}{x m_S^2 + (1-x)\,m_{\ell'}^2 - x\,(1-x)\,m_\ell^2}. \tag{4.25}$$

4.3.2 Charged scalar boson

The general structure of the magnetic dipole moment and electric dipole moment in figure 4.1b are

$$a_\ell = -\frac{Q_S}{Q_\ell}\frac{m_\ell}{8\pi^2}\int_0^1 dx\,(1-x)\,x\frac{(1-x)\,m_\ell\left(g_s^* g_s + g_p^* g_p\right) + m_{\ell'}\left(g_s^* g_s - g_p^* g_p\right)}{x m_{\ell'}^2 + (1-x)\,m_S^2 - x\,(1-x)\,m_\ell^2}, \tag{4.26}$$

$$d_\ell = i\frac{eQ_S}{16\pi^2}\int_0^1 dx\,(1-x)\,x\frac{m_{\ell'}\left(g_s^* g_p - g_s g_p^*\right)}{x m_{\ell'}^2 + (1-x)\,m_S^2 - x\,(1-x)\,m_\ell^2}. \tag{4.27}$$

4.3.3 Neutral vector boson

The general structure of the magnetic dipole moment and electric dipole moment in figure 4.2a are

$$\begin{aligned} a_\ell = & \frac{Q_{\ell'}}{Q_\ell}\frac{m_\ell}{4\pi^2}\int_0^1 dx\,(1-x)\,x\frac{\left[2m_{\ell'}\left(g_v^* g_v - g_a^* g_a\right) - (1+x)\,m_\ell\left(g_v^* g_v + g_a^* g_a\right)\right]}{x m_V^2 + (1-x)\,m_{\ell'}^2 - x\,(1-x)\,m_\ell^2} \\ & + \frac{Q_{\ell'}}{Q_\ell}\frac{1}{8\pi^2}\frac{m_\ell}{m_V^2}\int_0^1 dx\,(1-x)^2 \\ & \times \frac{m_{\ell'}\left[g_v^* g_v\,(m_\ell - m_{\ell'})^2 - g_a^* g_a\,(m_\ell + m_{\ell'})^2\right] + x m_\ell\left[g_v^* g_v\,(m_\ell - m_{\ell'})^2 + g_a^* g_a\,(m_\ell + m_{\ell'})^2\right]}{x m_V^2 + (1-x)\,m_{\ell'}^2 - x\,(1-x)\,m_\ell^2}, \end{aligned} \tag{4.28}$$

$$\begin{aligned} d_\ell = & -i\frac{eQ_{\ell'}}{4\pi^2}\int_0^1 dx\,(1-x)\,x\frac{m_{\ell'}\left(g_v^* g_a - g_v g_a^*\right)}{x m_V^2 + (1-x)\,m_{\ell'}^2 - x\,(1-x)\,m_\ell^2} \\ & + i\frac{eQ_{\ell'}}{16\pi^2}\frac{m_\ell^2 - m_{\ell'}^2}{m_V^2}\int_0^1 dx\,(1-x)^2\,\frac{m_{\ell'}\left(g_v^* g_a - g_v g_a^*\right)}{x m_V^2 + (1-x)\,m_{\ell'}^2 - x\,(1-x)\,m_\ell^2}. \end{aligned} \tag{4.29}$$

In the expression above, the first term is the contribution from the vector boson and the second term is the one obtained by replacing the vector boson with an unphysical scalar boson.

4.3.4 Charged vector boson

The general structure of the magnetic dipole moment and electric dipole moment in figure 5.1c are

$$\begin{aligned} a_\ell = & \frac{G}{eQ_\ell}\frac{m_\ell}{8\pi^2}\int_0^1 dx(1-x)^2\frac{m_\ell(3-2x)(g_v^* g_v + g_a^* g_a) - 3m_{\ell'}(g_v^* g_v - g_a^* g_a)}{x m_{\ell'}^2 + (1-x)m_V^2 - x(1-x)m_\ell^2} \\ & - \frac{\widetilde{G}}{eQ_\ell}\frac{1}{8\pi^2}\frac{m_\ell}{m_V}\int_0^1 dx(1-x)^2\frac{m_\ell(g_v^* g_v + g_a^* g_a) - m_{\ell'}(g_v^* g_v - g_a^* g_a)}{x m_{\ell'}^2 + (1-x)m_V^2 - x(1-x)m_\ell^2} \\ & - \frac{Q_V}{Q_\ell}\frac{1}{8\pi^2}\frac{m_\ell}{m_V^2}\int_0^1 dx\,(1-x)\,x \\ & \times\left\{\frac{(1-x)\,m_\ell\left[g_v^* g_v(m_\ell - m_{\ell'})^2 + g_a^* g_a(m_\ell + m_{\ell'})^2\right]}{x m_{\ell'}^2 + (1-x)\,m_V^2 - x\,(1-x)\,m_\ell^2}\right. \\ & \qquad\left. + \frac{m_{\ell'}\left[g_v^* g_v(m_\ell - m_{\ell'})^2 - g_a^* g_a(m_\ell + m_{\ell'})^2\right]}{x m_{\ell'}^2 + (1-x)\,m_V^2 - x\,(1-x)\,m_\ell^2}\right\}, \end{aligned} \tag{4.30}$$

$$
\begin{aligned}
d_\ell = & \, i\frac{G}{16\pi^2}\int_0^1 dx(1-x)^2\frac{3m_{\ell'}(g_v^* g_a - g_v g_a^*)}{xm_{\ell'}^2+(1-x)m_V^2-x(1-x)m_\ell^2} \\
& + i\frac{\widetilde{G}}{16\pi^2 m_V}\int_0^1 dx(1-x)^2\frac{m_\ell(g_v^* g_a + g_v g_a^*) - m_{\ell'}(g_v^* g_a - g_v g_a^*)}{xm_{\ell'}^2+(1-x)m_V^2-x(1-x)m_\ell^2} \\
& + i\frac{eQ_V}{16\pi^2}\frac{m_{\ell'}^2-m_\ell^2}{m_V^2}\int_0^1 dx(1-x)x\frac{m_{\ell'}(g_v^* g_a - g_v g_a^*)}{xm_{\ell'}^2+(1-x)m_V^2-x(1-x)m_\ell^2}.
\end{aligned} \tag{4.31}
$$

In the expression above, the first term is the contribution from the vector boson, the second term is the one obtained by replacing one of the vector bosons with an unphysical scalar boson, and the last term is obtained by replacing all two vector bosons with the unphysical scalar bosons. For the diagrams with vector bosons, the contribution from the vector boson itself is always dominant, as we can see from the general expression. The contributions from the unphysical scalar bosons are suppressed by the heavy mass of the vector boson.

In the next chapter, we will apply the general formulas to the model of vector-like leptons. It would be convenient if we can express the combinations of couplings in the form of left-handed and right-handed couplings. The Lagrangians (4.16) and (4.19) can be rewritten in the form of $\bar{\ell}'(g_L P_L + g_R P_R)\ell S^*$ and $\bar{\ell}'\gamma^\mu(g_L P_L + g_R P_R)\ell V_\mu^*$, where $P_{L,R}$ are the projection operators. Couplings $g_{s,v}$ and $g_{p,a}$ are related to their corresponding g_L and g_R by

$$
g_{s,v} = \frac{1}{2}(g_L + g_R) \ , \ g_{p,a} = \frac{1}{2}(-g_L + g_R). \tag{4.32}
$$

From them, we then obtain the following relations,

$$
g_{s,v}^* g_{s,v} + g_{p,a}^* g_{p,a} = \frac{1}{2}(|g_L|^2 + |g_R|^2), \tag{4.33}
$$

$$
g_{s,v}^* g_{s,v} - g_{p,a}^* g_{p,a} = \mathrm{Re}(g_L g_R^*), \tag{4.34}
$$

$$
g_{s,v}^* g_{p,a} + g_{s,v} g_{p,a}^* = -\frac{1}{2}(|g_L|^2 - |g_R|^2), \tag{4.35}
$$

$$
g_{s,v}^* g_{p,a} - g_{s,v} g_{p,a}^* = -i\,\mathrm{Im}(g_L g_R^*), \tag{4.36}
$$

where the scalar-type and vector-type couplings are paired independently. For example, in eq. (4.33) it should be read as $g_s^* g_s + g_p^* g_p$ or $g_v^* g_v + g_a^* g_a$.

4.4 An example: muon $g-2$ in the SM

In this section, we apply the formulas obtained above to the one-loop electroweak contribution of muon $g-2$ in the SM. Let us compute the contribution from Z boson first. Since the lepton mass is much smaller than the boson mass, we neglect the second term in eq. (4.28). In this case, $m_V = m_Z$ and $m_\ell = m_{\ell'} = m_\mu$. The muon mass is ignored in the denominator. The couplings of Z boson are

$$g_v = -\frac{g}{4\cos\theta_W}(-1+4\sin^2\theta_W), \tag{4.37}$$

$$g_a = -\frac{g}{4\cos\theta_W}. \tag{4.38}$$

Then we have

$$\begin{aligned} a_\mu^{\mathrm{Z}} &= \frac{m_\mu^2}{4\pi^2 m_Z^2}\int_0^1 dx\,(1-x)\left[g_v^* g_v(1-x) - g_a^* g_a(3+x)\right] \\ &= \frac{m_\mu^2}{4\pi^2 m_Z^2}\frac{g^2}{16\cos^2\theta_W}\int_0^1 dx\,(1-x)\left[(-1+4\sin^2\theta_W)^2(1+x)+(-3+x)\right] \\ &= \frac{m_\mu^2}{4\pi^2 m_Z^2}\frac{g^2}{16\cos^2\theta_W}\frac{4}{3}(-1-2\sin^2\theta_W+4\sin^4\theta_W) \\ &= -\frac{m_\mu^2 G_F}{8\sqrt{2}\pi^2}\frac{4}{3}(1+2\sin^2\theta_W-4\sin^4\theta_W), \end{aligned} \tag{4.39}$$

where $G_F = \sqrt{2}g^2/8m_W^2$ is the Fermi coupling constant.

Next, we compute the contribution from the W boson. In this case, $m_V = m_W$ and $m_\ell = m_{\ell'} = m_\mu$. The muon mass is ignored in the denominator. We also neglect the third term in eq. (4.30) because it is suppressed by the large mass of the W boson. The couplings of W boson are

$$g_v = -g_a = -\frac{g}{2\sqrt{2}}, \tag{4.40}$$

$$G = -e, \tag{4.41}$$

$$\widetilde{G} = em_W. \tag{4.42}$$

Then we have

$$\begin{aligned} a_\mu^{\rm W} &= \frac{1}{8\pi^2}\frac{m_\mu^2}{m_W^2}\int_0^1 dx(1-x)[(3-2x)(g_v^* g_v + g_a^* g_a) - 3(g_v^* g_v - g_a^* g_a)] \\ &\quad + \frac{1}{8\pi^2}\frac{m_\mu^2}{m_W^2}\int_0^1 dx(1-x)[(g_v^* g_v + g_a^* g_a) - (g_v^* g_v - g_a^* g_a)] \\ &= \frac{1}{8\pi^2}\frac{m_\mu^2}{m_W^2}\frac{g^2}{8}\int_0^1 dx(1-x)[(6-4x)+2] \\ &= \frac{1}{8\pi^2}\frac{m_\mu^2}{m_W^2}\frac{g^2}{8}\frac{10}{3} = \frac{m_\mu^2 G_F}{8\sqrt{2}\pi^2}\frac{10}{3}. \end{aligned} \tag{4.43}$$

The final piece of the one-loop electroweak contribution comes from the Higgs boson. In this case, $m_S = m_h$ and $m_\ell = m_{\ell'} = m_\mu$. The couplings of Higgs boson are

$$g_s = -\frac{m_\mu}{v}\ ,\ g_p = 0. \tag{4.44}$$

Then we have

$$a_\mu^{\rm Higgs} = \frac{m_\mu^2}{8\pi^2}\frac{m_\mu^2}{v^2}\int_0^1 dx \frac{(1-x)^2(1+x)}{x m_h^2 + (1-x)^2 m_\mu^2} = \frac{m_\mu^4 G_F}{4\sqrt{2}\pi^2}\frac{1}{m_h^2}\int_0^1 dx \frac{(1-x)^2(1+x)}{x + (1-x)^2 m_\mu^2/m_h^2}. \tag{4.45}$$

It turns out that the contribution from Higgs is several orders of magnitude smaller than the Z and W contributions, and thus can be safely ignored.

Combining the results from the Z and W contributions, we obtain

$$a_\mu^{\rm EW(1)} = \frac{m_\mu^2 G_F}{8\sqrt{2}\pi^2}\frac{1}{3}\left[5 + (1-4\sin^2\theta_W)^2\right], \tag{4.46}$$

which reproduces the one-loop contribution written in the White Paper [48].

4.5 Remarks

Let us consider a simple case with the contribution from a scalar boson mediation. The magnetic and electric dipole moments of SM lepton are induced by the Yukawa couplings of the lepton with new particles. It is, therefore, useful to give expressions of these quantities for such cases in a generic manner. Suppose that the SM leptons ℓ couple to a

new lepton ℓ' and a scalar S via the following Lagrangian terms:

$$\mathcal{L}_{\rm int} = -\bar{\ell'}(g_L P_L + g_R P_R)\ell S^* + \text{h.c.}. \tag{4.47}$$

The charge and mass of ℓ' (S) are denoted by $Q_{\ell'}$ (Q_S) and $M_{\ell'}$ (M_S), respectively. These interactions induce the leptonic anomalous magnetic dipole moment at the one-loop level:

$$\begin{aligned}\Delta a_\ell =& \frac{m_\ell}{8\pi^2}\frac{M_{\ell'}}{M_S^2}\text{Re}\left(g_L g_R^*\right)\left[-Q_{\ell'}G_{\ell'}\left(\frac{M_{\ell'}^2}{M_S^2}\right)+Q_S G_S\left(\frac{M_{\ell'}^2}{M_S^2}\right)\right] \\ &+\frac{1}{8\pi^2}\frac{m_\ell^2}{M_S^2}\left(|g_L|^2+|g_R|^2\right)\left[-Q_{\ell'}F_{\ell'}\left(\frac{M_{\ell'}^2}{M_S^2}\right)+Q_S F_S\left(\frac{M_{\ell'}^2}{M_S^2}\right)\right],\end{aligned} \tag{4.48}$$

where

$$G_{\ell'}(x) = -\frac{3-4x+x^2+2\ln x}{2(1-x)^3}\,, \tag{4.49}$$

$$G_S(x) = \frac{1-x^2+2x\ln x}{2(1-x)^3}\,, \tag{4.50}$$

$$F_{\ell'}(x) = \frac{2+3x-6x^2+x^3+6x\ln x}{12(1-x)^4}\,, \tag{4.51}$$

$$F_S(x) = \frac{1-6x+3x^2+2x^3-6x^2\ln x}{12(1-x)^4}\,. \tag{4.52}$$

These functions are obtained from the integrations of the generic expression in the corresponding category of the diagram, namely the diagrams with neutral or charged scalar bosons, with the SM lepton masses neglected.

The EDMs are also induced at the one-loop level:

$$d_\ell = \frac{e}{16\pi^2}\frac{M_{\ell'}}{M_S^2}\text{Im}\left(g_L g_R^*\right)\left[-Q_{\ell'}G_{\ell'}\left(\frac{M_{\ell'}^2}{M_S^2}\right)+Q_S G_S\left(\frac{M_{\ell'}^2}{M_S^2}\right)\right]. \tag{4.53}$$

From this expression, we see that the EDMs vanish if $g_L = 0$ or $g_R = 0$, whilst there still exist non-vanishing terms for Δa_ℓ. This clearly violates the assumption (i) in section 3.3. In this case, the interactions in eq. (4.47) conserve the CP symmetry; for instance, if $g_L = 0$, the CP phase in g_R can be rotated out by the field redefinition of S and thus is not physical, and vice versa.

The first term in eq. (4.48), and eq. (4.53) are proportional to the fermion mass $M_{\ell'}$, which provides an additional source of chirality flip and thus spoils the assumption (iii) discussed in section 3.3. If $M_{\ell'} \gg m_\ell$, the first term dominates the second term eq. (4.48). In this

case, we have a simple relation between Δa_ℓ and d_ℓ:

$$d_\ell \simeq \frac{e}{2m_\ell} \times \tan\left[\arg\left(g_L g_R^*\right)\right] \times \Delta a_\ell \ , \tag{4.54}$$

which corresponds to eq. (3.27) for $\ell = \mu$. We show a plot to visualize the dependence of the muon EDM on the muon $g-2$ and the CP-violating phase in figure 4.4. In the region consistent with the deviation of muon $g-2$ in 2σ enclosed by two vertical dashed lines, the the proposed experiments at Fermilab and J-PARC can cover the region with large phases while the experiment at PSI is able to probe region with much smaller phases due to its high sensitivity.

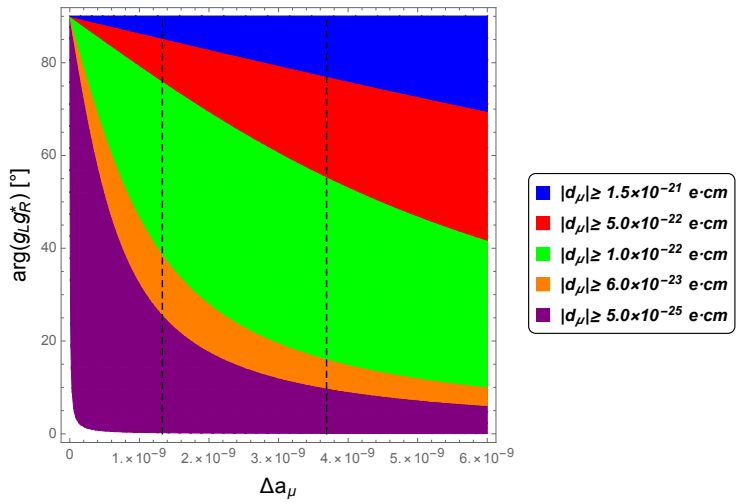

FIGURE 4.4: The dependence of muon EDM on the deviation of muon $g-2$ and the the CP-violating phase in the scenario with new scalar sector. The region enclosed by the vertical dashed lines is the 2σ region of Δa_μ.

Chapter 5

Model of Vector-like leptons

Now we know that the assumption of three generations of matter in the SM describes the experimental results very well. However, we still do not understand why it should be so. It is therefore natural to suspect that there are some additional fermions in Nature. We can build models containing new fermions, with their properties determined by some theoretical assumptions, and see how they affect the SM predictions. In general, these new fermions can couple to the electroweak bosons and result in measurable deviations from the SM prediction, such as particle mass, cross-section, decay branching ratio, etc.

At first thought, a simple and naive option is to introduce more generations of new fermions which are also chiral as their SM partners, that is, the left-handed and right-handed leptons behave differently under the symmetry transformations of the theory, and thus lead to different interactions, e.g. the weak charged current interacts only with the left-handed particles in the SM. However, the null results from the experimental searches have put strong constraints on these new chiral fermions, and their masses are restricted to be huge [47]. Since the mass of these chiral fermions is generated by the Yukawa couplings with the Higgs boson, it means that their Yukawa couplings must be relatively large and may violate the unitarity bound. To avoid the severe constraints, another approach of extension to the SM fermion sector is preferable: the vector-like fermions. Unlike the chiral fermions, the vector-like fermions can acquire their masses from mass terms independent of Yukawa couplings, and therefore are less constrained than extra chiral families, as we can choose the mass parameters to be relatively large.

Models with extra vector-like leptons (VLLs) have been discussed previously as being possible explanations of the muon $g-2$ deviation between the experimental and theoretical sides [80, 81, 82, 83]. Inspired by these studies, we discuss an SM extension with two vector-like leptons, one $SU(2)_L$ doublet and one $SU(2)_L$ singlet, and investigate the electromagnetic dipole moments in the model. In particular, we are interested in the possible new sources of CP-violation in the model, which can generate sizable muon EDM. Looking forward to the experiments of EDM measurement, we perform the computation of the prediction for the muon EDM and see whether it is suitable for the proposed projects of the muon EDM measurement.

5.1 Lagrangian

	μ_L	μ_R	H	$L_{L,R}$	$E_{L,R}$
$SU(3)_C$	**1**	**1**	**1**	**1**	**1**
$SU(2)_L$	**2**	**1**	**2**	**2**	**1**
$U(1)_Y$	$-\frac{1}{2}$	-1	$\frac{1}{2}$	$-\frac{1}{2}$	-1

TABLE 5.1: This table shows the quantum numbers of SM and extra vector-like leptons. As usual, the electric charge is given by $Q = T_3 + Y$, where T_3 is the weak isospin, which is $+1/2$ for for the first component and -1/2 for the second one of a doublet, respectively.

We consider an extension to the SM by one doublet (L) and one singlet (E) vector-like leptons. For simplicity, we consider the minimal scenario where only the couplings of the vector-like leptons to the second generation of lepton exist and the couplings of the vector-like leptons to other generations are unchanged from their SM values.[1] Therefore, the electron and tau do not mix with extra vector-like leptons and their masses totally originate from the Higgs Yukawa couplings. The quantum numbers of the fields necessary for the analysis are listed in table 5.1, where the lowercase letters denote fields in the SM and the uppercase letters denote the vector-like leptons. As can be seen from the table, $L_{L,R}$ and $E_{L,R}$ have the same quantum numbers as their chiral partners μ_L and μ_R in the SM, respectively. In the discussion below, our notation basically follows the one used in [82].

[1] Such kind of structure may be realized by imposing specific flavor symmetries to the model, for example, $U(1)_{L_\mu}$ or $U(1)_{L_\mu - L_\tau}$ symmetry which we studied in [84, 85]. The neutrino masses can be generated by breaking these symmetries with the mass term of right-handed neutrinos. In general, couplings with other leptons are possible, but it complicates the model and analysis, so in this work, we focus on couplings with muon directly related to muon dipole moments and assume that other couplings are negligibly small. Considering the concrete model in this framework, especially for the explanation of the neutrino mixing, is not trivial, we devote the more general couplings and neutrino sector to our future work.

The components of the doublet fields are labeled as

$$\ell_L = \begin{pmatrix} \nu_{L\mu} \\ \mu_L \end{pmatrix}, \; L_{L,R} = \begin{pmatrix} L^0_{L,R} \\ L^-_{L,R} \end{pmatrix}, \; H = \frac{1}{\sqrt{2}} \begin{pmatrix} 0 \\ v+h \end{pmatrix}, \tag{5.1}$$

where $v = 246.22$ GeV is the vacuum expectation value of the Higgs field.

Without loss of generality, we work in the basis where the Yukawa matrix of the leptons in the SM sector is already diagonal. The most relevant part of the Lagrangin is the Yukawa interactions among the muon and the vector-like leptons and the mass term of the vector-like leptons, which are given by

$$\begin{aligned} \mathcal{L} \supset & - y_\mu \bar{\ell}_L \mu_R H - \lambda_E \bar{\ell}_L E_R H - \lambda_L \bar{L}_L \mu_R H - \lambda \bar{L}_L E_R H - \bar{\lambda} H^\dagger \bar{E}_L L_R \\ & - M_L \bar{L}_L L_R - M_E \bar{E}_L E_R + \text{h.c.}. \end{aligned} \tag{5.2}$$

The parameters $y_\mu, \lambda_E, \lambda_L, \lambda, \bar{\lambda}, M_L, M_E$ are in general complex. However, most of the complex phases are not physical since they can be removed via the field redefinition. It turns out that in the model there are two independent complex phases

$$\phi_y = \arg\left(y_\mu \lambda_L^* \lambda_E^* \lambda\right) \;, \tag{5.3}$$

$$\phi_M = \arg\left(\lambda \bar{\lambda} M_L^* M_E^*\right), \tag{5.4}$$

which are invariant under the phase rotation of the fields and therefore can serve as the sources of new CP violation. In this work, we take the two CP phases to be the phases of $\bar{\lambda}$ and λ_E.

After the spontaneous symmetry breaking of the Higgs field, the leptons acquire masses and the mass matrix of charged leptons is given by

$$\bar{\ell}_L M \ell_R = (\bar{\mu}_L, \bar{L}^-_L, \bar{E}_L) \begin{pmatrix} y_\mu v/\sqrt{2} & 0 & \lambda_E v/\sqrt{2} \\ \lambda_L v/\sqrt{2} & M_L & \lambda v/\sqrt{2} \\ 0 & \bar{\lambda} v/\sqrt{2} & M_E \end{pmatrix} \begin{pmatrix} \mu_R \\ L^-_R \\ E_R \end{pmatrix}. \tag{5.5}$$

Following the notation I adapted for the SM, the leptons in the flavor eigenbasis are denoted collectively as $\ell_L = (\mu_L, L^-_L, E_L)^T$ and $\ell_R = (\mu_R, L^-_R, E_R)^T$.

We can diagonalize the mass matrix in eq. (5.5) by a bi-unitary transformation with two unitary matrices U_L and U_R:

$$U_L^\dagger \begin{pmatrix} y_\mu v & 0 & \lambda_E v \\ \lambda_L v & M_L & \lambda v \\ 0 & \bar{\lambda} v & M_E \end{pmatrix} U_R = \begin{pmatrix} m_\mu & 0 & 0 \\ 0 & m_4 & 0 \\ 0 & 0 & m_5 \end{pmatrix}, \tag{5.6}$$

where the eigenmass m_2 is set to be the mass of muon, m_μ, and the mass ordering is fixed as $m_2 < m_4 < m_5$.

We also note that the mass of the neutral component of the doublet L, $L^0 \equiv \nu_4$, solely originates from the mass term $-M_L \bar{L}_L L_R$ and hence its mass is simply determined by the value of M_L.

5.2 Muon mass

In order to perform the numerical calculations of this model, we need to input the values of the free parameters. In particular, these parameters must be chosen in such a way that the eigenvalue of m_2 after the diagonalization of the mass matrix corresponds to the real value of the muon mass measured in the experiment, namely, $m_\mu = 105.6583755(23)$ MeV [47]. We choose to fix all the parameters except the Yukawa coupling of muon to the Higgs boson, y_μ, and solve the value of y_μ for the correct m_μ.

From the daigonalization of mass matrix, we have

$$U_L^\dagger M_\ell M_\ell^\dagger U_L = \begin{pmatrix} m_\mu^2 & 0 & 0 \\ 0 & m_4^2 & 0 \\ 0 & 0 & m_5^2 \end{pmatrix}. \tag{5.7}$$

We then subtract on both sides the muon mass squared to obtain

$$U_L^\dagger (M_\ell M_\ell^\dagger - m_\mu^2) U_L = \begin{pmatrix} 0 & 0 & 0 \\ 0 & m_4^2 - m_\mu^2 & 0 \\ 0 & 0 & m_5^2 - m_\mu^2 \end{pmatrix}. \tag{5.8}$$

This means that the determinant of the quantity $M_\ell M_\ell^\dagger - m_\mu^2 I$ is zero,

$$\det(M_\ell M_\ell^\dagger - m_\mu^2 I) = 0. \tag{5.9}$$

By substituting the mass matrix in eq. (5.5) to the determinant, we get a quadratic function of y_μ,

$$\frac{8}{v^6}\det(M_\ell M_\ell^\dagger - m_\mu^2 I) = c_2 y_\mu^2 + c_1 y_\mu + c_0 = 0\ ,\ c_k = \sum_{n=0}^{3} c_k^{2n}\left(\frac{\sqrt{2}m_\mu}{v}\right)^{2n}, \tag{5.10}$$

with the coefficients c_k^{2n} given by

$$\begin{cases} c_0^0 = \lambda^2|\lambda_E|^2|\bar{\lambda}|^2, \\ c_0^2 = -\lambda^2|\bar{\lambda}|^2 - |\lambda_E|^2|\bar{\lambda}|^2 - \lambda_L^2|\bar{\lambda}|^2 - \lambda_L^2|\lambda_E|^2 - r_L^2|\lambda_E|^2 - r_E^2\lambda_L^2 - r_L^2 r_E^2 + 4r_L r_E \lambda \mathrm{Re}(\bar{\lambda}), \\ c_0^4 = \lambda^2 + \lambda_L^2 + |\bar{\lambda}|^2 + |\lambda_E|^2 + r_L^2 + r_E^2, \\ c_0^6 = -1, \end{cases} \tag{5.11}$$

$$\begin{cases} c_1^0 = 2\lambda_L\left[r_L r_E \mathrm{Re}(\lambda_E\bar{\lambda}) - \lambda|\bar{\lambda}|^2\mathrm{Re}(\lambda_E)\right] \\ c_1^2 = 2\lambda\lambda_L\mathrm{Re}(\lambda_E), \\ c_1^4 = 0, \\ c_1^6 = 0, \end{cases} \tag{5.12}$$

$$\begin{cases} c_2^0 = \lambda^2|\bar{\lambda}|^2 + r_L^2 r_E^2 - 2r_L r_E \lambda\bar{\lambda}, \\ c_2^2 = \lambda^2 - |\bar{\lambda}|^2 - r_L^2 - r_E^2, \\ c_2^4 = 1, \\ c_2^6 = 0. \end{cases} \tag{5.13}$$

Since it is a quadratic function of y_μ, we know that there are in general two solutions for each set of 6 free parameters, $(\lambda_E, \lambda_L, \lambda, \bar{\lambda}, M_L, M_E)$.

5.3 Interactions

In this section, the quantities related to the flavor basis are indexed by Greek alphabets $(\alpha, \beta, \gamma, \cdots)$, while the quantities related to the mass basis are indexed by Latin alphabets $(a, b, c, \cdots)$. For the flavor indices, we have $2 = \mu, 4 = L$ and $5 = E$.

5.3.1 Higgs boson couplings

Since the couplings related to electron and tau are not modified by the vector-like leptons, their couplings with Higgs boson are the SM values $\lambda_{e,\tau} = -m_{e,\tau}/v$. Other couplings of charged leptons to Higgs boson is modified by the mixing with the vector-like leptons. The Yukawa interaction in the flavor basis is given by

$$\mathcal{L}_Y \supset -\frac{1}{\sqrt{2}}\,\bar{\ell}_{L\rho}\,Y_{\rho\sigma}\,\ell_{R\sigma}\,h + \text{h.c.}. \tag{5.14}$$

This can be transformed to the the mass basis given by

$$\mathcal{L}_Y \supset -\frac{1}{\sqrt{2}}\sum_{\rho,\sigma=2,4,5}\bar{\ell}_{La}(U_L^\dagger)_{a\rho}\,Y_{\rho\sigma}\,(U_R)_{\sigma b}\,\ell_{Rb}\,h + \text{h.c.} \equiv \bar{\ell}_{La}\,\lambda_{ab}\,\ell_{Rb}\,h + \text{h.c.}, \tag{5.15}$$

where the Yukawa matrix is written as

$$Y = \begin{pmatrix} y_\mu & 0 & \lambda_E \\ \lambda_L & 0 & \lambda \\ 0 & \bar{\lambda} & 0 \end{pmatrix}, \tag{5.16}$$

and the Yukawa couplings in the mass basis is

$$\lambda_{ab} = -\frac{1}{\sqrt{2}}\sum_{\rho,\sigma=2,4,5}(U_L^\dagger)_{a\rho}Y_{\rho\sigma}\,(U_R)_{\sigma b}\,. \tag{5.17}$$

We notice that the Yukawa coupling in the flavor basis is similar to the mass matrix of the charged leptons with the absence of the masses of vector-like leptons, that is, $Yv/\sqrt{2} = M - \text{diag}(0, M_L, M_E)$. With this relation, the Higgs boson couplings in the

mass basis can be written as:

$$-\lambda v = U_L^\dagger \begin{pmatrix} y_\mu v/\sqrt{2} & 0 & \lambda_E v/\sqrt{2} \\ \lambda_L v/\sqrt{2} & M_L & \lambda v/\sqrt{2} \\ 0 & \bar{\lambda} v/\sqrt{2} & M_E \end{pmatrix} U_R - U_L^\dagger \begin{pmatrix} 0 & 0 & 0 \\ 0 & M_L & 0 \\ 0 & 0 & M_E \end{pmatrix} U_R \tag{5.18}$$

$$= \begin{pmatrix} m_\mu & 0 & 0 \\ 0 & m_4 & 0 \\ 0 & 0 & m_5 \end{pmatrix} - U_L^\dagger \begin{pmatrix} 0 & 0 & 0 \\ 0 & M_L & 0 \\ 0 & 0 & M_E \end{pmatrix} U_R. \tag{5.19}$$

In this expression, we can see clearly that the first term has a simple form which is the same as the Yukawa couplings in the SM. It originates from the mixings between muons and vector-like leptons. The second term corresponds solely to the contributions from the mass term of the vector-like leptons.

5.3.2 Z boson couplings

The couplings of leptons to the Z boson come from the kinetic term of the leptons. Due to the mixing among muon and vector-like leptons, the kinetic term is modified to

$$\mathcal{L}_{\text{kin}} \supset \bar{\ell}_{L\alpha} i \not{D}_\alpha \ell_{L\alpha} + \bar{\ell}_{R\alpha} i \not{D}_\alpha \ell_{R\alpha} = \bar{\ell}_{La} (U_L^\dagger)_{a\sigma} i \not{D}_\sigma (U_L)_{\sigma b} \ell_{Lb} + \bar{\ell}_{Ra} (U_R^\dagger)_{a\sigma} i \not{D}_\sigma (U_R)_{\sigma b} \ell_{Rb}. \tag{5.20}$$

The covariant derivative $D_{\mu\alpha}$ is defined as

$$D_{\mu\sigma} = \partial_\mu + i \frac{g}{\cos\theta_W} (T_\sigma^3 - Q_\sigma \sin^2\theta_W) Z_\mu + ieQ_\sigma A_\mu, \tag{5.21}$$

where T^3 and Q are the weak isospin and electric charge of leptons obtained from the quantum numbers listed in table 5.1.

The couplings of the Z boson to charged leptons ℓ_a and ℓ_b are defined in the Lagrangian

$$\mathcal{L}_Z \supset \left[\bar{\ell}_{La} \gamma^\mu (g_L^Z)_{ab} \ell_{Lb} + \bar{\ell}_{Ra} \gamma^\mu (g_R^Z)_{ab} \ell_{Rb} \right] Z_\mu. \tag{5.22}$$

Couplings of left-handed and right-handed charged leptons with Z boson are given by

$$(g_L^Z)_{ab} = -\frac{g}{\cos\theta_W} \sum_{\sigma=2,4,5} (T^3_{L\sigma} - \sin^2\theta_W Q_\sigma)(U_L^\dagger)_{a\sigma}(U_L)_{\sigma b}, \tag{5.23}$$

$$(g_R^Z)_{ab} = -\frac{g}{\cos\theta_W} \sum_{\sigma=2,4,5} (T^3_{R\sigma} - \sin^2\theta_W Q_\sigma)(U_R^\dagger)_{a\sigma}(U_R)_{\sigma b}, \tag{5.24}$$

where the electric charge Q_σ and the third component of weak isospins $T^3_{L\sigma}$ and $T^3_{R\sigma}$ for each flavor are summarized in the following table 5.2.

Flavor	2	4	5
Q_σ	-1	-1	-1
$T^3_{L\sigma}$	-1/2	-1/2	0
$T^3_{R\sigma}$	0	-1/2	0

TABLE 5.2: This table shows the electric charge Q_σ and the third component of weak isospins $T^3_{L\sigma}$ and $T^3_{R\sigma}$ for each flavor considered in the mixing of charged leptons. Recall that in the flavor basis, we have $2 = \mu, 4 = L$, and $5 = E$.

Since the electric charge Q_σ is the same for all the charged leptons considered, no modification is made on the couplings of photon with charged leptons. On the other hand, because of the different weak isospins of the charged leptons in the mixing, the couplings of the Z boson in eq. (5.23) and eq. (5.24) are modified from their SM values. In $(g_L^Z)_{ab}$, we have

$$-\frac{g}{\cos\theta_W}\left\{\left(-\frac{1}{2}+\sin^2\theta_W\right)[(U_L^\dagger)_{a2}(U_L)_{2b}+(U_L^\dagger)_{a4}(U_L)_{4b}]+\sin^2\theta_W(U_L^\dagger)_{a5}(U_L)_{5b}\right\}. \tag{5.25}$$

To see the modification to the SM coupling, we can arrange and separate eq. (5.23) in two parts. The first one is

$$-\frac{g}{\cos\theta_W}\left\{\left(-\frac{1}{2}+\sin^2\theta_W\right)[(U_L^\dagger)_{a2}(U_L)_{2b}+(U_L^\dagger)_{a4}(U_L)_{4b}+(U_L^\dagger)_{a5}(U_L)_{5b}]\right\}. \tag{5.26}$$

By the unitarity of the matrix U_L, we have $\sum_{\sigma=2,4,5}(U_L^\dagger)_{a\sigma}(U_L)_{\sigma b} = \delta_{ab}$. This gives the form of the SM coupling of Z boson with the left-handed leptons

$$(g_L^Z)^{\rm SM}_{ab} = -\frac{g}{\cos\theta_W}\left(-\frac{1}{2}+\sin^2\theta_W\right)\delta_{ab}. \tag{5.27}$$

The second one corresponds to the modification of the SM coupling,

$$(\delta g_L^Z)_{ab} = -\frac{g}{2\cos\theta_W}(U_L^\dagger)_{a5}(U_L)_{5b}. \tag{5.28}$$

Similarly, we can separate eq. (5.24) in parts of the SM coupling

$$(g_R^Z)_{ab}^{\rm SM} = -\frac{g}{\cos\theta_W}\sin^2\theta_W\,\delta^{ab} \tag{5.29}$$

and the modification

$$(\delta g_R^Z)_{ab} = \frac{g}{2\cos\theta_W}(U_R^\dagger)_{a4}(U_R)_{4b}. \tag{5.30}$$

5.3.3 W boson couplings

The couplings of W with leptons are also derived from the kinetic term. Since the charged lepton E is an $SU(2)_L$ singlet, it decouples from the interaction with W boson. The kinetic term is given by

$$\mathcal{L}_{\rm kin} \supset -\frac{g}{\sqrt{2}}\left(\bar\nu_{L\mu}\gamma^\mu\mu_L + \bar L_L^0\gamma^\mu L_L^- + \bar L_R^0\gamma^\mu L_R^-\right)W_\mu^+ + h.c. \tag{5.31}$$

$$= -\frac{g}{\sqrt{2}}\left(\bar\nu_{L2}\gamma^\mu(U_L)_{2b}\ell_{Lb} + \bar\nu_{L4}\gamma^\mu(U_L)_{4b}\ell_{Lb} + \bar\nu_{R4}\gamma^\mu(U_R)_{4b}\ell_{Rb}\right)W_\mu^+ + h.c.. \tag{5.32}$$

This can be written in a more compact form

$$\mathcal{L}_W \supset \left[\bar\nu_{La}\gamma^\mu(g_L^W)_{ab}\ell_{Lb} + \bar\nu_{Ra}\gamma^\mu(g_R^W)_{ab}\ell_{Rb}\right]W_\mu^+ + h.c., \tag{5.33}$$

and the couplings of W boson with leptons are defined as

$$(g_L^W)_{2b} = -\frac{g}{\sqrt{2}}(U_L)_{2b}, \qquad (g_L^W)_{4b} = -\frac{g}{\sqrt{2}}(U_L)_{4b}, \tag{5.34}$$

$$(g_R^W)_{4b} = -\frac{g}{\sqrt{2}}(U_R)_{4b}. \tag{5.35}$$

5.4 One-loop diagrams for the muon dipole moments

In this section, we perform the computation of the one-loop contributions to the electromagnetic dipole moments of muon by applying the general formulas discussed in chapter

4. In this model, we need to consider the diagrams of the Higgs, Z boson and W boson mediations, see figure 5.1. These correspond to the neutral scalar boson (section 4.3.1), neutral vector boson (section 4.3.3), and charged vector boson (section 4.3.1), respectively.

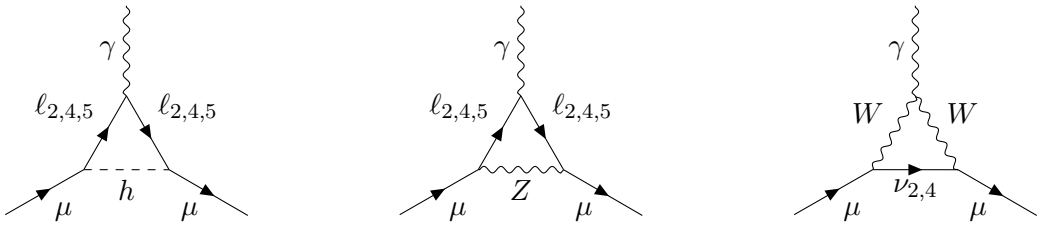

(a) Higgs boson (b) Z boson (c) W boson

FIGURE 5.1: One-loop contributions considered in the model.

5.4.1 Higgs boson mediation

As we discussed in the previous section, the interaction of the Higgs boson with the charged leptons is

$$\bar{\ell}_{Li}\,\lambda_{ij}\,\ell_{Rj}\,h + \bar{\ell}_{Ri}\,\lambda^*_{ji}\,\ell_{Lj}\,h = \bar{\ell}_i(\lambda_{ij}P_R + \lambda^*_{ji}P_L)\ell_j\,h, \tag{5.36}$$

where $P_{L,R}$ are the projection operators for the left-handed and right-handed components of the leptons. This can be rearranged in the form of the scalar and pseudoscalar couplings

$$\bar{\ell}_i(g_s + g_p\gamma_5)\ell_j\,h, \tag{5.37}$$

where

$$g_s = \frac{1}{2}(\lambda_{ij} + \lambda^*_{ji})\ ,\ g_p = \frac{1}{2}(\lambda_{ij} - \lambda^*_{ji}). \tag{5.38}$$

Substituting these couplings, with $j = 2$, into the general formulas, we obtain the contribution to the muon $g-2$ as

$$\Delta a^h_\mu = \frac{m_\mu}{8\pi^2}\sum_{i=2,4,5}\int_0^1 dx\,(1-x)^2\,\frac{m_i \mathrm{Re}(\lambda_{i2}\lambda_{2i}) + x m_\mu(|\lambda_{i2}|^2 + |\lambda_{2i}|^2)/2}{x m_h^2 + (1-x)\,m_i^2}. \tag{5.39}$$

For simplicity, we have neglected terms higher than $\mathcal{O}(m_\mu^2/m_h^2)$ in the integral. In this case, the integration can be carried out easily as

$$g_h(r_i) = \int_0^1 \frac{(1-x)^2}{x+(1-x)r_i}dx = -\frac{r_i^2 - 4r_i + 3 + 2\ln(r_i)}{2(1-r_i)^3}, \tag{5.40}$$

$$f_h(r_i) = \frac{1}{2}\int_0^1 \frac{x(1-x)^2}{x+(1-x)r_i}dx = \frac{r_i^3 - 6r_i^2 + 3r_i + 2 + 6r_i\ln(r_i)}{12(1-r_i)^4}, \tag{5.41}$$

where $r_i = m_i^2/m_h^2$ and $i = 2, 4, 5$.

Then, we obtain the contribution to muon $g-2$ from the Higgs boson,

$$\Delta a_\mu^h = \frac{m_\mu}{8\pi^2 m_h^2}\sum_{i=2,4,5}\left[\left(|\lambda_{i2}|^2 + |\lambda_{2i}|^2\right)m_\mu f_h(r_i) + \mathrm{Re}\left(\lambda_{i2}\lambda_{2i}\right)m_i g_h(r_i)\right]. \tag{5.42}$$

The contribution to the muon EDM can be obtained similarly and the result is

$$d_\mu^h = -\frac{e}{16\pi^2 m_h^2}\sum_{i=2,4,5}\mathrm{Im}(\lambda_{i2}\lambda_{2i})m_i g_h(r_i). \tag{5.43}$$

5.4.2 Z boson mediation

The interaction of charged leptons with Z boson can be written as

$$\bar{\ell}_i\gamma^\mu\left(g_v^Z + g_a^Z\gamma_5\right)\ell_j Z_\mu, \tag{5.44}$$

where

$$g_v^Z = \frac{1}{2}\left[(g_L^Z)_{ij} + (g_R^Z)_{ij}\right]\ ,\ g_a^Z = \frac{1}{2}\left[(-g_L^Z)_{ij} + (g_R^Z)_{ij}\right]. \tag{5.45}$$

By applying the general formula, with $j = 2$, for the case with neutral vector boson, we obtain

$$\begin{aligned}\Delta a_\mu^Z =& \\ \sum_{i=2,4,5}&\frac{m_\mu}{4\pi^2}\int_0^1 dx\,(1-x)\,x\frac{2m_i\mathrm{Re}\left[(g_L^Z)_{i2}(g_R^Z)_{i2}^*\right] - (1+x)\,m_\mu\left[|(g_L^Z)_{i2}|^2 + |(g_R^Z)_{i2}|^2\right]/2}{xm_Z^2 + (1-x)\,m_i^2} \\ &+\frac{m_\mu}{8\pi^2}\int_0^1 dx\,(1-x)^2\,\frac{r_i\left\{m_i\mathrm{Re}\left[(g_L^Z)_{i2}(g_R^Z)_{i2}^*\right] + m_\mu(x-2)\left[|(g_L^Z)_{i2}|^2 + |(g_R^Z)_{i2}|^2\right]/2\right\}}{xm_Z^2 + (1-x)\,m_i^2},\end{aligned} \tag{5.46}$$

where $r_i = m_i^2/m_Z^2$ and $i = 2, 4, 5$. For simplicity, we have neglected terms higher than $\mathcal{O}(m_\mu^2/m_Z^2)$ in the integral. In this case, the integration can be carried out easily as

$$g_Z(r_i) = \int_0^1 \frac{4x(1-x) + r_i(1-x)^2}{x + (1-x)r_i} dx = -\frac{r_i^3 + 3r_i - 4 - 6r_i \ln(r_i)}{2(1-r_i)^3}, \tag{5.47}$$

$$\begin{aligned} f_Z(r_i) &= \frac{1}{2}\int_0^1 \frac{-2x(1-x^2) + r_i(x-2)(1-x)^2}{x + (1-x)r_i} dx \\ &= -\frac{5r_i^4 - 14r_i^3 + 39r_i^2 - 38r_i + 8 - 18r_i^2 \ln(r_i)}{12(1-r_i)^4}. \end{aligned} \tag{5.48}$$

The contribution to muon $g-2$ from the Z boson is now given by

$$\Delta a_\mu^Z = \frac{m_\mu}{8\pi^2 m_Z^2} \sum_{i=2,4,5} \left\{ \left[|(g_L^Z)_{i2}|^2 + |(g_R^Z)_{i2}|^2 \right] m_\mu f_Z(r_i) + \mathrm{Re}\left[(g_L^Z)_{i2} (g_R^{Z*})_{i2} \right] m_i g_Z(r_i) \right\}. \tag{5.49}$$

Similarly, we can calculate the contribution to muon EDM and the result is

$$d_\mu^Z = \frac{e}{16\pi^2 m_Z^2} \sum_{i=2,4,5} \mathrm{Im}\left[(g_L^Z)_{i2} (g_R^{Z*})_{i2} \right] m_i g_Z(r_i). \tag{5.50}$$

5.4.3 W boson mediation

The interaction of charged leptons with W boson can be written as

$$\bar{\nu}_i \gamma^\mu \left(g_v^W + g_a^W \gamma_5 \right) \ell_j W_\mu^+, \tag{5.51}$$

where

$$g_v^W = \frac{1}{2}\left[(g_L^W)_{ij} + (g_R^W)_{ij} \right] \ , \ g_a^W = \frac{1}{2}\left[(-g_L^W)_{ij} + (g_R^W)_{ij} \right]. \tag{5.52}$$

By applying the general formula, with $j = 2$, for the case with charged vector boson, we obtain

$$\begin{aligned}
\Delta a_\mu^W = & \sum_{i=2,4} \\
& \frac{m_\mu}{8\pi^2}\int_0^1 dx(1-x)^2 \frac{m_\mu(3-2x)\left[|(g_L^W)_{i2}|^2+|(g_R^W)_{i2}|^2/2\right]-3m_{\nu i}\mathrm{Re}\left[(g_L^W)_{i2}(g_R^W)_{i2}^*\right]}{xm_{\nu i}^2+(1-x)m_W^2} \\
+ & \frac{m_\mu}{8\pi^2}\int_0^1 dx(1-x)^2 \frac{m_\mu\left[|(g_L^W)_{i2}|^2+|(g_R^W)_{i2}|^2/2\right]-m_{\nu i}\mathrm{Re}\left[(g_L^W)_{i2}(g_R^W)_{i2}^*\right]}{xm_{\nu i}^2+(1-x)m_W^2} \\
- & \frac{m_\mu}{8\pi^2}\int_0^1 dx\, r_i\left\{\frac{-x\left(1-x^2\right)m_\mu\left[|(g_L^W)_{i2}|^2+|(g_R^W)_{i2}|^2/2\right]+x(1-x)\mathrm{Re}\left[(g_L^W)_{i2}(g_R^W)_{i2}^*\right]}{xm_{\nu i}^2+(1-x)\,m_W^2}\right\}.
\end{aligned} \tag{5.53}$$

where $m_{\nu 2} = m_{\nu_\mu} \simeq 0$, $m_{\nu 4} = M_L$, $r_2 = m_{\nu_\mu}^2/m_W^2$ and $r_4 = M_L^2/m_W^2$. For simplicity, we have neglected terms higher than $\mathcal{O}(m_\mu^2/m_W^2)$ in the integral. In this case, the integration can be carried out easily as

$$g_W(r) = -\int_0^1 \frac{3(1-x)^2+(1-x)^2+rx(1-x)}{(1-x)+xr}dx = \frac{r^3-12r^2+15r-4+6r^2\ln(r)}{2(1-r)^3}, \tag{5.54}$$

$$\begin{aligned}
f_W(r) &= \frac{1}{2}\int_0^1 \frac{(3-2x)(1-x)^2+(1-x)^2+rx(1-x^2)}{(1-x)+xr}dx \\
&= \frac{4r^4-49r^3+78r^2-43r+10+18r^3\ln(r)}{12(1-r)^4}.
\end{aligned} \tag{5.55}$$

Neglecting the vanishingly small mass of the muon neutrino, the contribution from W boson is then given by

$$\Delta a_\mu^W = \sum_{i=2,4}\frac{m_\mu}{8\pi^2 m_W^2}\left\{\left[|(g_L^W)_{i2}|^2+|(g_R^W)_{i2}|^2\right]m_\mu f_W(r_i)\right\}+\mathrm{Re}\left[(g_L^W)_{42}(g_R^{W*})_{42}\right]M_L g_W(r_4), \tag{5.56}$$

while the muon EDM originates from the W mediation can be calculated similarly and the result is

$$d_\mu^W = \frac{e}{16\pi^2 m_W^2}\mathrm{Im}\left[(g_L^W)_{42}(g_R^{W*})_{42}\right]M_L g_W(r_4). \tag{5.57}$$

As we discussed in section 4.5, all electromagnetic dipole moments from different diagrams acquire enhancements from the new sources of chirality flip provided by the mass of extra vector-like leptons, m_4, m_5, or M_L.

Because the contributions from the SM are also contained in the modified $\mu - \mu - h$, $\mu - \mu - Z$, and $\mu - \nu_\mu - W$ couplings, in the results presented below we subtract the SM contributions from the values obtained in the calculations above. We note that in the parameter space consistent with experimental constraints in this work, the new-physics contributions from these couplings are small compared to the ones from mixings with vector-like leptons. According to the numerical results we obtained, they are typically at the level of 0.1% for the magnetic dipole moment and 0.001% for the electric dipole moment. Therefore these contributions can be safely ignored under our consideration.

5.5 Constraints

In this section, we consider the constraints to the model of vector-like leptons. These include the constraints from precision electroweak measurements, the electron EDM, the Higgs decay such as $h \to \mu^+\mu^-$, and the heavy charged leptons.

5.5.1 Precision electroweak measurements

Since muon and muon neutrino mix with extra vector-like leptons in this model, the gauge couplings in the mass basis are modified, as we have seen in section 5.3. Therefore, several electroweak observables are affected correspondingly, such as the muon lifetime, decay asymmetries involving muons, partial widths of W and Z bosons, etc. These constraints have been considered in the previous analysis [80] and can be translated into upper bounds of the couplings λ_L and λ_E given by

$$\frac{\lambda_L v}{\sqrt{2}M_L} \lesssim 0.04 \ , \ \frac{\lambda_E v}{\sqrt{2}M_E} \lesssim 0.03, \tag{5.58}$$

whose maximum values are adapted in our analysis.

5.5.2 $h \to \mu^+\mu^-$

Since the Yukawa coupling of muon is also modified from its SM value, the deviation from the SM prediction is expected in the decay channel of Higgs boson to a muon pair, $h \to \mu^+\mu^-$. It has been a long history for pursuing the search of dimuon productions

in the Higgs decay, as presented in a series of competitive studies between the ATLAS and CMS groups at CERN [86, 87, 88, 89, 90], with gradually decreasing upper limits on the deviation from the SM prediction. Recently, CMS group claimed that it found the first evidence of the Higgs-to-dimuon decay channel [42] with a significance of 3 standard deviations. Currently, the branching fraction of $h \to \mu^+\mu^-$ is constrained to be within the range $0.8 \times 10^{-4} < \mathcal{B}(h \to \mu^+\mu^-) < 4.5 \times 10^{-4}$ at 95% confidence level. This can be transformed into

$$0.369 < R(h \to \mu^+\mu^-) \equiv \frac{\Gamma(h \to \mu^+\mu^-)}{\Gamma(h \to \mu^+\mu^-)_{\rm SM}} < 2.07, \tag{5.59}$$

which we adapt as a constraint in this analysis.

5.5.3 Electron EDM

The latest measurement of electron EDM is performed by the ACME collaboration [43], which measured the precession of electron spin in a superposition of the quantum states of an electron inside a strong intramolecular electric field. The group obtained a rather strong upper limit on the value of electron EDM,

$$|d_e| < 1.1 \times 10^{-29}\ e \cdot \text{cm} \tag{5.60}$$

at 90% confidence level. Therefore, we need to make sure that all models which can generate an electron EDM must not exceed this upper limit. If there is no parameter space for a value smaller than the bound, then the model should be considered as already excluded. We note that in obtaining the above limit, possible contributions to the spin precession frequency from the CP-odd electron-nucleon scalar coupling are set to zero. In the case of the model of vector-like leptons, such kinds of coupling exist as higher-order quantum effects and therefore can be safely ignored in our analysis.

In the framework of this model, the mixings among muon and extra vector-like leptons may also contribute to a sizable electron EDM. These contributions appear in the internal lepton loop of the two-loop Barr-Zee diagrams shown in figure 5.2, where all possible combinations of muon and vector-like leptons contribute to the inner loop, as shown in figure 5.3.

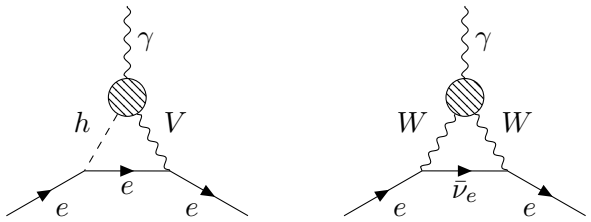

FIGURE 5.2: Contributions to the electron EDM from the Barr-Zee diagram induced by the vector-like leptons.

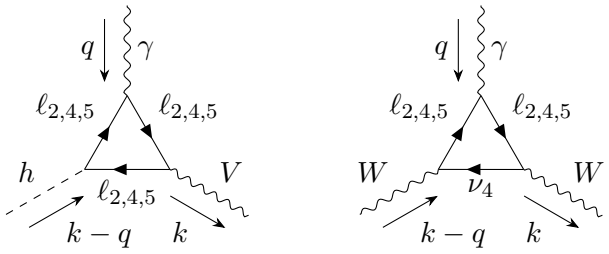

FIGURE 5.3: The inner loop inside the blob of figure 5.2.

To obtain the value of the electron EDM, let us first discuss the left diagram in figure 5.2. The first step is to extract the effective vertex $\Gamma^{\mu\nu}_{hV\gamma}$ from the inner loop. By the gauge invariance of the on-shell photon, $q_\mu \Gamma^{\mu\nu} = 0$, the effective vertex must have the form of [91]

$$i\Gamma^{\mu\nu}_{hV\gamma}(q,k) = i\int_0^1 dx \left[c_E(q^\nu k^\mu - q\cdot k\, g^{\mu\nu}) + ic_O \epsilon^{\mu\nu\alpha\beta} q_\alpha k_\beta\right]. \tag{5.61}$$

We can perform similar calculations as the ones we have done in the one-loop contributions, except that this time we extract coefficients c_E and c_O of the corresponding combinations of momenta. Applying the general Feynman rules listed in section 4.2, we obtain

$$c_E^{ij} = \frac{eQ_i}{4\pi^2}\frac{m_i(1-x)^3(g_s^{ij}g_v^{*ij} - g_p^{ij}g_a^{*ij}) + m_j x^2(1-x)(g_s^{ij}g_v^{*ij} + g_p^{ij}g_a^{*ij})}{-x(1-x)k^2 + (1-x)m_i^2 + xm_j^2}, \tag{5.62}$$

$$c_O^{ij} = \frac{eQ_i}{4\pi^2}\frac{m_i(1-x)^2(g_s^{ij}g_a^{*ij} - g_p^{ij}g_v^{*ij}) - m_j x(1-x)(g_s^{ij}g_a^{*ij} + g_p^{ij}g_v^{*ij})}{-x(1-x)k^2 + (1-x)m_i^2 + xm_j^2}, \tag{5.63}$$

where $i,j = 2,4,5$. The electron EDM can be obtained by attaching the effective vertex to the electron line, which produces the mathematical expression corresponding to the $hV\gamma$ diagram. We notice that for each diagram of $\Gamma^{\mu\nu}_{hV\gamma}$, we need to consider the diagrams with the exchange of propagators of Higgs boson and vector boson, and also with the crossing

between the photon and the vector boson in the inner loop. After a lengthy calculation, we get

$$d_e^{ij} = \frac{-e}{32\pi^4}\int_0^1 dx\Big[\mathrm{Im}(c_E^{ij}g_v^{eV}g_p^{eh*}) - \mathrm{Im}(c_E^{ij}g_a^{eV}g_s^{eh*}) \\ +\mathrm{Im}(c_O^{ij}g_v^{eV}g_s^{eh*}) - \mathrm{Im}(c_O^{ij}g_a^{eV}g_p^{eh*})\Big] \times I_{hV}^{ij}, \tag{5.64}$$

where $i,j = 2,4,5$, g^{eV}s are the couplings of the electron with vector boson and g^{eh}s are the couplings of the electron with Higgs boson. The momentum integration over k in the outer loop, I_{hV}^{ij}, is given by

$$I_{hV}^{ij} = \frac{1}{m_h^2}\left[F\left(x,\frac{m_V^2}{m_h^2},\frac{\Delta_{ij}}{m_h^2}\right) - F\left(x,\frac{m_V^2}{m_h^2},\frac{\Delta_{ij}}{m_V^2}\right)\right], \tag{5.65}$$

where

$$F(x,y,z) = \frac{\ln\frac{z}{x(1-x)}}{(1-y)[z-x(1-x)]}, \tag{5.66}$$

$$\Delta_{ij} = (1-x)m_i^2 + xm_j^2. \tag{5.67}$$

In the expression of d_e^{ij}, particle i is defined as the one who interacts with the external photon, accompanied by particle j in the inner loop of the Barr-Zee diagram. The total contribution is obtained by summing all possible combinations of ij.

For the case that V is a photon, the expression can be greatly simplified because in the inner loop only one type of lepton can exist. Also, we have

$$g_s^{ij} = \frac{1}{2}(\lambda+\lambda^\dagger)_{ij}\ ,\ g_s^{eh} = -\frac{m_e}{v}, \tag{5.68}$$

$$g_p^{ij} = \frac{1}{2}(\lambda-\lambda^\dagger)_{ij}\ ,\ g_p^{eh} = 0, \tag{5.69}$$

$$g_v^{ij} = g_v^{e\gamma} = e, \tag{5.70}$$

$$g_a^{ij} = g_a^{e\gamma} = 0. \tag{5.71}$$

Therefore, only one term, $\mathrm{Im}(c_O^{ij}g_v^{eV}g_s^{eh*})$, remains in the expression of eq. (5.64). With $c_O^{ii} = -em_i(1-x)g_p^{ii}$, the electron EDM from the $h\gamma\gamma$ diagrams is then given by

$$d_e^{h\gamma\gamma} = \sum_{i=2,4,5} -\frac{e^3 m_e m_i}{32\pi^4}\mathrm{Im}(g_p^{ii})\int_0^1 dx(1-x)I_{h\gamma}^{ii}. \tag{5.72}$$

We note that there is a factor of 2 compared to eq. (5.64) beacuse we can cross the two photon lines in the diagram.

For the case that V is a Z boson, we have

$$g_s^{ij} = \frac{1}{2}(\lambda + \lambda^\dagger)_{ij} \ , \ g_s^{eh} = -\frac{m_e}{v}, \tag{5.73}$$

$$g_p^{ij} = \frac{1}{2}(\lambda - \lambda^\dagger)_{ij} \ , \ g_p^{eh} = 0, \tag{5.74}$$

$$g_v^{ij} = \frac{1}{2}(g_L^Z + g_R^Z)_{ij} \ , \ g_v^{eZ} = -\frac{g}{4\cos\theta_W}(-1 + 4\sin^2\theta_{\rm W}), \tag{5.75}$$

$$g_a^{ij} = \frac{1}{2}(-g_L^Z + g_R^Z)_{ij} \ , \ g_a^{eZ} = -\frac{g}{4\cos\theta_W}. \tag{5.76}$$

In this case, we need to sum all possible combinations of charged leptons to obtain the contribution from the $hZ\gamma$ diagrams.

Another class of diagrams is the ones with two W bosons as shown in the right diagram of figure 5.2. In this case, the contribution to the electron EDM originates from the the interaction of the heavy neutrino ν_4 with the charged leptons, and is given by

$$d_e^{WW\gamma} = \frac{eg^2}{256\pi^4} \sum_{i=2,4,5} \frac{m_e m_i M_L}{m_W^2} \mathrm{Im}\left[(g_L^W)_{4i}(g_R^{W*})_{4i}\right] \int_0^1 dx I_{WW}^{4i}, \tag{5.77}$$

where

$$I_{WW}^{4i} = \frac{(1-x)\ln\frac{(1-x)m_i^2 + xM_L^2}{x(1-x)m_W^2}}{-x(1-x)m_W^2 + (1-x)m_i^2 + xM_L^2}. \tag{5.78}$$

5.5.4 Heavy leptons mass

It is possible that the extra vector-like leptons can decay via charged or neutral weak currents through the mixing with the SM leptons of the second generation. The LEP experiment searched for such kinds of decays and set a lower bound on the mass of these new particles [92]. The lower bound is around 100 GeV for these heavy leptons.

5.6 Results

In this section, we show the results of our analysis on the model of vector-like leptons. In the following figures we perform scans through several different parameters, with other

parameters fixed mainly by one specific parameter set

$$\lambda = 0.2\ ,\ |\bar{\lambda}| = 0.58\ ,\ \arg(\bar{\lambda}) = \arg(\lambda_E) = \frac{\pi}{2}\ ,\ M_L = 4\ \text{TeV}\ ,\ M_E = 8\ \text{TeV}, \tag{5.79}$$

and with λ_L and $|\lambda_E|$ determined by their maximum values in eq. (5.58), namely, $\lambda_L \sim 2.3 \times 10^{-4} M_L/\text{GeV}$ and $\lambda_E \sim 1.7 \times 10^{-4} M_E/\text{GeV}$. The Higgs Yukawa coupling of muon, y_μ, chosen to be the larger one of its two solutions. For clarity, we put the values of fixed parameters on the top of each plot. We note that the mass of the vector-like leptons is chosen to be at the TeV scale, therefore the constraints on the heavy leptons discussed above can be safely ignored in this analysis.

The prediction of contribution to the muon $g-2$ as a function of $R(h \to \mu^+\mu^-)$ is shown in figure 5.4, where the region enclosed by the two vertical dotted lines is the one constrained by CMS experiment in [42]. We have examined the behavior over a broad range of the mass parameter M_L. As can be seen from the plot, large M_L around 4 TeV can successfully reproduce the central value of muon $g-2$ within the constraint on $R(h \to \mu^+\mu^-)$ set by CMS, while small M_L fails to reproduce the correct Δa_μ in this case. It is possible to make M_L small, but we need to carefully fine-tune the parameters such that the prediction can barely fit in the region around the 2σ boundary of Δa_μ within the constrained region of $R(h \to \mu^+\mu^-)$ and is therefore not favored.

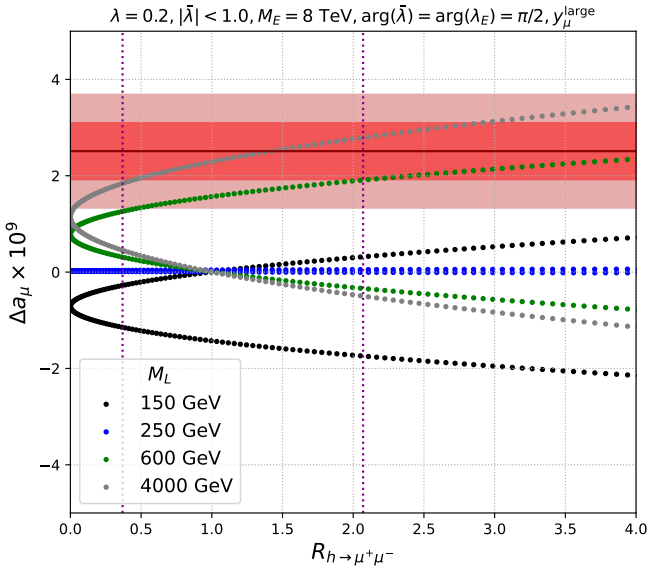

FIGURE 5.4: The prediction of muon $g-2$ as a function of $R(h \to \mu^+\mu^-)$. In this plot, we pick up 4 values of M_L and let $|\bar{\lambda}|$ run through -1 to 1. The region enclosed by the two vertical dotted lines is the one constrained by CMS experiment in [42].

Here, we discuss an interesting feature related to the muon $g-2$ in the model of vector-like lepton. Assuming the vector-like leptons are very heavy, then after integrating them out in the Lagrangian, we obtain an effective Lagrangian including the following terms [93]

$$\begin{aligned}\mathcal{L}_{\text{eff}} \supset & - y_\mu \bar{\ell}_L \mu_R H - C_{\mu H} \bar{\ell}_L \mu_R H \left(H^\dagger H\right) \\ & - C_{\mu B} \bar{\ell}_L \sigma^{\alpha\beta} \mu_R H B_{\alpha\beta} + C_{\mu W} \bar{\ell}_L \sigma^{\alpha\beta} \mu_R \tau^3 H W^3_{\alpha\beta} + \text{h.c.},\end{aligned} \tag{5.80}$$

where $\ell_L = (\nu_\mu, \mu_L)^T$, Cs are the Wilson coefficients of the corresponding operators, $B_{\alpha\beta} = \partial_\alpha B_\beta - \partial_\beta B_\alpha$, and $W^3_{\alpha\beta} = \partial_\alpha W^3_\beta - \partial_\beta W^3_\alpha$. We note that all parameters in $\mathcal{L}_{\text{eff}}$ can be complex in general. We denote the Pauli matrix σ^3 by τ^3 to avoid confusion with $\sigma^{\alpha\beta}$. After expanding the Higgs field in terms of $(0, v+h)^T/\sqrt{2}$, the second term in the first line of $\mathcal{L}_{\text{eff}}$ induces contributions to the mass of muon and the Yukawa coupling of muon to Higgs boson. The terms in the second line give contributions to muon dipole moments. From this effective Lagrangian, we obtain the mass term of muon as $-|m_\mu| \bar{\mu} e^{i\gamma_5 \phi_{m_\mu}} \mu$, where $|m_\mu| = |y_\mu v/\sqrt{2} + C_{\mu H} v^3/2\sqrt{2}|$ and $\tan\phi_{m_\mu} = \text{Im}(m_\mu)/\text{Re}(m_\mu)$. We can transform it into a basis where the mass of muon is real and positive by the chiral transformation of the spinors, $\mu \to e^{-i\gamma_5 \phi_{m_\mu}/2}\mu$ and $\bar{\mu} \to \bar{\mu} e^{-i\gamma_5 \phi_{m_\mu}/2}$. Then, from eq. (5.80) we have [41]

$$\mathcal{L}_{\text{eff}} \supset -m_\mu \bar{\mu}\mu - \left(\lambda^h_{\mu\mu} \bar{\mu} P_R \mu h + \text{h.c.}\right) + \frac{e\Delta a_\mu}{4m_\mu} \bar{\mu}\sigma^{\alpha\beta}\mu F_{\alpha\beta} - i\frac{d_\mu}{2}\bar{\mu}\sigma^{\alpha\beta}\gamma_5 \mu F_{\alpha\beta}, \tag{5.81}$$

with

$$m_\mu = \left(\frac{y_\mu v}{\sqrt{2}} + \frac{C_{\mu H} v^3}{2\sqrt{2}}\right) e^{-i\phi_{m_\mu}}, \tag{5.82}$$

$$\lambda^h_{\mu\mu} = \left(\frac{y_\mu}{\sqrt{2}} + 3\frac{C_{\mu H} v^2}{2\sqrt{2}}\right) e^{-i\phi_{m_\mu}}, \tag{5.83}$$

$$\Delta a_\mu = -\frac{4m_\mu v}{e\sqrt{2}} \text{Re}\left(C_{\mu\gamma} e^{-i\phi_{m_\mu}}\right), \tag{5.84}$$

$$d_\mu = \frac{2v}{\sqrt{2}} \text{Im}\left(C_{\mu\gamma} e^{-i\phi_{m_\mu}}\right), \tag{5.85}$$

where $F_{\alpha\beta} = \partial_\alpha A_\beta - \partial_\beta A_\alpha$ and $C_{\mu\gamma} = C_{\mu B}\cos\theta_W - C_{\mu W}\sin\theta_W$. m_μ, Δa_μ and d_μ correspond to the muon mass, muon $g-2$, muon EDM and they are all real numbers, while the muon Yukawa coupling $\lambda^h_{\mu\mu}$ is complex in general. We see that the phase rotation in muon mass generically contributes to the muon Yukawa coupling, $g-2$, and EDM.[2]

[2]We note that the chiral transformations do not affect the QED interactions, because QED conserves CP symmetry and thus even in the complex formalism, it does not give contribution to the EDM. Actually, it has been shown that such kind of complex phase is redundant in QED [94]. Therefore, the phase can

To see the relation between muon $g-2$ and muon mass, it is convenient to first consider all parameters to be real. In this case, the mass of muon can be simply separated into two terms, $m_\mu = m_\mu^H + m_\mu^{LE}$, where m_μ^H is the mass term from the direct Yukawa interaction of muon with the Higgs boson, $y_\mu v/\sqrt{2}$, while m_μ^{LE} is the contribution from the mixing with vector-like leptons. Then, we can construct a relation between muon $g-2$ and m_μ^{LE} as

$$\Delta a_\mu \simeq -\frac{m_\mu m_\mu^{LE}}{8\pi^2 v^2} \tag{5.86}$$

Therefore, in the limit of heavy vector-like lepton masses, muon $g-2$ and m_μ^{LE} are anticorrelated linearly. This means we need a negative m_μ^{LE} to reproduce the correct value of muon $g-2$. In fact, we can obtain a simple approximation for Δa_μ even in the region of lighter vector-like leptons. In this case, the coefficient -1 is replaced by a function c of the mass of vector-like lepton, and Δa_μ can be approximated as

$$\Delta a_\mu \simeq c\,\frac{m_\mu m_\mu^{LE}}{8\pi^2 v^2} \simeq 0.93\, c\, \Delta a_\mu^{\rm exp} \frac{m_\mu^{LE}}{m_\mu}, \tag{5.87}$$

where c is typically an $\mathcal{O}(1)$ coefficient given by $c = c_W + c_Z + c_h$.[3] We note that although it deviates from the simple linear relation when the imaginary parts of the parameters increase, the approximation is good as we will see in the result on the $\{|\bar{\lambda}|, \arg(\bar{\lambda})\}$-plane that the anticorrelation holds in the parameter region consistent with experimental constraints.

In figure 5.5, we demonstrate the simple linear relation between muon $g-2$ and the contribution to the muon mass from the lepton mixing discussed above. It shows that muon $g-2$ and m_μ^{LE} are positively (negatively) correlated when the value of M_L is small (large). This can be understood by looking at the behavior of the coefficient c and the muon mass contribution from m_μ^{LE}. In the left plot of figure 5.6, we show the predictions of these quantities as a function of M_L, with other parameters fixed by the values in eq. (5.79). All three components of c from the Higgs, W, and Z bosons are also shown explicitly. Intriguing features are that the contributions from the Higgs and Z bosons are

always be rotated away without affecting QED results. We can make the muon mass real from the beginning, or at the end of the loop calculation. Either way, EDM would not be induced.

[3] In the large mass limit, $m_4 \sim M_L$ and $m_5 \sim M_E$, and these functions can be approximated as

$$c_W \sim -2 g_W(r_W)\ ,\ c_Z \sim -g_Z(r_Z)\ ,\ c_h \sim -2\, r_{h4}\, g_h(r_{h4}) - r_{h5}\, g_h(r_{h5}), \tag{5.88}$$

where $r_W = M_L^2/m_W^2$, $r_Z = m_5^2/m_Z^2$, and $r_{h4,5} = m_{4,5}^2/m_h^2$.

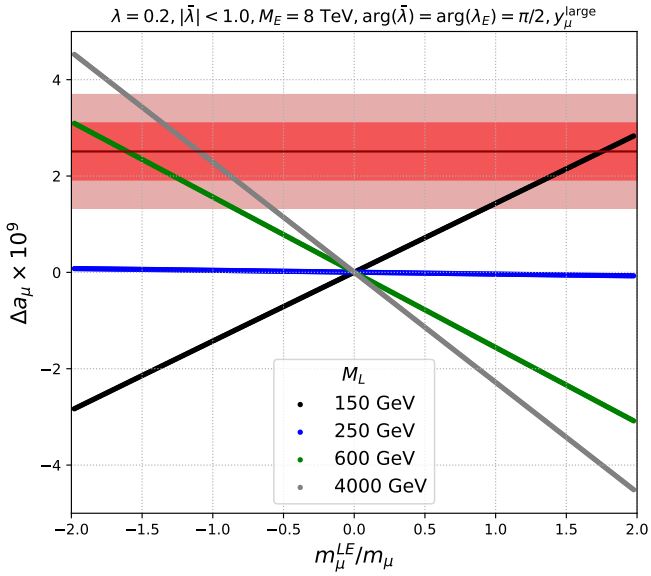

FIGURE 5.5: The prediction of muon $g-2$ as a function of the ratio m_μ^{LE}/m_μ. In this plot, we pick up 4 values of M_L and let $\bar{\lambda}$ run through -1 to 1. We can see a clear linear relation between the muon $g-2$ and m_μ^{LE} from the plot. This linear relation has been discussed in, for example, [80, 82].

opposite to the one from the W boson, and their sum equals minus 2 in a large range of M_L, while the contribution of the W boson decreases to an asymptotic value 1 as M_L increases. These quantities depend on the behavior of the loop functions g_h, g_Z and g_W given in section 5.4. As a result, it shows that the coefficient c is around 1 at $M_L = 100$ GeV and decreases as M_L increases. It then flips the sign when M_L goes across ~ 250 GeV. This means that for the relation (5.87), the slope changes from positive to negative when M_L becomes larger and larger. In our choice of parameters, the mass ratio m_μ^{LE}/m_μ is negative, so in this case, the positive product of $c \cdot m^{LE}/m^\mu$ is available in the large M_L limit where c is also negative and is, therefore, possible to reproduce the correct value of muon $g-2$ when M_L is heavy enough. This is shown explicitly in the right plot of figure 5.6, where the contributions from Higgs, W, and Z bosons are also given separately. For the case with a positive m^{LE}/m^μ, the conclusion on the correlation between the muon $g-2$ and M_L becomes opposite, as can be seen in figure 5.5. In this case, small M_L is necessary for reproducing the muon $g-2$ correctly.

Next, we move on to the prediction of muon EDM in this model. Figure 5.7 shows the predicted muon EDM as a function of M_L, with two specific values of the CP-violating phase in $\bar{\lambda}$, 1.55 and 1.8, which are chosen to show the typical size of the generated muon EDM in the model. The three different contributions from the one-loop diagrams with

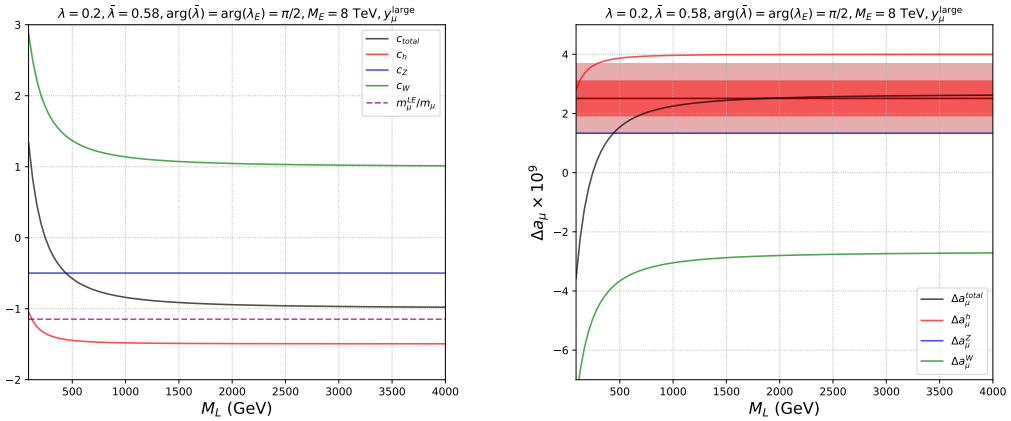

FIGURE 5.6: The left figure shows the behavior of the coefficient c in the relation between the muon $g-2$ and the muon mass contribution from the charged lepton mixing. With the chosen parameters, m^{LE}/m^{μ} is negative. The right figure shows the prediction of the muon $g-2$ as a function of M_L. We see that in the large M_L limit, the prediction lies inside the 1σ band and is very close to the observed central value. All three contributions from the Higgs, W and Z bosons are also given in the plots.

Higgs, W, and Z bosons are also given in the plots. Similar to the result of muon $g-2$, in a large range of M_L the contributions from Higgs and Z bosons are opposite to the one from the W boson. In the large M_L limit considered in this work, the typical size of the muon EDM is around $\mathcal{O}(10^{-23} \sim 10^{-22})\ e \cdot \text{cm}$, whose value is just appropriate for the search of muon EDM at PSI with the frozen-spin technique [72].

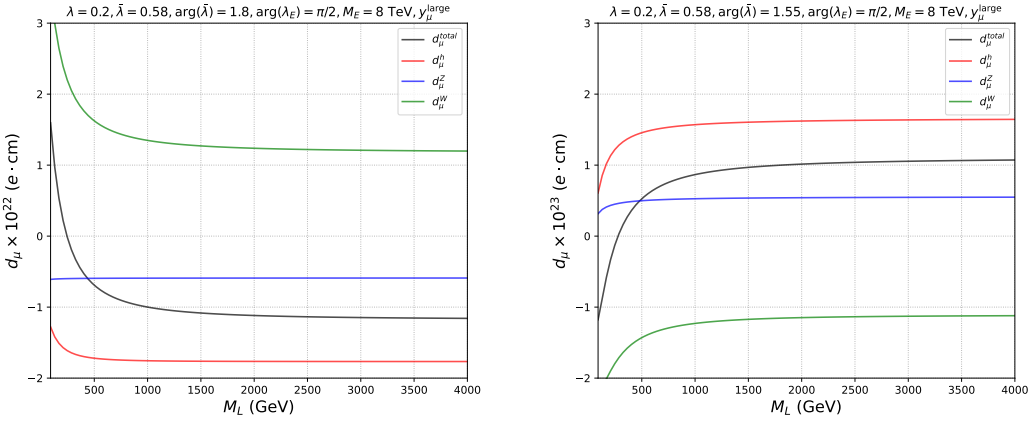

FIGURE 5.7: The prediction of muon EDM at two different values, 1.55 and 1.8, of the CP-violating phase in $\bar{\lambda}$ as a function of M_L. In the large M_L limit considered in this work, the typical size of the muon EDM is $\mathcal{O}(10^{-23} \sim 10^{-22})\ e \cdot \text{cm}$, which is able to be searched at PSI using the frozen-spin technique [72].

We are now ready to present the main result of this analysis. In figure 5.8, the prediction of muon dipole moments are shown on the $\{|\bar{\lambda}|, \arg(\bar{\lambda})\}$-plane, with other parameters

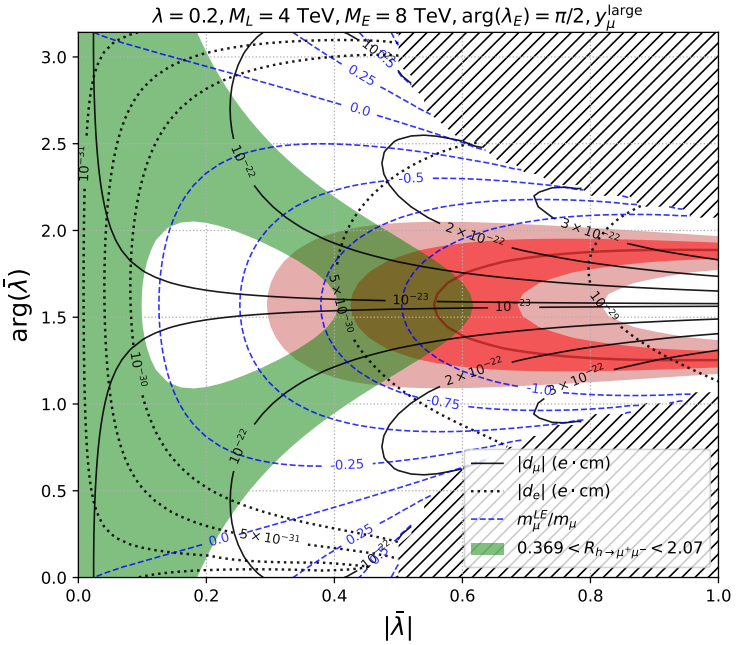

FIGURE 5.8: Predictions of muon dipole moments on the $\{|\bar{\lambda}|, \arg(\bar{\lambda})\}$-plane, with other fixed parameters shown above the plot. The red line and bands are consistent with the central value, 1σ and 2σ regions of muon $g-2$ deviation. Black solid (dotted) lines are the contours of muon (electron) EDM. Blue dashed lines correspond to the mass ratio m_μ^{LE}/m_μ. The green region represents the constraint from the $R(h \to \mu^+\mu^-)$ [42]. In the hatched regions, no correct muon mass is generated after the mass diagonalization.

fixed by the values given in eq. (5.79). The central value, 1σ and 2σ regions of muon $g-2$ deviation is plotted in red. The black solid (dotted) lines are the contours of muon (electron) EDM. The blue dashed lines correspond to the contours of the mass ratio m_μ^{LE}/m_μ indicating the muon mass contribution from the charged lepton mixing. The green region represents the constraint from the $R(h \to \mu^+\mu^-)$ measurement by CMS [42]. The hatched regions are those which do not have a solution to the quadratic equation of y_μ and therefore cannot produce the correct muon mass after the mass diagonalization. We see that the region of muon $g-2$ being consistent with the $R(h \to \mu^+\mu^-)$ constraint lies in $0.3 \lesssim |\bar{\lambda}| \lesssim 0.6$ and $1.0 \lesssim \arg(\bar{\lambda}) \lesssim 2.0$, where the charged lepton mixing tends to give a negative contribution to the muon mass. The typical size of the induced muon EDM is $\mathcal{O}(10^{-23} \sim 10^{-22})$ $e\cdot$cm as mentioned above, while the typical electron EDMs generated are of order $\mathcal{O}(10^{-30})$ $e\cdot$cm. With our choice of parameters, it turns out that the electron EDM serves not as a constraint but more as a prediction that can be searched in future experiments. For example, it is suitable for the proposed experiment in [95], where the NL-eEDM collaboration in the Netherlands plans to measure the electron EDM

in the Barium monofluoride (BaF) molecules with a sensitivity of $\sim 5 \times 10^{-30}\ e \cdot \mathrm{cm}$.

Finally, we show the dependence of the muon and electron EDMs on the two CP-violating phases, $\arg(\bar{\lambda})$ and $\arg(\lambda_E)$, in figure 5.9. As can be seen from the plots, there is a relatively simple correlation between the muon EDM and the two CP-violating phases, while in the case of the electron EDM it is nontrivial because of the complex structure of the two-loop contributions. The gray bands in the figures indicate those with no correct muon mass after the mass diagonalization.

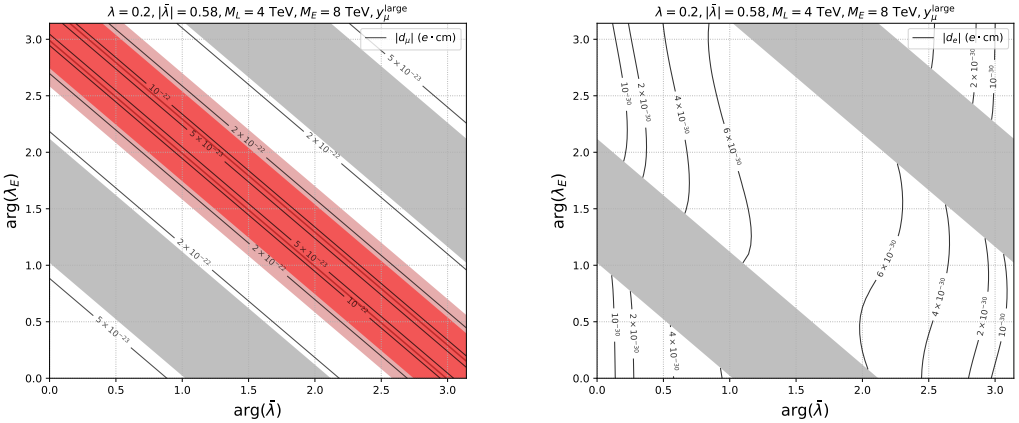

FIGURE 5.9: The dependence of the muon and electron EDMs on the two CP-violating phases $\arg(\bar{\lambda})$ and $\arg(\lambda_E)$. The gray bands correspond to the parameter region which cannot give the correct muon mass after the mass diagonalization.

Chapter 6

Conclusions and outlook

The high-energy physics community has come to an era of precise measurement. Here, physicists pursue the very-precise values of the fundamental physical quantities, such as those listed in the Review of Particle Physics summarized by the Particle Data Group [47]. As the experimental techniques develop and improve, experimentalists have successfully pushed the precision of the measurement to an incredible level. As an instance, in the measurement of the anomalous magnetic dipole moment of the muon, the measured value has been pushed to the 11 digits after the decimal points [21], which is truly amazing work. In the meantime, theoreticians also have made significant progress in the predictions of physical quantities such that the uncertainties become smaller and smaller. It has become so precise that any deviations between the experimental results and the theoretical predictions are speculated to be the signs of physics beyond the SM.

In particular, any discoveries of the EDM of elementary particles are unambiguous signs of new physics, since the SM contribution to such kind of EDM signal is too small and beyond the scope of the current experiment sensitivity. In addition, it is also possible that these new sources of particle EDMs can also solve one of the big puzzles in modern physics, the matter-antimatter asymmetry. In general, it requires new CP-violating processes for the explanation of the observed asymmetry in the universe [24]. Therefore, it is important to continue the search for the EDM of elementary particles.

In order to cope with the proposed experiments on the muon EDM measurements, and also inspired by the deviation on the muon $g-2$ between the experiment and theoretical values, in this thesis, we perform an analysis on the model of vector-like leptons, in

which one $SU(2)_L$ doublet and one $SU(2)_L$ singlet vector-like leptons are introduced as an extension of the SM. We focus on the interaction between the muon and these extra vector-like leptons and take the electromagnetic dipole moments of the muon as useful probes for physics beyond the SM.

In order to fit in the strong constraint of the Higgs-to-dimuon decay channel [42], the mass of vector-like leptons above the TeV scale is preferable, which safely avoids the mass constraint of new lepton searches. In the result in the $\{|\bar{\lambda}|, \arg(\bar{\lambda})\}$-plane, we found that with an appropriate choice of the free parameters in the model, $\lambda = 0.2$, $M_L = 4$ TeV, $M_E = 8$ TeV, $\lambda_L \simeq 0.9$, $|\lambda_E| \simeq 1.4$, $\arg(\lambda_E) = \pi/2$ and the large root of y_μ, the observed deviation of muon $g-2$ can be explained in the available parameter region around $0.3 \lesssim |\bar{\lambda}| \lesssim 0.6$ and $1.0 \lesssim \arg(\bar{\lambda}) \lesssim 2.0$. In this region, the contribution to the muon mass from the charged lepton mixings anticorrelates with muon $g-2$, and the typical size of the induced muon and electron EDMs are of order $\mathcal{O}(10^{-23} \sim 10^{-22})\ e \cdot \mathrm{cm}$ and $\mathcal{O}(5 \times 10^{-30})\ e \cdot \mathrm{cm}$, respectively, which are suitable for the proposed experiments. Muon EDM can be probed by the muEDM collaboration at PSI [72] with a sensitivity of $6 \times 10^{-23}\ e \cdot \mathrm{cm}$ and electron EDM can be searched by the NL-eEDM collaboration in the Netherlands [95] with a sensitivity of $5 \times 10^{-30}\ e \cdot \mathrm{cm}$.

We are looking forward to the real execution of these experiments and to seeing whether there are any signs of the muon EDM. Once the signal is observed, it shows the concrete existence of the physics beyond the SM, and the model of vector-like leptons is one possible candidate, with these heavy extra leptons to be searched in other experiments, such as the LHC at CERN.

Acknowledgement

During the five years of the GSGC program at the University of Tokyo, I would like to express my greatest appreciation to my supervisor, Koichi Hamaguchi, for helping me in all aspects, from physics research to life in Japan. He has always encouraged me to start new things and collaborate with others. When I get lost, a brief discussion with Koichi can make me recover quickly. I can feel his enthusiasm for physics and gain some power for keeping up with research. I cannot thank Koichi enough for accepting me as a member of his research group.

I would also like to express my sincere gratitude to Natsumi Nagata, for the helpful advice and suggestions he gave during the collaboration. I have learned a lot of experience from his impressive insight into physics research, and of how to tackle research problems appropriately.

I am also grateful to all of my collaborators during the past few years, including Kento Asai, Chia-Hung Chang, Chuan-Ren Chen, Shu-Yu Ho, Kazunori Nakayama, Genta Osaki, Koji Tsumura, Juntaro Wada. I thank them so much for all the efforts they spent on the collaboration.

Special thanks to the members of the wakuwaku anime screening party: Kento Asai and Kazunori Nakayama. I am pleased to participate in this activity and we have been doing this for about four years!

I thank all my friends in Japan and Taiwan. Without their company, I may not be able to get through the hard times in my life.

Finally, I would like to show my best appreciation to all the members of the particle physics theory group at the University of Tokyo. I would say that joining this group is the best choice I have made in my life.

This dissertation is based on the work supported by JSPS KAKENHI Grant No.20J22214.

Appendix A

Calculations of the one-loop contributions to dipole moments

In this appendix, we show more details of the calculation of the general one-loop diagrams discussed in chapter 4.

A.1 The vertex function

Here, let us quickly recap the content of the electromagnetic vertex function of the charged leptons. The amplitude related to the electromagnetic dipole moments is given by

$$iM = -ieQ_\ell \overline{u}\left(\ell'\right)\Gamma^\mu\left(q^2\right)u\left(p\right)A_\mu, \tag{A.1}$$

with the vertex function defined by

$$\Gamma^\mu = F_1\left(q^2\right)\gamma^\mu + F_2\left(q^2\right)\frac{i}{2m_\ell}\sigma^{\mu\nu}q_\nu - F_3\left(q^2\right)\sigma^{\mu\nu}q_\nu\gamma_5, \tag{A.2}$$

where

$$q^\mu = p'^\mu - p^\mu. \tag{A.3}$$

The electric charge and electromagnetic dipole moments are related to the form factors in the limit of zero momentum transfer of the vertex function by

$$F_1(0) = 1, \tag{A.4}$$

$$F_2(0) = a_\ell, \tag{A.5}$$

$$F_3(0) = \frac{d_\ell}{eQ_\ell}. \tag{A.6}$$

The Gordon identity is extremely useful in the computation of the dipole moments, which is given by

$$\overline{u}(p')\gamma^\mu u(p) = \frac{1}{2m_\ell}\overline{u}(p')\left[(p'+p)^\mu + i\sigma^{\mu\nu}(p'-p)_\nu\right]u(p). \tag{A.7}$$

A.2 Convention of the momentum flow

Here, we give the convention of momentum directions in the Feynman diagram.

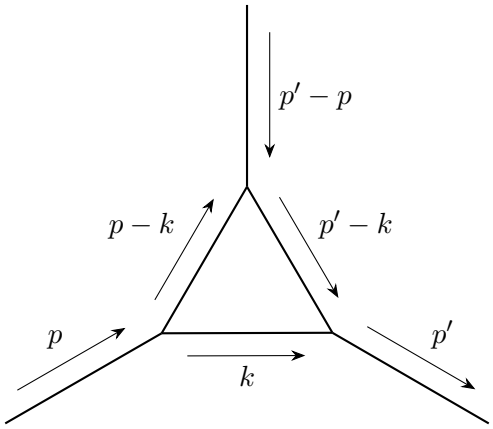

A.3 Scalar boson contribution

In this section, we perform the calculation of the general formulation in the scalar sector. For the Feynman diagrams and the corresponding Feynman rules, please refer to section 4.1.

A.3.1 Neutral scalar boson

The vertex function is given by

$$
\begin{aligned}
-ieQ_\ell\Gamma^\mu = -i^6 eQ_{\ell'} \int \frac{d^4k}{(2\pi)^4} \\
\left(g_s^* - g_p^*\gamma_5\right) \frac{\not{p}' - \not{k} + m_{\ell'}}{(p'-k)^2 - m_{\ell'}^2}\gamma^\mu \frac{\not{p} - \not{k} + m_{\ell'}}{(p-k)^2 - m_{\ell'}^2} \left(g_s + g_p\gamma_5\right) \frac{1}{k^2 - m_S^2}.
\end{aligned} \tag{A.8}
$$

The denominator can be combined by applying the Feynman formula

$$
\frac{1}{A_1 \cdots A_n} = \int dF_n \frac{1}{(x_1A_1 + \cdots + x_nA_n)^n}, \tag{A.9}
$$

where the integration measure over the Feynman parameters x_i is

$$
\int dF_n = (n-1)! \int_0^1 dx_1 \cdots dx_n \delta\left(x_1 + \cdots + x_n - 1\right). \tag{A.10}
$$

In our case, it becomes

$$
\begin{aligned}
\frac{1}{\left[(p'-k)^2 - m_{\ell'}^2\right]\left[(p-k)^2 - m_{\ell'}^2\right]\left(k^2 - m_S^2\right)} = \\
\int dF_3 \frac{1}{\left\{x_1\left[(p'-k)^2 - m_{\ell'}^2\right] + x_2\left[(p-k)^2 - m_{\ell'}^2\right] + x_3\left(k^2 - m_S^2\right)\right\}^3}.
\end{aligned} \tag{A.11}
$$

We can simplify the expression in the denominator:

$$
\begin{aligned}
& x_1\left[\left(p'-k\right)^2 - m_{\ell'}^2\right] + x_2\left[(p-k)^2 - m_{\ell'}^2\right] + x_3\left(k^2 - m_S^2\right) \\
&= x_1p'^2 - 2x_1p'\cdot k + x_1k^2 - x_1m_{\ell'}^2 + x_2p^2 - 2x_2p\cdot k + x_2k^2 - x_2m_{\ell'}^2 + x_3k^2 - x_3m_S^2 \\
&= \left[k - \left(x_1p' + x_2p\right)\right]^2 - \left(x_1p' + x_2p\right)^2 + x_1p'^2 + x_2p^2 - \left(x_1 + x_2\right)m_{\ell'}^2 - x_3m_S^2 \\
&= \ell^2 - D,
\end{aligned} \tag{A.12}
$$

where

$$
\ell \equiv k - \left(x_1p' + x_2p\right), \tag{A.13}
$$

$$
\begin{aligned}
D &\equiv -x_1\left(1-x_1\right)p'^2 - x_2\left(1-x_2\right)p^2 + 2x_1x_2\left(p'\cdot p\right) + \left(x_1+x_2\right)m_{\ell'}^2 + x_3m_S^2 \\
&= -x_1\left(1-x_1\right)m_\ell^2 - x_2\left(1-x_2\right)m_\ell^2 + 2x_1x_2\left(m_\ell^2 - \frac{q^2}{2}\right) + \left(x_1+x_2\right)m_{\ell'}^2 + x_3m_S^2 \\
&= -x_1x_2q^2 + \left(x_1+x_2\right)\left(x_1+x_2-1\right)m_\ell^2 + \left(x_1+x_2\right)m_{\ell'}^2 + x_3m_S^2.
\end{aligned}
\tag{A.14}
$$

In the numerator, we have

$$
\begin{aligned}
&\left(g_s^* - g_p^*\gamma_5\right)\left(\not{p}' - \not{k} + m_{\ell'}\right)\gamma^\mu\left(\not{p} - \not{k} + m_{\ell'}\right)\left(g_s + g_p\gamma_5\right) \\
&= \left(g_s^* - g_p^*\gamma_5\right)\left(\not{p}' - \left(\not{\ell} + x_1\not{p}' + x_2\not{p}\right) + m_{\ell'}\right)\gamma^\mu\left(\not{p} - \left(\not{\ell} + x_1\not{p}' + x_2\not{p}\right) + m_{\ell'}\right)\left(g_s + g_p\gamma_5\right) \\
&= \left(g_s^* - g_p^*\gamma_5\right)\left(-\not{\ell} + \left(1-x_1\right)\not{p}' - x_2\not{p} + m_{\ell'}\right)\gamma^\mu\left(-\not{\ell} - x_1\not{p}' + \left(1-x_2\right)\not{p} + m_{\ell'}\right)\left(g_s + g_p\gamma_5\right) \\
&= \left(g_s^* - g_p^*\gamma_5\right)\not{\ell}\gamma^\mu\not{\ell}\left(g_s + g_p\gamma_5\right) + N^\mu + \text{terms linear in } \ell,
\end{aligned}
\tag{A.15}
$$

where

$$
N^\mu \equiv \left(g_s^* - g_p^*\gamma_5\right)\left[\left(1-x_1\right)\not{p}' - x_2\not{p} + m_{\ell'}\right]\gamma^\mu\left[-x_1\not{p}' + \left(1-x_2\right)\not{p} + m_{\ell'}\right]\left(g_s + g_p\gamma_5\right).
\tag{A.16}
$$

The first term in the last line of eq. (A.15) does not contribute to a_ℓ and d_ℓ since the dipole moment must be finite without divergences, and terms linear in ℓ vanishes after the integration over ℓ. Therefore, what we need to calculate is N^μ, which can be expanded into the following 9 terms. As an illustrative example, we perform the full and direct calculation of N^μ term by term.

1.

$$
\begin{aligned}
&-x_1\left(1-x_1\right)\left(g_s^* - g_p^*\gamma_5\right)\not{p}'\gamma^\mu\not{p}'\left(g_s + g_p\gamma_5\right) \\
&= -x_1\left(1-x_1\right)\left(g_s^*g_s\not{p}'\gamma^\mu\not{p}' + g_s^*g_p\not{p}'\gamma^\mu\not{p}'\gamma_5 - g_sg_p^*\gamma_5\not{p}'\gamma^\mu\not{p}' - g_p^*g_p\gamma_5\not{p}'\gamma^\mu\not{p}'\gamma_5\right) \\
&= -x_1\left(1-x_1\right)\left[\left(g_s^*g_s + g_p^*g_p\right)\not{p}'\gamma^\mu\not{p}' + \left(g_s^*g_p + g_sg_p^*\right)\not{p}'\gamma^\mu\not{p}'\gamma_5\right] \\
&= -x_1\left(1-x_1\right)\left[\left(g_s^*g_s + g_p^*g_p\right)\not{p}'\left(2p'^\mu - \not{p}'\gamma^\mu\right) + \left(g_s^*g_p + g_sg_p^*\right)\not{p}'\left(2p'^\mu - \not{p}'\gamma^\mu\right)\gamma_5\right] \\
&= -x_1\left(1-x_1\right)\left[\left(g_s^*g_s + g_p^*g_p\right)\left(2m_\ell p'^\mu - m_\ell^2\gamma^\mu\right) + \left(g_s^*g_p + g_sg_p^*\right)\left(2m_\ell p'^\mu - m_\ell^2\gamma^\mu\right)\gamma_5\right].
\end{aligned}
$$

2.

$$
\begin{aligned}
&(1-x_1)(1-x_2)\left(g_s^*-g_p^*\gamma_5\right)\not{p}'\gamma^\mu\not{p}\left(g_s+g_p\gamma_5\right)\\
=&(1-x_1)(1-x_2)\left(g_s^*g_s\not{p}'\gamma^\mu\not{p}+g_s^*g_p\not{p}'\gamma^\mu\not{p}\gamma_5-g_sg_p^*\gamma_5\not{p}'\gamma^\mu\not{p}-g_p^*g_p\gamma_5\not{p}'\gamma^\mu\not{p}\gamma_5\right)\\
=&(1-x_1)(1-x_2)\left[\left(g_s^*g_s+g_p^*g_p\right)\not{p}'\gamma^\mu\not{p}+\left(g_s^*g_p+g_sg_p^*\right)\not{p}'\gamma^\mu\not{p}\gamma_5\right]\\
=&(1-x_1)(1-x_2)\,m_\ell^2\left[\left(g_s^*g_s+g_p^*g_p\right)\gamma^\mu-\left(g_s^*g_p+g_sg_p^*\right)\gamma^\mu\gamma_5\right].
\end{aligned}
$$

3.

$$
\begin{aligned}
&(1-x_1)\,m_{\ell'}\left(g_s^*-g_p^*\gamma_5\right)\not{p}'\gamma^\mu\left(g_s+g_p\gamma_5\right)\\
=&(1-x_1)\,m_{\ell'}\left(g_s^*g_s\not{p}'\gamma^\mu+g_s^*g_p\not{p}'\gamma^\mu\gamma_5-g_sg_p^*\gamma_5\not{p}'\gamma^\mu-g_p^*g_p\gamma_5\not{p}'\gamma^\mu\gamma_5\right)\\
=&(1-x_1)\,m_{\ell'}\left[\left(g_s^*g_s-g_p^*g_p\right)\not{p}'\gamma^\mu+\left(g_s^*g_p-g_sg_p^*\right)\not{p}'\gamma^\mu\gamma_5\right]\\
=&(1-x_1)\,m_{\ell'}m_\ell\left[\left(g_s^*g_s-g_p^*g_p\right)\gamma^\mu+\left(g_s^*g_p-g_sg_p^*\right)\gamma^\mu\gamma_5\right].
\end{aligned}
$$

4.

$$
\begin{aligned}
&x_1x_2\left(g_s^*-g_p^*\gamma_5\right)\not{p}\gamma^\mu\not{p}'\left(g_s+g_p\gamma_5\right)\\
=&\,x_1x_2\left(g_s^*g_s\not{p}\gamma^\mu\not{p}'+g_s^*g_p\not{p}\gamma^\mu\not{p}'\gamma_5-g_sg_p^*\gamma_5\not{p}\gamma^\mu\not{p}'-g_p^*g_p\gamma_5\not{p}\gamma^\mu\not{p}'\gamma_5\right)\\
=&\,x_1x_2\left[\left(g_s^*g_s+g_p^*g_p\right)\not{p}\gamma^\mu\not{p}'+\left(g_s^*g_p+g_sg_p^*\right)\not{p}\gamma^\mu\not{p}'\gamma_5\right]\\
=&\,x_1x_2\left(g_s^*g_s+g_p^*g_p\right)\left(2\not{p}'p^\mu-2\left(p'\cdot p\right)\gamma^\mu+2\not{p}p'^\mu-\not{p}'\gamma^\mu\not{p}\right)\\
+&\,x_1x_2\left(g_s^*g_p+g_sg_p^*\right)\left(2\not{p}'p^\mu-2\left(p'\cdot p\right)\gamma^\mu+2\not{p}p'^\mu-\not{p}'\gamma^\mu\not{p}\right)\gamma_5\\
=&\,x_1x_2\left(g_s^*g_s+g_p^*g_p\right)\left(2m_\ell p^\mu-2\left(p'\cdot p\right)\gamma^\mu+2m_\ell p'^\mu-m_\ell^2\gamma^\mu\right)\\
+&\,x_1x_2\left(g_s^*g_p+g_sg_p^*\right)\left(2m_\ell p^\mu-2\left(p'\cdot p\right)\gamma^\mu-2m_\ell p'^\mu+m_\ell^2\gamma^\mu\right)\gamma_5.
\end{aligned}
$$

5.

$$
\begin{aligned}
&-x_2(1-x_2)\left(g_s^*-g_p^*\gamma_5\right)\not{p}\gamma^\mu\not{p}\left(g_s+g_p\gamma_5\right)\\
=&-x_2(1-x_2)\left(g_s^*g_s\not{p}\gamma^\mu\not{p}+g_s^*g_p\not{p}\gamma^\mu\not{p}\gamma_5-g_sg_p^*\gamma_5\not{p}\gamma^\mu\not{p}-g_p^*g_p\gamma_5\not{p}\gamma^\mu\not{p}\gamma_5\right)\\
=&-x_2(1-x_2)\left[\left(g_s^*g_s+g_p^*g_p\right)\not{p}\gamma^\mu\not{p}+\left(g_s^*g_p+g_sg_p^*\right)\not{p}\gamma^\mu\not{p}\gamma_5\right]\\
=&-x_2(1-x_2)\left[\left(g_s^*g_s+g_p^*g_p\right)\left(2p^\mu-\gamma^\mu\not{p}\right)\not{p}+\left(g_s^*g_p+g_sg_p^*\right)\left(2p^\mu-\gamma^\mu\not{p}\right)\not{p}\gamma_5\right]\\
=&-x_2(1-x_2)\left[\left(g_s^*g_s+g_p^*g_p\right)\left(2m_\ell p^\mu-m_\ell^2\gamma^\mu\right)-\left(g_s^*g_p+g_sg_p^*\right)\left(2m_\ell p^\mu+m_\ell^2\gamma^\mu\right)\gamma_5\right].
\end{aligned}
$$

6.

$$
\begin{aligned}
&- x_2 m_{\ell'} \left(g_s^* - g_p^* \gamma_5\right) \not{p} \gamma^\mu \left(g_s + g_p \gamma_5\right) \\
=& - x_2 m_{\ell'} \left(g_s^* g_s \not{p} \gamma^\mu + g_s^* g_p \not{p} \gamma^\mu \gamma_5 - g_s g_p^* \gamma_5 \not{p} \gamma^\mu - g_p^* g_p \gamma_5 \not{p} \gamma^\mu \gamma_5\right) \\
=& - x_2 m_{\ell'} \left[\left(g_s^* g_s - g_p^* g_p\right) \not{p} \gamma^\mu + \left(g_s^* g_p - g_s g_p^*\right) \not{p} \gamma^\mu \gamma_5\right] \\
=& - x_2 m_{\ell'} \left[\left(g_s^* g_s - g_p^* g_p\right) \left(2p^\mu - \gamma^\mu \not{p}\right) + \left(g_s^* g_p - g_s g_p^*\right) \left(2p^\mu - \gamma^\mu \not{p}\right) \gamma_5\right] \\
=& - x_2 m_{\ell'} \left[\left(g_s^* g_s - g_p^* g_p\right) \left(2p^\mu - m_\ell \gamma^\mu\right) + \left(g_s^* g_p - g_s g_p^*\right) \left(2p^\mu + m_\ell \gamma^\mu\right) \gamma_5\right].
\end{aligned}
$$

7.

$$
\begin{aligned}
&- x_1 m_{\ell'} \left(g_s^* - g_p^* \gamma_5\right) \gamma^\mu \not{p}' \left(g_s + g_p \gamma_5\right) \\
=& - x_1 m_{\ell'} \left(g_s^* g_s \gamma^\mu \not{p}' + g_s^* g_p \gamma^\mu \not{p}' \gamma_5 - g_s g_p^* \gamma_5 \gamma^\mu \not{p}' - g_p^* g_p \gamma_5 \gamma^\mu \not{p}' \gamma_5\right) \\
=& - x_1 m_{\ell'} \left[\left(g_s^* g_s - g_p^* g_p\right) \gamma^\mu \not{p}' + \left(g_s^* g_p - g_s g_p^*\right) \gamma^\mu \not{p}' \gamma_5\right] \\
=& - x_1 m_{\ell'} \left[\left(g_s^* g_s - g_p^* g_p\right) \left(2p'^\mu - \not{p}' \gamma^\mu\right) + \left(g_s^* g_p - g_s g_p^*\right) \left(2p'^\mu - \not{p}' \gamma^\mu\right) \gamma_5\right] \\
=& - x_1 m_{\ell'} \left[\left(g_s^* g_s - g_p^* g_p\right) \left(2p'^\mu - m_\ell \gamma^\mu\right) + \left(g_s^* g_p - g_s g_p^*\right) \left(2p'^\mu - m_\ell \gamma^\mu\right) \gamma_5\right].
\end{aligned}
$$

8.

$$
\begin{aligned}
&\left(1 - x_2\right) m_{\ell'} \left(g_s^* - g_p^* \gamma_5\right) \gamma^\mu \not{p} \left(g_s + g_p \gamma_5\right) \\
=& \left(1 - x_2\right) m_{\ell'} \left(g_s^* g_s \gamma^\mu \not{p} + g_s^* g_p \gamma^\mu \not{p} \gamma_5 - g_s g_p^* \gamma_5 \gamma^\mu \not{p} - g_p^* g_p \gamma_5 \gamma^\mu \not{p} \gamma_5\right) \\
=& \left(1 - x_2\right) m_{\ell'} \left[\left(g_s^* g_s - g_p^* g_p\right) \gamma^\mu \not{p} + \left(g_s^* g_p - g_s g_p^*\right) \gamma^\mu \not{p} \gamma_5\right] \\
=& \left(1 - x_2\right) m_{\ell'} m_\ell \left[\left(g_s^* g_s - g_p^* g_p\right) \gamma^\mu - \left(g_s^* g_p - g_s g_p^*\right) \gamma^\mu \gamma_5\right].
\end{aligned}
$$

9.

$$
\begin{aligned}
&m_{\ell'}^2 \left(g_s^* - g_p^* \gamma_5\right) \gamma^\mu \left(g_s + g_p \gamma_5\right) \\
=& \, m_{\ell'}^2 \left(g_s^* g_s \gamma^\mu + g_s^* g_p \gamma^\mu \gamma_5 - g_s g_p^* \gamma_5 \gamma^\mu - g_p^* g_p \gamma_5 \gamma^\mu \gamma_5\right) \\
=& \, m_{\ell'}^2 \left[\left(g_s^* g_s + g_p^* g_p\right) \gamma^\mu - \left(g_s^* g_p + g_s g_p^*\right) \gamma^\mu \gamma_5\right].
\end{aligned}
$$

In the above calculation, the relations $\gamma^\mu \gamma^\nu = 2g^{\mu\nu} - \gamma^\nu \gamma^\mu$ and $\gamma_5 \gamma^\mu = -\gamma^\mu \gamma_5$ are used repeatedly. In the last line of each calculation, the momenta of the on-shell leptons are

replaced by their masses via the equations of motion

$$\not{p} u(p) = m_\ell u(p), \tag{A.17}$$

$$\overline{u}(p') \not{p}' = m_\ell \overline{u}(p'). \tag{A.18}$$

Now we have all ingredients for the one-loop contribution of dipole moments. Let us first collect terms proportional to p^μ and p'^μ in the previous calculation. For the anomalous magnetic dipole moment, we need to keep terms without γ_5:

$$2m_\ell \left(g_s^* g_s + g_p^* g_p\right)\left[(x_1+x_2-1)\left(x_1 p'^\mu + x_2 p^\mu\right)\right] - 2m_{\ell'}\left(g_s^* g_s - g_p^* g_p\right)\left(x_1 p'^\mu + x_2 p^\mu\right). \tag{A.19}$$

The next step is to rewrite eq. (A.19) in the form with terms proportional to $(p'+p)^\mu$ and $(p'-p)^\mu$ and keep the contributions from the former. We obtain

$$m_\ell \left(g_s^* g_s + g_p^* g_p\right)(x_1+x_2)(x_1+x_2-1)\left(p'+p\right)^\mu - m_{\ell'}\left(g_s^* g_s - g_p^* g_p\right)(x_1+x_2)\left(p'+p\right)^\mu. \tag{A.20}$$

By using the Gordon identity eq. (A.7), we can extract terms proportional to $\sigma^{\mu\nu}\left(p'-p\right)_\nu$:

$$\left[m_\ell \left(g_s^* g_s + g_p^* g_p\right)(x_1+x_2)(x_1+x_2-1) - m_{\ell'}\left(g_s^* g_s - g_p^* g_p\right)(x_1+x_2)\right]\left[-i\sigma^{\mu\nu}\left(p'-p\right)_\nu\right]. \tag{A.21}$$

The vertex function now reads

$$\begin{aligned}
\Gamma^\mu_{a_\ell}(q^2) =& -i\frac{Q_{\ell'}}{Q_\ell}\int dF_3 \int \frac{d^4\ell}{(2\pi)^4}\frac{1}{\left(\ell^2 - D\right)^3} \\
&\times \left[m_\ell \left(g_s^* g_s + g_p^* g_p\right)(x_1+x_2)(x_1+x_2-1) - m_{\ell'}\left(g_s^* g_s - g_p^* g_p\right)(x_1+x_2)\right](i\sigma^{\mu\nu}q_\nu) \\
=& -i\frac{Q_{\ell'}}{Q_\ell}\int dF_3 \frac{-i}{32\pi^2 D} \\
&\times \left[m_\ell \left(g_s^* g_s + g_p^* g_p\right)(x_1+x_2)(x_1+x_2-1) - m_{\ell'}\left(g_s^* g_s - g_p^* g_p\right)(x_1+x_2)\right](i\sigma^{\mu\nu}q_\nu) \\
=& \frac{Q_{\ell'}}{Q_\ell}\frac{2m_\ell}{32\pi^2}\int dF_3 \\
&\frac{m_{\ell'}\left(g_s^* g_s - g_p^* g_p\right)(x_1+x_2) - m_\ell\left(g_s^* g_s + g_p^* g_p\right)(x_1+x_2)(x_1+x_2-1)}{-x_1x_2q^2 + (x_1+x_2)(x_1+x_2-1)m_\ell^2 + (x_1+x_2)m_{\ell'}^2 + x_3 m_S^2}\left(\frac{i\sigma^{\mu\nu}q_\nu}{2m_\ell}\right) \\
=& F_2(q^2)\frac{i\sigma^{\mu\nu}q_\nu}{2m_\ell},
\end{aligned} \tag{A.22}$$

where we have Wick-rotated the four-momentum ℓ and the result after integration is

$$\int \frac{d^4\ell}{(2\pi)^4} \frac{1}{\left(\ell^2 - D\right)^3} = -\frac{i}{32\pi^2 D}. \tag{A.23}$$

Finally, we obtain the one-loop contribution to the anomalous magnetic dipole moment:

$$\begin{aligned}
a_\ell &= F_2(0) \\
&= \frac{Q_{\ell'}}{Q_\ell}\frac{m_\ell}{16\pi^2}\, 2\int_0^1 dx_3 \int_0^{1-x_3} dx_2 \int_0^{1-x_3-x_2} dx_1\; \delta(x_1+x_2+x_3-1) \\
&\quad \times \frac{m_{\ell'}\left(g_s^* g_s - g_p^* g_p\right)(x_1+x_2) - m_\ell\left(g_s^* g_s + g_p^* g_p\right)(x_1+x_2)(x_1+x_2-1)}{(x_1+x_2)(x_1+x_2-1)\, m_\ell^2 + (x_1+x_2)\, m_{\ell'}^2 + x_3 m_S^2} \\
&= \frac{Q_{\ell'}}{Q_\ell}\frac{m_\ell}{8\pi^2}\int_0^1 dx_3 \int_0^{1-x_3} dx_2 \frac{m_{\ell'}\left(g_s^* g_s - g_p^* g_p\right)(1-x_3) - m_\ell\left(g_s^* g_s + g_p^* g_p\right)(1-x_3)(-x_3)}{(1-x_3)(-x_3)\, m_\ell^2 + (1-x_3)\, m_{\ell'}^2 + x_3 m_S^2} \\
&= \frac{Q_{\ell'}}{Q_\ell}\frac{m_\ell}{8\pi^2}\int_0^1 dx_3 (1-x_3)^2 \frac{m_{\ell'}\left(g_s^* g_s - g_p^* g_p\right) + x_3 m_\ell\left(g_s^* g_s + g_p^* g_p\right)}{x_3 m_S^2 + (1-x_3)\, m_{\ell'}^2 - x_3(1-x_3)\, m_\ell^2}.
\end{aligned} \tag{A.24}$$

For the electric dipole moment, we need to keep terms with γ_5 in the numerator:

$$\begin{aligned}
&2m_\ell\left(g_s^* g_p + g_s g_p^*\right)\left[-x_1(1-x_1)\, p'^\mu + x_2(1-x_2)\, p^\mu - x_1 x_2\left(p'-p\right)^\mu\right]\gamma_5 \\
&\qquad - 2m_{\ell'}\left(g_s^* g_p - g_s g_p^*\right)\left(x_1 p'^\mu + x_2 p^\mu\right)\gamma_5.
\end{aligned} \tag{A.25}$$

Following the same steps, we rewrite eq. (A.25) and keep terms proportional to $(p'+p)^\mu$:

$$\left\{m_\ell\left(g_s^* g_p + g_s g_p^*\right)\left[x_2(1-x_2) - x_1(1-x_1)\right] - m_{\ell'}\left(g_s^* g_p - g_s g_p^*\right)(x_1+x_2)\right\}\left(p'+p\right)^\mu \gamma_5. \tag{A.26}$$

By using the Gordon identity eq. (A.7), we can extract terms proportional to $\sigma^{\mu\nu}\left(p'-p\right)_\nu$:

$$\begin{aligned}
&\left\{m_\ell\left(g_s^* g_p + g_s g_p^*\right)\left[x_2(1-x_2) - x_1(1-x_1)\right] - m_{\ell'}\left(g_s^* g_p - g_s g_p^*\right)(x_1+x_2)\right\} \\
&\qquad \times\left[-i\sigma^{\mu\nu}\left(p'-p\right)_\nu\right]\gamma_5.
\end{aligned} \tag{A.27}$$

The vertex function then reads

$$\begin{aligned}
\Gamma^{\mu}_{d_\ell}\left(q^2\right) =& -\frac{Q_{\ell'}}{Q_\ell}\int dF_3 \int \frac{d^4\ell}{(2\pi)^4}\frac{1}{\left(\ell^2-D\right)^3} \\
& \times\left\{m_\ell\left(g_s^* g_p + g_s g_p^*\right)\left[x_2\left(1-x_2\right)-x_1\left(1-x_1\right)\right] - m_{\ell'}\left(g_s^* g_p - g_s g_p^*\right)\left(x_1+x_2\right)\right\} \\
& \times\left(-\sigma^{\mu\nu}q_\nu\gamma_5\right) \\
=& -\frac{Q_{\ell'}}{Q_\ell}\int dF_3\ \frac{-i}{32\pi^2 D}\left[-m_{\ell'}\left(g_s^* g_p - g_s g_p^*\right)\left(x_1+x_2\right)\right]\left(-\sigma^{\mu\nu}q_\nu\gamma_5\right) \\
=& -i\frac{Q_{\ell'}}{Q_\ell}\frac{1}{32\pi^2}\int dF_3 \\
& \frac{m_{\ell'}\left(g_s^* g_p - g_s g_p^*\right)\left(x_1+x_2\right)}{-x_1x_2q^2+\left(x_1+x_2\right)\left(x_1+x_2-1\right)m_\ell^2+\left(x_1+x_2\right)m_{\ell'}^2+x_3m_S^2}\left(-\sigma^{\mu\nu}q_\nu\gamma_5\right) \\
=& \ F_3\left(q^2\right)\left(-\sigma^{\mu\nu}q_\nu\gamma_5\right).
\end{aligned} \tag{A.28}$$

In the above calculation, the term proportional to m_ℓ vanishes after we integrate over the Feynman parameters since this part is antisymmetric under the exchange of x_1 and x_2. Then, we obtain the one-loop contribution to the electric dipole moment:

$$\begin{aligned}
d_\ell =& \ eQ_\ell F_3\left(0\right) \\
=& -i\frac{eQ_{\ell'}}{32\pi^2}\ 2\int_0^1 dx_3\int_0^{1-x_3}dx_2\int_0^{1-x_3-x_2}dx_1\ \delta\left(x_1+x_2+x_3-1\right) \\
& \times\frac{m_{\ell'}\left(g_s^* g_p - g_s g_p^*\right)\left(x_1+x_2\right)}{\left(x_1+x_2\right)\left(x_1+x_2-1\right)m_\ell^2+\left(x_1+x_2\right)m_{\ell'}^2+x_3m_S^2} \\
=& -i\frac{eQ_{\ell'}}{16\pi^2}\int_0^1 dx_3\int_0^{1-x_3}dx_2\frac{m_{\ell'}\left(g_s^* g_p - g_s g_p^*\right)\left(1-x_3\right)}{\left(1-x_3\right)\left(-x_3\right)m_\ell^2+\left(1-x_3\right)m_{\ell'}^2+x_3m_S^2} \\
=& -i\frac{eQ_{\ell'}}{16\pi^2}\int_0^1 dx_3\left(1-x_3\right)^2\frac{m_{\ell'}\left(g_s^* g_p - g_s g_p^*\right)}{x_3m_S^2+\left(1-x_3\right)m_{\ell'}^2-x_3\left(1-x_3\right)m_\ell^2}.
\end{aligned} \tag{A.29}$$

A.3.2 Charged scalar boson

The vertex function is written as

$$\begin{aligned}
-ieQ_\ell\Gamma^\mu =& -i^6 eQ_S\int\frac{d^4k}{(2\pi)^4} \\
& \left(g_s^*-g_p^*\gamma_5\right)\frac{\not{k}+m_{\ell'}}{k^2-m_{\ell'}^2}\left(g_s+g_p\gamma_5\right)\left(p'+p-2k\right)^\mu\frac{1}{\left(p'-k\right)^2-m_S^2}\frac{1}{\left(p-k\right)^2-m_S^2}.
\end{aligned} \tag{A.30}$$

The denominator can be rewritten as

$$\frac{1}{\left[(p'-k)^2-m_S^2\right]\left[(p-k)^2-m_S^2\right]\left(k^2-m_{\ell'}^2\right)}= \int dF_3 \frac{1}{\left\{x_1\left[(p'-k)^2-m_S^2\right]+x_2\left[(p-k)^2-m_S^2\right]+x_3\left(k^2-m_{\ell'}^2\right)\right\}^3}. \quad \text{(A.31)}$$

Then we can simplify the expression:

$$\begin{aligned} & x_1\left[\left(p'-k\right)^2-m_S^2\right]+x_2\left[(p-k)^2-m_S^2\right]+x_3\left(k^2-m_{\ell'}^2\right) \\ &= x_1 p'^2-2x_1 p'\cdot k+x_1 k^2-x_1 m_S^2+x_2 p^2-2x_2 p\cdot k+x_2 k^2-x_2 m_S^2+x_3 k^2-x_3 m_{\ell'}^2 \\ &= \left[k-\left(x_1 p'+x_2 p\right)\right]^2-\left(x_1 p'+x_2 p\right)^2+x_1 p'^2+x_2 p^2-\left(x_1+x_2\right)m_S^2-x_3 m_{\ell'}^2 \\ &= \ell^2-D, \end{aligned} \quad \text{(A.32)}$$

where

$$\ell \equiv k-\left(x_1 p'+x_2 p\right), \quad \text{(A.33)}$$

$$\begin{aligned} D &\equiv -x_1\left(1-x_1\right)p'^2-x_2\left(1-x_2\right)p^2+2x_1x_2\left(p'\cdot p\right)+\left(x_1+x_2\right)m_S^2+x_3 m_{\ell'}^2 \\ &= -x_1\left(1-x_1\right)m_\ell^2-x_2\left(1-x_2\right)m_\ell^2+2x_1x_2\left(m_\ell^2-\frac{q^2}{2}\right)+\left(x_1+x_2\right)m_S^2+x_3 m_{\ell'}^2 \\ &= -x_1x_2q^2+\left(x_1+x_2\right)\left(x_1+x_2-1\right)m_\ell^2+\left(x_1+x_2\right)m_S^2+x_3 m_{\ell'}^2. \end{aligned} \quad \text{(A.34)}$$

In the numerator, we have

$$\begin{aligned} & \left(g_s^*-g_p^*\gamma_5\right)\left(\not{k}+m_{\ell'}\right)\left(g_s+g_p\gamma_5\right)\left(p'+p-2k\right)^\mu \\ &= \left(g_s^*-g_p^*\gamma_5\right)\left(\not{\ell}+x_1\not{p}'+x_2\not{p}+m_{\ell'}\right)\left(g_s+g_p\gamma_5\right)\left[p'+p-2\left(\ell+x_1p'+x_2p\right)\right]^\mu. \end{aligned} \quad \text{(A.35)}$$

Following the same argument as we discussed in the previous section, we keeping only terms independent of ℓ, we have

$$\left(g_s^*-g_p^*\gamma_5\right)\left(x_1\not{p}'+x_2\not{p}+m_{\ell'}\right)\left(g_s+g_p\gamma_5\right)\left[\left(1-2x_1\right)p'+\left(1-2x_2\right)p\right]^\mu. \quad \text{(A.36)}$$

Then we simplify the numerator by performing a lengthy computation with the gamma matrix algebra. Since the calculation is similar to the one perform in the previous section, to save the space we skip this procedure. The vertex function for the anomalous magnetic

dipole moment is given by

$$\begin{aligned}
\Gamma^{\mu}_{a_\ell}\left(q^2\right) =& -i\frac{Q_S}{Q_\ell}\int dF_3 \int \frac{d^4\ell}{\left(2\pi\right)^4}\frac{1}{\left(\ell^2-D\right)^3} \\
&\times\left[m_\ell\left(x_1+x_2\right)\left(g_s^*g_s+g_p^*g_p\right)+m_{\ell'}\left(g_s^*g_s-g_p^*g_p\right)\right]\left(1-x_1-x_2\right)\left[i\sigma^{\mu\nu}\left(p'-p\right)_\nu\right] \\
=& -i\frac{Q_S}{Q_\ell}\int dF_3\ \frac{-i}{32\pi^2 D} \\
&\times\left[m_\ell\left(x_1+x_2\right)\left(g_s^*g_s+g_p^*g_p\right)+m_{\ell'}\left(g_s^*g_s-g_p^*g_p\right)\right]\left(1-x_1-x_2\right)\left(i\sigma^{\mu\nu}q_\nu\right) \\
=& -\frac{Q_S}{Q_\ell}\frac{2m_\ell}{32\pi^2}\int dF_3 \\
&\frac{\left[m_\ell\left(x_1+x_2\right)\left(g_s^*g_s+g_p^*g_p\right)+m_{\ell'}\left(g_s^*g_s-g_p^*g_p\right)\right]\left(1-x_1-x_2\right)}{-x_1x_2q^2+\left(x_1+x_2\right)\left(x_1+x_2-1\right)m_\ell^2+\left(x_1+x_2\right)m_S^2+x_3m_{\ell'}^2}\left(\frac{i\sigma^{\mu\nu}q_\nu}{2m_\ell}\right) \\
=& F_2\left(q^2\right)\frac{i\sigma^{\mu\nu}q_\nu}{2m_\ell}.
\end{aligned} \tag{A.37}$$

We obtain the one-loop contribution to the anomalous magnetic dipole moment:

$$\begin{aligned}
a_\ell =& F_2\left(0\right) \\
=& -\frac{Q_S}{Q_\ell}\frac{m_\ell}{16\pi^2}\ 2\int_0^1 dx_3\int_0^{1-x_3}dx_2\int_0^{1-x_3-x_2}dx_1\ \delta\left(x_1+x_2+x_3-1\right) \\
&\times\frac{\left[m_\ell\left(x_1+x_2\right)\left(g_s^*g_s+g_p^*g_p\right)+m_{\ell'}\left(g_s^*g_s-g_p^*g_p\right)\right]\left(1-x_1-x_2\right)}{\left(x_1+x_2\right)\left(x_1+x_2-1\right)m_\ell^2+\left(x_1+x_2\right)m_S^2+x_3m_{\ell'}^2} \\
=& -\frac{Q_S}{Q_\ell}\frac{m_\ell}{8\pi^2}\int_0^1 dx_3\int_0^{1-x_3}dx_2\frac{\left[m_\ell\left(1-x_3\right)\left(g_s^*g_s+g_p^*g_p\right)+m_{\ell'}\left(g_s^*g_s-g_p^*g_p\right)\right]x_3}{-x_3\left(1-x_3\right)m_\ell^2+\left(1-x_3\right)m_S^2+x_3m_{\ell'}^2} \\
=& -\frac{Q_S}{Q_\ell}\frac{m_\ell}{8\pi^2}\int_0^1 dx_3\left(1-x_3\right)x_3\frac{\left(1-x_3\right)m_\ell\left(g_s^*g_s+g_p^*g_p\right)+m_{\ell'}\left(g_s^*g_s-g_p^*g_p\right)}{x_3m_{\ell'}^2+\left(1-x_3\right)m_S^2-x_3\left(1-x_3\right)m_\ell^2}.
\end{aligned} \tag{A.38}$$

For the contribution to the electric dipole moment, the vertex function is given by

$$\begin{aligned}
\Gamma^{\mu}_{d_\ell}\left(q^2\right) =& -\frac{Q_S}{Q_\ell}\int dF_3\int\frac{d^4\ell}{\left(2\pi\right)^4}\frac{1}{\left(\ell^2-D\right)^3}\ m_{\ell'}\left(g_s^*g_s-g_p^*g_p\right)\left(1-x_1-x_2\right)\left(-\sigma^{\mu\nu}q_\nu\gamma_5\right) \\
=& -\frac{Q_S}{Q_\ell}\int dF_3\ \frac{-i}{32\pi^2 D}\ m_{\ell'}\left(g_s^*g_s-g_p^*g_p\right)\left(1-x_1-x_2\right)\left(-\sigma^{\mu\nu}q_\nu\gamma_5\right) \\
=& i\frac{Q_S}{Q_\ell}\frac{1}{32\pi^2}\int dF_3 \\
&\frac{m_{\ell'}\left(g_s^*g_s-g_p^*g_p\right)\left(1-x_1-x_2\right)}{-x_1x_2q^2+\left(x_1+x_2\right)\left(x_1+x_2-1\right)m_\ell^2+\left(x_1+x_2\right)m_S^2+x_3m_{\ell'}^2}\left(-\sigma^{\mu\nu}q_\nu\gamma_5\right) \\
=& F_3\left(q^2\right)\left(-\sigma^{\mu\nu}q_\nu\gamma_5\right).
\end{aligned} \tag{A.39}$$

The one-loop contribution to the electric dipole moment is then

$$\begin{aligned} d_\ell &= eQ_\ell F_3(0) \\ &= i\frac{eQ_S}{32\pi^2}\,2\int_0^1 dx_3\int_0^{1-x_3} dx_2\int_0^{1-x_3-x_2} dx_1\;\delta(x_1+x_2+x_3-1) \\ &\quad\times\frac{m_{\ell'}\left(g_s^*g_s-g_p^*g_p\right)(1-x_1-x_2)}{(x_1+x_2)(x_1+x_2-1)m_\ell^2+(x_1+x_2)m_S^2+x_3m_{\ell'}^2} \\ &= i\frac{eQ_S}{16\pi^2}\int_0^1 dx_3\int_0^{1-x_3} dx_2\frac{m_{\ell'}\left(g_s^*g_s-g_p^*g_p\right)x_3}{(1-x_3)(-x_3)m_\ell^2+(1-x_3)m_S^2+x_3m_{\ell'}^2} \\ &= i\frac{eQ_S}{16\pi^2}\int_0^1 dx_3\,(1-x_3)\,x_3\frac{m_{\ell'}\left(g_s^*g_p-g_sg_p^*\right)}{x_3m_{\ell'}^2+(1-x_3)m_S^2-x_3(1-x_3)m_\ell^2}. \end{aligned} \tag{A.40}$$

A.4 Vector boson contribution

In this section, we perform the calculation of the general formulation in the vector sector. For the Feynman diagrams and the corresponding Feynman rules, please refer to section 4.1.

A.4.1 Neutral vector boson

The vertex function is given by

$$\begin{aligned} -ieQ_\ell\Gamma^\mu = i^6eQ_{\ell'}\int\frac{d^4k}{(2\pi)^4} \\ \gamma^\rho\left(g_v^*+g_a^*\gamma_5\right)\frac{\not{p}'-\not{k}+m_{\ell'}}{(p'-k)^2-m_{\ell'}^2}\gamma^\mu\frac{\not{p}-\not{k}+m_{\ell'}}{(p-k)^2-m_{\ell'}^2}\gamma^\sigma\left(g_v+g_a\gamma_5\right)\frac{g_{\rho\sigma}}{k^2-m_V^2}. \end{aligned} \tag{A.41}$$

We can rewrite the denominator as

$$\begin{aligned} \frac{1}{\left[(p'-k)^2-m_{\ell'}^2\right]\left[(p-k)^2-m_{\ell'}^2\right]\left(k^2-m_V^2\right)} = \\ \int dF_3\frac{1}{\left\{x_1\left[(p'-k)^2-m_{\ell'}^2\right]+x_2\left[(p-k)^2-m_{\ell'}^2\right]+x_3\left(k^2-m_V^2\right)\right\}^3}. \end{aligned} \tag{A.42}$$

It has the same structure as the denominator of the neutral scalar mediation, with the scalar boson replaced by a vector boson. Therefore, the denominator can be simplified to

$$\int dF_3\frac{1}{\left(\ell^2-D\right)^3}, \tag{A.43}$$

where

$$\ell \equiv k - \left(x_1 p' + x_2 p\right), \tag{A.44}$$

$$D \equiv -x_1 x_2 q^2 + (x_1 + x_2)(x_1 + x_2 - 1) m_\ell^2 + (x_1 + x_2) m_{\ell'}^2 + x_3 m_V^2. \tag{A.45}$$

After the index contraction, the numerator becomes

$$\begin{aligned} &\gamma^\rho \left(g_v^* + g_a^* \gamma_5\right) \left(\not{p}' - \not{k} + m_{\ell'}\right) \gamma^\mu \left(\not{p} - \not{k} + m_{\ell'}\right) \gamma_\rho \left(g_v + g_a \gamma_5\right) \\ &= \gamma^\rho \left(g_v^* + g_a^* \gamma_5\right) \left(-\not{\ell} + (1 - x_1)\not{p}' - x_2 \not{p} + m_{\ell'}\right) \gamma^\mu \\ &\qquad \times \left(-\not{\ell} - x_1 \not{p}' + (1 - x_2)\not{p} + m_{\ell'}\right) \gamma_\rho \left(g_v + g_a \gamma_5\right). \end{aligned} \tag{A.46}$$

Following the same procedure of the simplification of the numerator (lengthy calculations with gamma matrix algebra), we obtain the vertex function for the anomalous magnetic dipole moment as

$$\begin{aligned} \Gamma_{a_\ell}^\mu \left(q^2\right) =& -i \frac{Q_{\ell'}}{Q_\ell} \int dF_3 \int \frac{d^4\ell}{(2\pi)^4} \frac{1}{\left(\ell^2 - D\right)^3} [-2m_\ell \left(g_v^* g_v + g_a^* g_a\right)(x_1 + x_2 - 1)(x_1 + x_2 - 2) \\ &\qquad + 4m_{\ell'} \left(g_v^* g_v - g_a^* g_a\right)(1 - x_1 - x_2)] \left(-i\sigma^{\mu\nu} q_\nu\right) \\ =& \, i \frac{Q_{\ell'}}{Q_\ell} \int dF_3 \, \frac{-i}{32\pi^2 D} [-2m_\ell \left(g_v^* g_v + g_a^* g_a\right)(x_1 + x_2 - 1)(x_1 + x_2 - 2) \\ &\qquad + 4m_{\ell'} \left(g_v^* g_v - g_a^* g_a\right)(1 - x_1 - x_2)] \left(i\sigma^{\mu\nu} q_\nu\right) \\ =& \frac{Q_{\ell'}}{Q_\ell} \frac{2m_\ell}{32\pi^2} \int dF_3 \\ &\frac{[-2m_\ell \left(g_v^* g_v + g_a^* g_a\right)(x_1 + x_2 - 1)(x_1 + x_2 - 2) + 4m_{\ell'} \left(g_v^* g_v - g_a^* g_a\right)(1 - x_1 - x_2)]}{-x_1 x_2 q^2 + (x_1 + x_2)(x_1 + x_2 - 1) m_\ell^2 + (x_1 + x_2) m_{\ell'}^2 + x_3 m_V^2} \\ &\qquad \times \left(\frac{i\sigma^{\mu\nu} q_\nu}{2m_\ell}\right) \\ =& \, F_2\left(q^2\right) \frac{i\sigma^{\mu\nu} q_\nu}{2m_\ell}. \end{aligned} \tag{A.47}$$

From this, we can extract the form factor and the anomalous magnetic is then given by

$$\begin{aligned}
a_\ell &= F_2(0) \\
&= \frac{Q_{\ell'}}{Q_\ell}\frac{m_\ell}{16\pi^2}\,2\int_0^1 dx_3\int_0^{1-x_3} dx_2\int_0^{1-x_3-x_2} dx_1\;\delta(x_1+x_2+x_3-1) \\
&\quad\times\frac{\left[-2m_\ell\left(g_v^*g_v+g_a^*g_a\right)(x_1+x_2-1)(x_1+x_2-2)+4m_{\ell'}\left(g_v^*g_v-g_a^*g_a\right)(1-x_1-x_2)\right]}{(x_1+x_2)(x_1+x_2-1)m_\ell^2+(x_1+x_2)m_{\ell'}^2+x_3m_V^2} \\
&= \frac{Q_{\ell'}}{Q_\ell}\frac{m_\ell}{8\pi^2}\int_0^1 dx_3\int_0^{1-x_3} dx_2\;x_3\frac{\left[-2m_\ell(1+x_3)\left(g_v^*g_v+g_a^*g_a\right)+4m_{\ell'}\left(g_v^*g_v-g_a^*g_a\right)\right]}{-x_3(1-x_3)m_\ell^2+(1-x_3)m_{\ell'}^2+x_3m_V^2} \\
&= \frac{Q_{\ell'}}{Q_\ell}\frac{m_\ell}{4\pi^2}\int_0^1 dx_3\,(1-x_3)\,x_3\frac{\left[2m_{\ell'}\left(g_v^*g_v-g_a^*g_a\right)-(1+x_3)m_\ell\left(g_v^*g_v+g_a^*g_a\right)\right]}{-x_3(1-x_3)m_\ell^2+(1-x_3)m_{\ell'}^2+x_3m_V^2}.
\end{aligned} \tag{A.48}$$

Since the calculation is done in the Feynman gauge, we need to consider the contribution from the unphysical scalar boson with a mass m_V. The diagram is the one with the neutral vector boson replaced by the unphysical neutral scalar boson, so the structure is exactly the same as the one of the neutral scalar result, eq. (A.24), except that the couplings are now replaced by the following relations:

$$g_s = \frac{g_v}{m_V}\left(m_\ell - m_{\ell'}\right), \tag{A.49}$$

$$g_p = -\frac{g_a}{m_V}\left(m_\ell + m_{\ell'}\right). \tag{A.50}$$

Then we have the complete expression for the contribution of the neutral vector mediation:

$$\begin{aligned}
a_\ell &= \frac{Q_{\ell'}}{Q_\ell}\frac{m_\ell}{4\pi^2}\int_0^1 dx_3\,(1-x_3)\,x_3\frac{\left[2m_{\ell'}\left(g_v^*g_v-g_a^*g_a\right)-(1+x_3)m_\ell\left(g_v^*g_v+g_a^*g_a\right)\right]}{x_3m_V^2+(1-x_3)m_{\ell'}^2-x_3(1-x_3)m_\ell^2} \\
&\quad+\frac{Q_{\ell'}}{Q_\ell}\frac{1}{8\pi^2}\frac{m_\ell}{m_V^2}\int_0^1 dx_3\,(1-x_3)^2 \\
&\quad\times\frac{m_{\ell'}\left[g_v^*g_v\left(m_\ell-m_{\ell'}\right)^2-g_a^*g_a\left(m_\ell+m_{\ell'}\right)^2\right]+x_3m_\ell\left[g_v^*g_v\left(m_\ell-m_{\ell'}\right)^2+g_a^*g_a\left(m_\ell+m_{\ell'}\right)^2\right]}{x_3m_V^2+(1-x_3)m_{\ell'}^2-x_3(1-x_3)m_\ell^2}.
\end{aligned} \tag{A.51}$$

The vertex function for the electric dipole moment is

$$\begin{aligned}
\Gamma^{\mu}_{d_\ell}\left(q^2\right) =& -i\frac{Q_{\ell'}}{Q_\ell}\int dF_3 \int \frac{d^4\ell}{(2\pi)^4}\frac{1}{\left(\ell^2-D\right)^3}\; 4m_{\ell'}\left(1-x_1-x_2\right)\left(g_v^* g_a - g_v g_a^*\right)\left(-i\sigma^{\mu\nu}q_\nu\gamma_5\right) \\
=& \frac{Q_{\ell'}}{Q_\ell}\int dF_3\; \frac{-i}{32\pi^2 D}\; 4m_{\ell'}\left(1-x_1-x_2\right)\left(g_v^* g_a - g_v g_a^*\right)\left(-\sigma^{\mu\nu}q_\nu\gamma_5\right) \\
=& -i\frac{Q_{\ell'}}{Q_\ell}\frac{1}{8\pi^2}\int dF_3 \\
& \frac{m_{\ell'}\left(1-x_1-x_2\right)\left(g_v^* g_a - g_v g_a^*\right)}{-x_1x_2q^2+\left(x_1+x_2\right)\left(x_1+x_2-1\right)m_\ell^2+\left(x_1+x_2\right)m_{\ell'}^2+x_3m_V^2}\left(-\sigma^{\mu\nu}q_\nu\gamma_5\right) \\
=& F_3\left(q^2\right)\left(-\sigma^{\mu\nu}q_\nu\gamma_5\right).
\end{aligned} \tag{A.52}$$

This gives

$$\begin{aligned}
d_\ell =& eQ_\ell F_3\left(0\right) \\
=& -i\frac{eQ_{\ell'}}{8\pi^2}\; 2\int_0^1 dx_3\int_0^{1-x_3}dx_2\int_0^{1-x_3-x_2}dx_1\;\delta\left(x_1+x_2+x_3-1\right) \\
& \times\frac{m_{\ell'}\left(1-x_1-x_2\right)\left(g_v^* g_a - g_v g_a^*\right)}{\left(x_1+x_2\right)\left(x_1+x_2-1\right)m_\ell^2+\left(x_1+x_2\right)m_{\ell'}^2+x_3m_V^2} \\
=& -i\frac{eQ_{\ell'}}{4\pi^2}\int_0^1 dx_3\int_0^{1-x_3}dx_2\frac{m_{\ell'}x_3\left(g_v^* g_a - g_v g_a^*\right)}{-x_3\left(1-x_3\right)m_\ell^2+\left(1-x_3\right)m_{\ell'}^2+x_3m_V^2} \\
=& -i\frac{eQ_{\ell'}}{4\pi^2}\int_0^1 dx_3\left(1-x_3\right)x_3\frac{m_{\ell'}\left(g_v^* g_a - g_v g_a^*\right)}{x_3m_V^2+\left(1-x_3\right)m_{\ell'}^2-x_3\left(1-x_3\right)m_\ell^2}.
\end{aligned} \tag{A.53}$$

Adding the contribution from the unphysical scalar diagram, we obtain the most general structure of the electric dipole moment,

$$\begin{aligned}
d_\ell =& -i\frac{eQ_{\ell'}}{4\pi^2}\int_0^1 dx_3\left(1-x_3\right)x_3\frac{m_{\ell'}\left(g_v^* g_a - g_v g_a^*\right)}{x_3m_V^2+\left(1-x_3\right)m_{\ell'}^2-x_3\left(1-x_3\right)m_\ell^2} \\
& +i\frac{eQ_{\ell'}}{16\pi^2}\frac{m_\ell^2-m_{\ell'}^2}{m_V^2}\int_0^1 dx_3\left(1-x_3\right)^2\frac{m_{\ell'}\left(g_v^* g_a - g_v g_a^*\right)}{x_3m_V^2+\left(1-x_3\right)m_{\ell'}^2-x_3\left(1-x_3\right)m_\ell^2}.
\end{aligned} \tag{A.54}$$

A.4.2 Charged vector boson

The vertex function is given by

$$
\begin{aligned}
&-ieQ_\ell\Gamma^\mu = i^6 eQ_{\ell'}\int\frac{d^4k}{(2\pi)^4}\gamma^\rho\left(g_v^*+g_a^*\gamma_5\right)\frac{\not{k}+m_{\ell'}}{k^2-m_{\ell'}^2}\gamma^\sigma\left(g_v+g_a\gamma_5\right)\frac{g_{\rho\beta}}{(p'-k)^2-m_V^2}\\
&\times G\left[g^{\alpha\beta}\left(p+p'-2k\right)^\mu+g^{\beta\mu}\left(p-2p'+k\right)^\alpha+g^{\mu\alpha}\left(-2p+p'+k\right)^\beta\right]\frac{g_{\alpha\sigma}}{(p-k)^2-m_V^2}.
\end{aligned}
\tag{A.55}
$$

We can rewrite the denominator as

$$
\begin{aligned}
&\frac{1}{\left[(p'-k)^2-m_V^2\right]\left[(p-k)^2-m_V^2\right]\left(k^2-m_{\ell'}^2\right)} =\\
&\qquad\int dF_3\frac{1}{\left\{x_1\left[(p'-k)^2-m_V^2\right]+x_2\left[(p-k)^2-m_V^2\right]+x_3\left(k^2-m_{\ell'}^2\right)\right\}^3}.
\end{aligned}
\tag{A.56}
$$

It has the same structure as the denominator of the charged scalar mediation, with the scalar boson replaced by a vector boson. Therefore, the denominator can be simplified to

$$
\int dF_3\frac{1}{\left(\ell^2-D\right)^3},
\tag{A.57}
$$

where

$$
\ell\equiv k-\left(x_1p'+x_2p\right),
\tag{A.58}
$$

$$
D\equiv -x_1x_2q^2+\left(x_1+x_2\right)\left(x_1+x_2-1\right)m_\ell^2+\left(x_1+x_2\right)m_V^2+x_3m_{\ell'}^2.
\tag{A.59}
$$

The numerator is given by

$$
\begin{aligned}
&\gamma^\alpha\left(g_v^*+g_a^*\gamma_5\right)\left(\not{k}+m_{\ell'}\right)\gamma_\alpha\left(g_v+g_a\gamma_5\right)\left(p-p'-2k\right)^\mu\\
&+\gamma^\mu\left(g_v^*+g_a^*\gamma_5\right)\left(\not{k}+m_{\ell'}\right)\left(\not{p}-2\not{p}'+\not{k}\right)\left(g_v+g_a\gamma_5\right)\\
&+\gamma^\mu\left(g_v^*+g_a^*\gamma_5\right)\left(\not{k}+m_{\ell'}\right)\left(\not{p}-2\not{p}'+\not{k}\right)\left(g_v+g_a\gamma_5\right).
\end{aligned}
\tag{A.60}
$$

After the simplification of the numerator, we obtain the vertex function for the anomalous magnetic dipole moment

$$\begin{aligned}
\Gamma^{\mu}_{a_\ell}\left(q^2\right) =& -i\frac{G}{eQ_\ell}\int dF_3 \int \frac{d^4\ell}{(2\pi)^4}\frac{1}{\left(\ell^2-D\right)^3}[m_\ell\left(x_1+x_2\right)\left(1+2x_1+2x_2\right)\left(g_v^* g_v+g_a^* g_a\right) \\
&\qquad -3m_{\ell'}\left(x_1+x_2\right)\left(g_v^* g_v-g_a^* g_a\right)]\left(-i\sigma^{\mu\nu}q_\nu\right) \\
=& -i\frac{G}{eQ_\ell}\int dF_3 \frac{-i}{32\pi^2 D}[m_\ell\left(x_1+x_2\right)\left(1+2x_1+2x_2\right)\left(g_v^* g_v+g_a^* g_a\right) \\
&\qquad -3m_{\ell'}\left(x_1+x_2\right)\left(g_v^* g_v-g_a^* g_a\right)]\left(-i\sigma^{\mu\nu}q_\nu\right) \\
=& \frac{G}{eQ_\ell}\frac{m_\ell}{16\pi^2}\int dF_3 \\
&\frac{[m_\ell\left(x_1+x_2\right)\left(1+2x_1+2x_2\right)\left(g_v^* g_v+g_a^* g_a\right)-3m_{\ell'}\left(x_1+x_2\right)\left(g_v^* g_v-g_a^* g_a\right)]}{-x_1x_2q^2+\left(x_1+x_2\right)\left(x_1+x_2-1\right)m_\ell^2+\left(x_1+x_2\right)m_V^2+x_3m_{\ell'}^2} \\
&\qquad \times\left(\frac{i\sigma^{\mu\nu}q_\nu}{2m_\ell}\right) \\
=& F_2\left(q^2\right)\frac{i\sigma^{\mu\nu}q_\nu}{2m_\ell}.
\end{aligned} \tag{A.61}$$

We obtain the anomalous magnetic dipole moment as

$$\begin{aligned}
a_\ell =& F_2(0) \\
=& \frac{G}{eQ_f}\frac{m_\ell}{16\pi^2}\,2\int_0^1 dx_3\int_0^{1-x_3}dx_2\int_0^{1-x_3-x_2}dx_1\;\delta\left(x_1+x_2+x_3-1\right) \\
&\frac{[m_\ell\left(x_1+x_2\right)\left(1+2x_1+2x_2\right)\left(g_v^* g_v+g_a^* g_a\right)-3m_{\ell'}\left(x_1+x_2\right)\left(g_v^* g_v-g_a^* g_a\right)]}{-x_1x_2q^2+\left(x_1+x_2\right)\left(x_1+x_2-1\right)m_\ell^2+\left(x_1+x_2\right)m_V^2+x_3m_{\ell'}^2} \\
=& \frac{G}{eQ_f}\frac{m_\ell}{8\pi^2}\int_0^1 dx_3\int_0^{1-x_3}dx_2 \\
&\frac{[m_\ell\left(1-x_3\right)\left(3+2x_3\right)\left(g_v^* g_v+g_a^* g_a\right)-3m_{\ell'}\left(1-x_3\right)\left(g_v^* g_v-g_a^* g_a\right)]}{-x_3\left(1-x_3\right)m_\ell^2+\left(1-x_3\right)m_V^2+x_3m_{\ell'}^2} \\
=& \frac{G}{eQ_f}\frac{m_\ell}{8\pi^2}\int_0^1 dx_3\left(1-x_3\right)^2\frac{[m_\ell\left(3+2x_3\right)\left(g_v^* g_v+g_a^* g_a\right)-3m_{\ell'}\left(g_v^* g_v-g_a^* g_a\right)]}{-x_3\left(1-x_3\right)m_\ell^2+\left(1-x_3\right)m_V^2+x_3m_{\ell'}^2}.
\end{aligned} \tag{A.62}$$

Since we are working in the Feynman gauge, we need to consider the contributions coming from the unphysical Goldstone boson. This can be done by replacing the vector bosons in the diagram with the scalar bosons of mass m_V. There are two more diagrams that need to be computed, one is the diagram with one of the two vector bosons replaced by a scalar boson and the other is the diagram with both vector bosons replaced by scalar bosons. We note that in the diagram with one scalar boson, there are two vector bosons for the

replacement, so there are actually two diagrams in the one scalar boson case. These two diagrams give the same contribution and therefore, in this case, we can simply twice the result. The vertex function of the case with one scalar boson is given by

$$-ieQ_\ell\Gamma^\mu = \widetilde{G}\int dF_3 \int \frac{d^4\ell}{(2\pi)^4}\frac{1}{(\ell-D)^3}\left(g_s^* - g_p^*\gamma_5\right)\left(\not{k}+m_{\ell'}\right)\gamma^\mu\left(g_v+g_a\gamma_5\right). \tag{A.63}$$

From this we obtain the vertex function

$$\begin{aligned}\Gamma^\mu =& -\frac{\widetilde{G}}{eQ_f}\frac{m_\ell}{16\pi^2}\int dF_3 \frac{x_2\left(g_v^*g_v - g_a^*g_a\right)}{-x_1x_2q^2+\left(x_1+x_2\right)\left(x_1+x_2-1\right)m_\ell^2+\left(x_1+x_2\right)m_V^2+x_3m_{\ell'}^2} \\ &\times\left(i\frac{\sigma^{\mu\nu}q_\nu}{2m_\ell}\right) \\ =& \; F_2\left(q^2\right)\left(i\frac{\sigma^{\mu\nu}q_\nu}{2m_\ell}\right).\end{aligned} \tag{A.64}$$

From this we can extract the anomalous magnetic moment from $F_2(0)$. The diagram with two scalar bosons is just what we have calculated at the beginning of the appendix, with the couplings replaced by the ones of the unphysical scalar boson, so we need not repeat it again and simply replace the couplings in the expression. The expression of the dipole moments are a bit complicated because we need to consider three different types of diagrams in this case. They are given by

$$\begin{aligned}a_\ell =& \frac{G}{eQ_\ell}\frac{m_\ell}{8\pi^2}\int_0^1 dx(1-x)^2\frac{m_\ell(3-2x)(g_v^*g_v+g_a^*g_a)-3m_{\ell'}(g_v^*g_v-g_a^*g_a)}{xm_{\ell'}^2+(1-x)m_V^2-x(1-x)m_\ell^2} \\ &-\frac{\widetilde{G}}{eQ_\ell}\frac{1}{8\pi^2}\frac{m_\ell}{m_V}\int_0^1 dx(1-x)^2\frac{m_\ell(g_v^*g_v+g_a^*g_a)-m_{\ell'}(g_v^*g_v-g_a^*g_a)}{xm_{\ell'}^2+(1-x)m_V^2-x(1-x)m_\ell^2} \\ &-\frac{Q_V}{Q_\ell}\frac{1}{8\pi^2}\frac{m_\ell}{m_V^2}\int_0^1 dx\,(1-x)\,x \\ &\times\left\{\frac{(1-x)\,m_\ell\left[g_v^*g_v(m_\ell-m_{\ell'})^2+g_a^*g_a(m_\ell+m_{\ell'})^2\right]}{xm_{\ell'}^2+(1-x)\,m_V^2-x\,(1-x)\,m_\ell^2}\right. \\ &\qquad\left.+\frac{m_{\ell'}\left[g_v^*g_v(m_\ell-m_{\ell'})^2-g_a^*g_a(m_\ell+m_{\ell'})^2\right]}{xm_{\ell'}^2+(1-x)\,m_V^2-x\,(1-x)\,m_\ell^2}\right\},\end{aligned} \tag{A.65}$$

$$
\begin{aligned}
d_\ell = & \, i\frac{G}{16\pi^2}\int_0^1 dx(1-x)^2\frac{3m_{\ell'}(g_v^* g_a - g_v g_a^*)}{xm_{\ell'}^2+(1-x)m_V^2-x(1-x)m_\ell^2} \\
& + i\frac{\widetilde{G}}{16\pi^2 m_V}\int_0^1 dx(1-x)^2\frac{m_\ell(g_v^* g_a + g_v g_a^*) - m_{\ell'}(g_v^* g_a - g_v g_a^*)}{xm_{\ell'}^2+(1-x)m_V^2-x(1-x)m_\ell^2} \\
& + i\frac{eQ_V}{16\pi^2}\frac{m_{\ell'}^2-m_\ell^2}{m_V^2}\int_0^1 dx(1-x)x\frac{m_{\ell'}(g_v^* g_a - g_v g_a^*)}{xm_{\ell'}^2+(1-x)m_V^2-x(1-x)m_\ell^2},
\end{aligned}
\tag{A.66}
$$

where the first, second, third terms correspond to the diagram with two vector bosons, one vector boson and one scalar boson, two scalar bosons, respectively.

Bibliography

[1] S. L. Glashow, *Partial Symmetries of Weak Interactions*, Nucl. Phys. **22** (1961) 579–588.

[2] S. Weinberg, *A Model of Leptons*, Phys. Rev. Lett. **19** (1967) 1264–1266.

[3] A. Salam, *Weak and Electromagnetic Interactions*, Conf. Proc. C **680519** (1968) 367–377.

[4] **ATLAS** Collaboration, *Observation of a new particle in the search for the Standard Model Higgs boson with the ATLAS detector at the LHC*, Phys. Lett. B **716** (2012) 1–29 [arXiv:1207.7214].

[5] **CMS** Collaboration, *Observation of a New Boson at a Mass of 125 GeV with the CMS Experiment at the LHC*, Phys. Lett. B **716** (2012) 30–61 [arXiv:1207.7235].

[6] M. Thomson, *Modern particle physics*. Cambridge University Press, New York, 2013.

[7] Y. Koide, *A Fermion - Boson Composite Model of Quarks and Leptons*, Phys. Lett. B **120** (1983) 161–165.

[8] Y. Sumino, *Family Gauge Symmetry as an Origin of Koide's Mass Formula and Charged Lepton Spectrum*, JHEP **05** (2009) 075 [arXiv:0812.2103].

[9] W. Rodejohann and H. Zhang, *Extension of an empirical charged lepton mass relation to the neutrino sector*, Phys. Lett. B **698** (2011) 152–156 [arXiv:1101.5525].

[10] P. Zenczykowski, *Remark on Koide's Z3-symmetric parametrization of quark masses*, Phys. Rev. D **86** (2012) 117303 [arXiv:1210.4125].

[11] F.-G. Cao, *Neutrino masses from lepton and quark mass relations and neutrino oscillations*, Phys. Rev. D **85** (2012) 113003 [arXiv:1205.4068].

[12] N. Arkani-Hamed, S. Dimopoulos, and G. R. Dvali, *The Hierarchy problem and new dimensions at a millimeter*, Phys. Lett. B **429** (1998) 263–272 [hep-ph/9803315].

[13] N. Craig and S. Koren, *IR Dynamics from UV Divergences: UV/IR Mixing, NCFT, and the Hierarchy Problem*, JHEP **03** (2020) 037 [arXiv:1909.01365].

[14] **Super-Kamiokande** Collaboration, *Evidence for oscillation of atmospheric neutrinos*, Phys. Rev. Lett. **81** (1998) 1562–1567 [hep-ex/9807003].

[15] **SNO** Collaboration, *Measurement of the rate of $\nu_e + d \to p + p + e^-$ interactions produced by ^8B solar neutrinos at the Sudbury Neutrino Observatory*, Phys. Rev. Lett. **87** (2001) 071301 [nucl-ex/0106015].

[16] V. Barger, D. Marfatia, and K. Whisnant, *The physics of neutrinos*. Princeton Univ. Pr., Princeton, USA, 2012.

[17] M. C. Gonzalez-Garcia and M. Maltoni, *Phenomenology with Massive Neutrinos*, Phys. Rept. **460** (2008) 1–129 [arXiv:0704.1800].

[18] **Planck** Collaboration, *Planck 2018 results. VI. Cosmological parameters*, Astron. Astrophys. **641** (2020) A6 [arXiv:1807.06209]. [Erratum: Astron.Astrophys. 652, C4 (2021)].

[19] R. J. Adler, B. Casey, and O. C. Jacob, *Vacuum catastrophe: An Elementary exposition of the cosmological constant problem*, Am. J. Phys. **63** (1995) 620–626.

[20] J. Martin, *Everything You Always Wanted To Know About The Cosmological Constant Problem (But Were Afraid To Ask)*, Comptes Rendus Physique **13** (2012) 566–665 [arXiv:1205.3365].

[21] **Muon g-2** Collaboration, *Measurement of the Positive Muon Anomalous Magnetic Moment to 0.46 ppm*, Phys. Rev. Lett. **126** (2021) 141801 [arXiv:2104.03281].

[22] M. Kobayashi and T. Maskawa, *CP Violation in the Renormalizable Theory of Weak Interaction*, Prog. Theor. Phys. **49** (1973) 652–657.

[23] M. Pospelov and A. Ritz, *Electric dipole moments as probes of new physics*, Annals Phys. **318** (2005) 119–169 [hep-ph/0504231].

[24] A. D. Sakharov, *Violation of CP Invariance, C asymmetry, and baryon asymmetry of the universe*, Pisma Zh. Eksp. Teor. Fiz. **5** (1967) 32–35.

[25] K. S. Babu, B. Dutta, and R. N. Mohapatra, *Enhanced electric dipole moment of the muon in the presence of large neutrino mixing*, Phys. Rev. Lett. **85** (2000) 5064–5067 [hep-ph/0006329].

[26] T. Ibrahim and P. Nath, *Slepton flavor nonuniversality, the muon EDM and its proposed sensitive search at Brookhaven*, Phys. Rev. D **64** (2001) 093002 [hep-ph/0105025].

[27] J. L. Feng, K. T. Matchev, and Y. Shadmi, *Theoretical expectations for the muon's electric dipole moment*, Nucl. Phys. B **613** (2001) 366–381 [hep-ph/0107182].

[28] A. Romanino and A. Strumia, *Electron and Muon Electric Dipoles in Supersymmetric Scenarios*, Nucl. Phys. B **622** (2002) 73–94 [hep-ph/0108275].

[29] J. R. Ellis, J. Hisano, S. Lola, and M. Raidal, *CP violation in the minimal supersymmetric seesaw model*, Nucl. Phys. B **621** (2002) 208–234 [hep-ph/0109125].

[30] J. R. Ellis, J. Hisano, M. Raidal, and Y. Shimizu, *Lepton electric dipole moments in nondegenerate supersymmetric seesaw models*, Phys. Lett. B **528** (2002) 86–96 [hep-ph/0111324].

[31] A. Bartl, W. Majerotto, W. Porod, and D. Wyler, *Effect of supersymmetric phases on lepton dipole moments and rare lepton decays*, Phys. Rev. D **68** (2003) 053005 [hep-ph/0306050].

[32] K. Cheung, O. C. W. Kong, and J. S. Lee, *Electric and anomalous magnetic dipole moments of the muon in the MSSM*, JHEP **06** (2009) 020 [arXiv:0904.4352].

[33] G. Hiller, K. Huitu, T. Ruppell, and J. Laamanen, *A Large Muon Electric Dipole Moment from Flavor?*, Phys. Rev. D **82** (2010) 093015 [arXiv:1008.5091].

[34] C. Cesarotti, Q. Lu, Y. Nakai, A. Parikh, and M. Reece, *Interpreting the Electron EDM Constraint*, JHEP **05** (2019) 059 [arXiv:1810.07736].

[35] W. Dekens, J. de Vries, M. Jung, and K. K. Vos, *The phenomenology of electric dipole moments in models of scalar leptoquarks*, JHEP **01** (2019) 069 [arXiv:1809.09114].

[36] W. Altmannshofer, S. Gori, H. H. Patel, S. Profumo, and D. Tuckler, *Electric dipole moments in a leptoquark scenario for the B-physics anomalies*, JHEP **05** (2020) 069 [arXiv:2002.01400].

[37] I. Bigaran and R. R. Volkas, *Reflecting on chirality: CP-violating extensions of the single scalar-leptoquark solutions for the (g-2)e,μ puzzles and their implications for lepton EDMs*, Phys. Rev. D **105** (2022) 015002 [arXiv:2110.03707].

[38] Y. Omura, E. Senaha, and K. Tobe, *τ- and μ-physics in a general two Higgs doublet model with $\mu - \tau$ flavor violation*, Phys. Rev. D **94** (2016) 055019 [arXiv:1511.08880].

[39] W.-S. Hou, G. Kumar, and S. Teunissen, *Charged lepton EDM with extra Yukawa couplings*, JHEP **01** (2022) 092 [arXiv:2109.08936].

[40] Y. Nakai, R. Sato, and Y. Shigekami, *Muon electric dipole moment as a probe of flavor-diagonal CP violation*, Phys. Lett. B **831** (2022) 137194 [arXiv:2204.03183].

[41] R. Dermisek, K. Hermanek, N. McGinnis, and S. Yoon, *The Ellipse of Muon Dipole Moments*, arXiv:2205.14243 (2022).

[42] **CMS** Collaboration, *Evidence for Higgs boson decay to a pair of muons*, JHEP **01** (2021) 148 [arXiv:2009.04363].

[43] **ACME** Collaboration, *Improved limit on the electric dipole moment of the electron*, Nature **562** (2018) 355–360.

[44] N. Cabibbo, *Unitary Symmetry and Leptonic Decays*, Phys. Rev. Lett. **10** (1963) 531–533.

[45] R. D. Peccei and H. R. Quinn, *CP Conservation in the Presence of Instantons*, Phys. Rev. Lett. **38** (1977) 1440–1443.

[46] R. D. Peccei and H. R. Quinn, *Constraints Imposed by CP Conservation in the Presence of Instantons*, Phys. Rev. D **16** (1977) 1791–1797.

[47] **Particle Data Group** Collaboration, *Review of Particle Physics*,. to be published (2022).

[48] T. Aoyama *et al.*, *The anomalous magnetic moment of the muon in the Standard Model*, Phys. Rept. **887** (2020) 1–166 [arXiv:2006.04822].

[49] T. Aoyama, M. Hayakawa, T. Kinoshita, and M. Nio, *Tenth-Order QED Contribution to the Electron g-2 and an Improved Value of the Fine Structure Constant*, Phys. Rev. Lett. **109** (2012) 111807 [arXiv:1205.5368].

[50] S. J. Brodsky and E. De Rafael, *SUGGESTED BOSON - LEPTON PAIR COUPLINGS AND THE ANOMALOUS MAGNETIC MOMENT OF THE MUON*, Phys. Rev. **168** (1968) 1620–1622.

[51] M. Gourdin and E. De Rafael, *Hadronic contributions to the muon g-factor*, Nucl. Phys. B **10** (1969) 667–674.

[52] S. Borsanyi *et al.*, *Leading hadronic contribution to the muon magnetic moment from lattice QCD*, Nature **593** (2021) 51–55 [arXiv:2002.12347].

[53] K. G. Wilson, *Confinement of Quarks*, Phys. Rev. D **10** (1974) 2445–2459.

[54] M. Cè *et al.*, *Window observable for the hadronic vacuum polarization contribution to the muon $g-2$ from lattice QCD*, arXiv:2206.06582 (2022).

[55] C. Alexandrou *et al.*, *Lattice calculation of the short and intermediate time-distance hadronic vacuum polarization contributions to the muon magnetic moment using twisted-mass fermions*, arXiv:2206.15084 (2022).

[56] G. Abbiendi *et al.*, *Measuring the leading hadronic contribution to the muon g-2 via μe scattering*, Eur. Phys. J. C **77** (2017) 139 [arXiv:1609.08987].

[57] **MUonE** Collaboration, *Status of the MUonE experiment*, PoS **ICHEP2020** (2021) 223 [arXiv:2012.07016].

[58] K. Asai, K. Hamaguchi, N. Nagata, S.-Y. Tseng, and J. Wada, *Probing the L_μ-L_τ Gauge Boson at the MUonE Experiment*, arXiv:2109.10093 (2021).

[59] S. Baek, N. G. Deshpande, X. G. He, and P. Ko, *Muon anomalous g-2 and gauged L(muon) - L(tau) models*, Phys. Rev. D **64** (2001) 055006 [hep-ph/0104141].

[60] E. Ma, D. P. Roy, and S. Roy, *Gauged L(mu) - L(tau) with large muon anomalous magnetic moment and the bimaximal mixing of neutrinos*, Phys. Lett. B **525** (2002) 101–106 [hep-ph/0110146].

[61] J. Heeck and W. Rodejohann, *Gauged $L_\mu - L_\tau$ Symmetry at the Electroweak Scale*, Phys. Rev. D **84** (2011) 075007 [arXiv:1107.5238].

[62] K. Harigaya, T. Igari, M. M. Nojiri, M. Takeuchi, and K. Tobe, *Muon g-2 and LHC phenomenology in the $L_\mu - L_\tau$ gauge symmetric model*, JHEP **03** (2014) 105 [arXiv:1311.0870].

[63] A. Czarnecki, W. J. Marciano, and A. Vainshtein, *Refinements in electroweak contributions to the muon anomalous magnetic moment*, Phys. Rev. D **67** (2003) 073006 [hep-ph/0212229]. [Erratum: Phys.Rev.D 73, 119901 (2006)].

[64] C. Gnendiger, D. Stöckinger, and H. Stöckinger-Kim, *The electroweak contributions to $(g-2)_\mu$ after the Higgs boson mass measurement*, Phys. Rev. D **88** (2013) 053005 [arXiv:1306.5546].

[65] C. Jarlskog, *Commutator of the Quark Mass Matrices in the Standard Electroweak Model and a Measure of Maximal CP Nonconservation*, Phys. Rev. Lett. **55** (1985) 1039.

[66] F. Hoogeveen, *The Standard Model Prediction for the Electric Dipole Moment of the Electron*, Nucl. Phys. B **341** (1990) 322–340.

[67] M. E. Pospelov and I. B. Khriplovich, *Electric dipole moment of the W boson and the electron in the Kobayashi-Maskawa model*, Sov. J. Nucl. Phys. **53** (1991) 638–640.

[68] M. J. Booth, *The Electric dipole moment of the W and electron in the Standard Model*, hep-ph/9301293 (1993).

[69] M. Pospelov and A. Ritz, *CKM benchmarks for electron electric dipole moment experiments*, Phys. Rev. D **89** (2014) 056006 [arXiv:1311.5537].

[70] D. Ghosh and R. Sato, *Lepton Electric Dipole Moment and Strong CP Violation*, Phys. Lett. B **777** (2018) 335–339 [arXiv:1709.05866].

[71] C. Abel *et al.*, *Measurement of the Permanent Electric Dipole Moment of the Neutron*, Phys. Rev. Lett. **124** (2020) 081803 [arXiv:2001.11966].

[72] A. Adelmann *et al.*, *Search for a muon EDM using the frozen-spin technique*, arXiv:2102.08838 (2021).

[73] D. Hanneke, S. Fogwell, and G. Gabrielse, *New Measurement of the Electron Magnetic Moment and the Fine Structure Constant*, Phys. Rev. Lett. **100** (2008) 120801 [arXiv:0801.1134].

[74] B. L. Roberts and W. J. Marciano, *Lepton dipole moments*, vol. 20. World Scientific, 2010.

[75] **Muon (g-2)** Collaboration, *An Improved Limit on the Muon Electric Dipole Moment*, Phys. Rev. D **80** (2009) 052008 [arXiv:0811.1207].

[76] **Muon g-2** Collaboration, *The muon EDM in the g-2 experiment at Fermilab*, EPJ Web Conf. **118** (2016) 01005.

[77] M. Abe *et al.*, *A New Approach for Measuring the Muon Anomalous Magnetic Moment and Electric Dipole Moment*, PTEP **2019** (2019) 053C02 [arXiv:1901.03047].

[78] F. J. M. Farley, *et al.*, *A New method of measuring electric dipole moments in storage rings*, Phys. Rev. Lett. **93** (2004) 052001 [hep-ex/0307006].

[79] A. Adelmann and K. Kirch, *Search for the muon electric dipole moment using a compact storage ring*, hep-ex/0606034 (2006).

[80] K. Kannike, M. Raidal, D. M. Straub, and A. Strumia, *Anthropic solution to the magnetic muon anomaly: the charged see-saw*, JHEP **02** (2012) 106 [arXiv:1111.2551]. [Erratum: JHEP 10, 136 (2012)].

[81] A. Falkowski, D. M. Straub, and A. Vicente, *Vector-like leptons: Higgs decays and collider phenomenology*, JHEP **05** (2014) 092 [arXiv:1312.5329].

[82] R. Dermisek and A. Raval, *Explanation of the Muon g-2 Anomaly with Vectorlike Leptons and its Implications for Higgs Decays*, Phys. Rev. D **88** (2013) 013017 [arXiv:1305.3522].

[83] Z. Poh and S. Raby, *Vectorlike leptons: Muon g-2 anomaly, lepton flavor violation, Higgs boson decays, and lepton nonuniversality*, Phys. Rev. D **96** (2017) 015032 [arXiv:1705.07007].

[84] K. Asai, K. Hamaguchi, N. Nagata, S.-Y. Tseng, and K. Tsumura, *Minimal Gauged $U(1)_{L_\alpha - L_\beta}$ Models Driven into a Corner*, Phys. Rev. D **99** (2019) 055029 [arXiv:1811.07571].

[85] K. Asai, K. Hamaguchi, N. Nagata, and S.-Y. Tseng, *Leptogenesis in the minimal gauged $U(1)_{L_\mu - L_\tau}$ model and the sign of the cosmological baryon asymmetry*, JCAP **11** (2020) 013 [arXiv:2005.01039].

[86] **ATLAS** Collaboration, *Search for the Standard Model Higgs boson decay to $\mu^+\mu^-$ with the ATLAS detector*, Phys. Lett. B **738** (2014) 68–86 [arXiv:1406.7663].

[87] **CMS** Collaboration, *Search for a standard model-like Higgs boson in the $^+$ and e^+e decay channels at the LHC*, Phys. Lett. B **744** (2015) 184–207 [arXiv:1410.6679].

[88] **ATLAS** Collaboration, *Search for the dimuon decay of the Higgs boson in pp collisions at $\sqrt{s}$ = 13 TeV with the ATLAS detector*, Phys. Rev. Lett. **119** (2017) 051802 [arXiv:1705.04582].

[89] **CMS** Collaboration, *Search for the Higgs boson decaying to two muons in proton-proton collisions at $\sqrt{s} = 13$ TeV*, Phys. Rev. Lett. **122** (2019) 021801 [arXiv:1807.06325].

[90] **ATLAS** Collaboration, *A search for the dimuon decay of the Standard Model Higgs boson with the ATLAS detector*, Phys. Lett. B **812** (2021) 135980 [arXiv:2007.07830].

[91] Y. Nakai and M. Reece, *Electric Dipole Moments in Natural Supersymmetry*, JHEP **08** (2017) 031 [arXiv:1612.08090].

[92] **L3** Collaboration, *Search for heavy neutral and charged leptons in e^+e^- annihilation at LEP*, Phys. Lett. B **517** (2001) 75–85 [hep-ex/0107015].

[93] A. Buras, *Gauge Theory of Weak Decays*. Cambridge University Press, 2020.

[94] B. H. J. McKellar and D.-d. Wu, *Quantum Electrodynamics with Complex Fermion Mass*, (1991).

[95] P. Aggarwal, *et al.*, *Measuring the electric dipole moment of the electron in BaF*, The European Physical Journal D **72** (2018) 1–10.